Hadronic Calorimeters

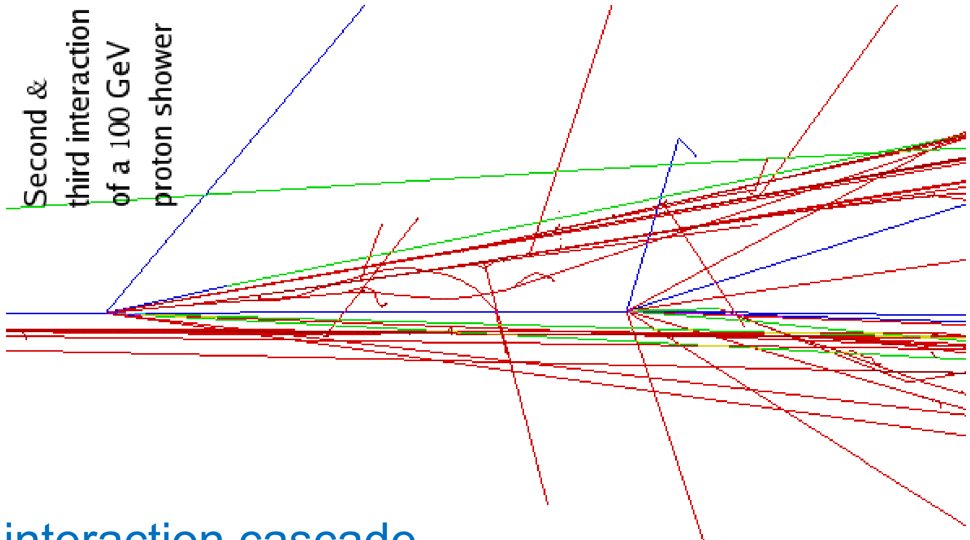

- Strong (nuclear) interaction cascade
- Similar to EM shower

$$\chi_0(EM) \rightarrow \lambda_I(had) \approx 35\, g\, cm^{-2}\, A^{1/3}$$

hadronic interaction length

$$\lambda_I > \chi_0$$

hadronic calorimeter
nearly always sampling calorimeters

- Shower length $\sim 5\lambda \sim 4m @ 100\, GeV$
  $\sim 13\lambda \sim 10m @ 1TeV$

- Energy Resolution
  - shower fluctuations
  - leakage of energy
  - invisible energy loss mechanisms

Sampling Calorimeter

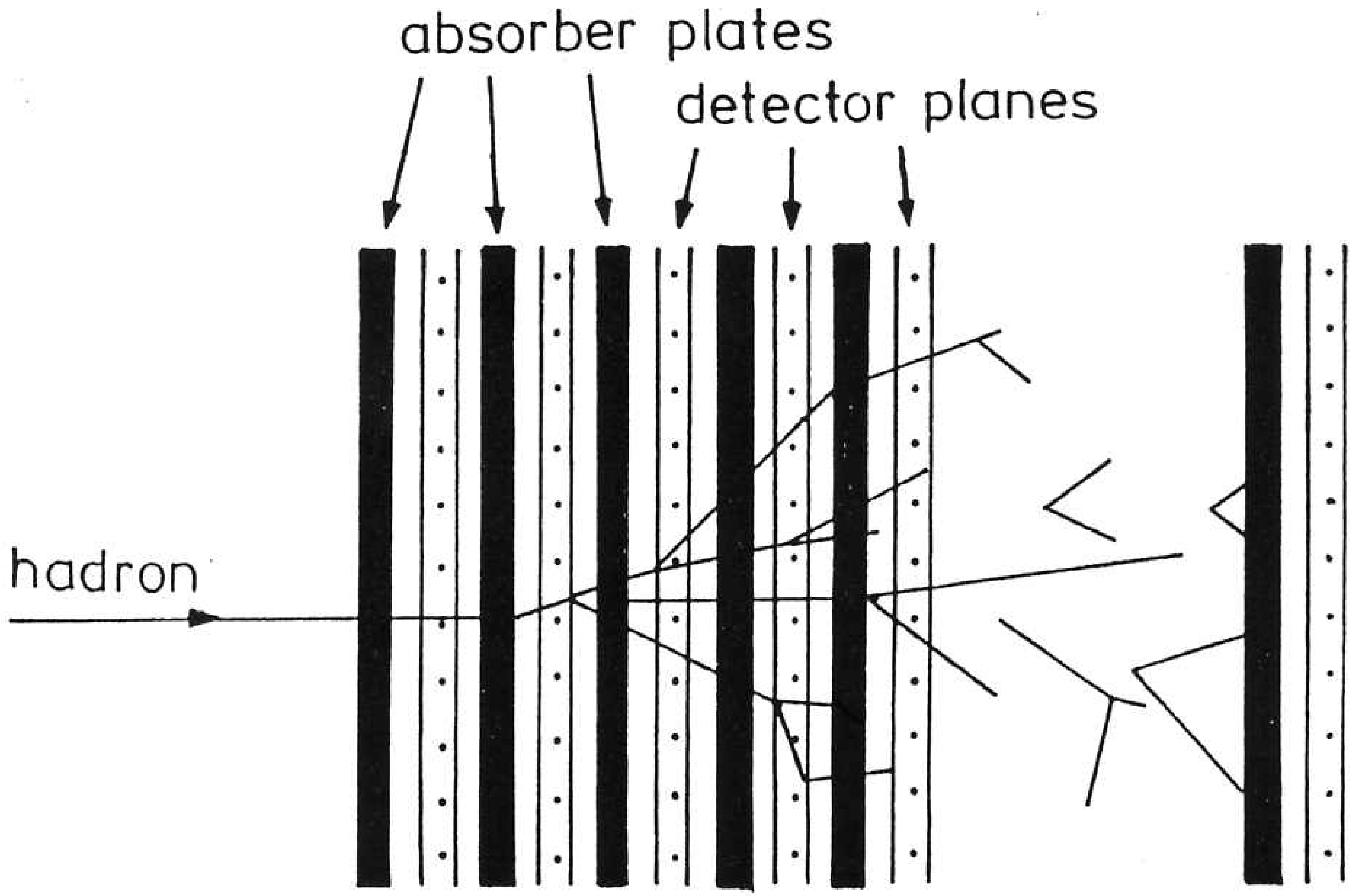

Hadronic Lateral Shower Profile

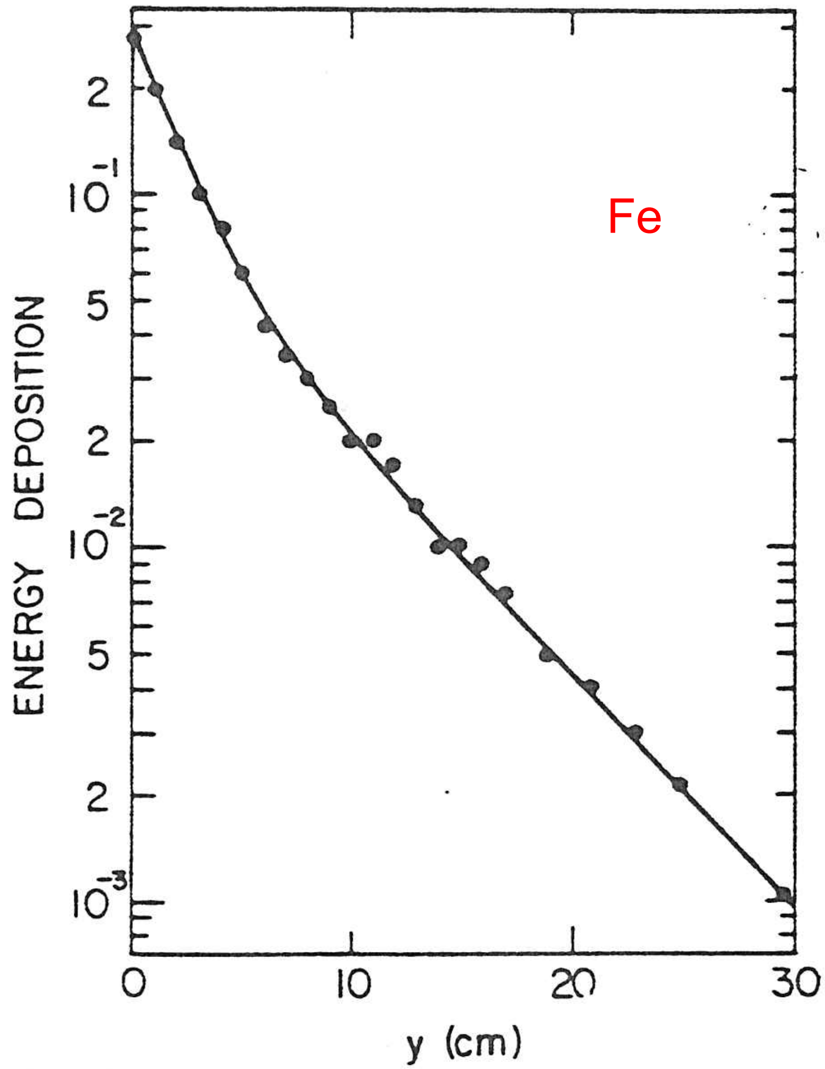

- Hadronic shower much broader than EM
  - Mean hadronic p_T versus MCS

Fe $\lambda_I \sim 16cm$

$\chi_0 \sim 1.8cm$

Hadronic Shower Longitudinal Development

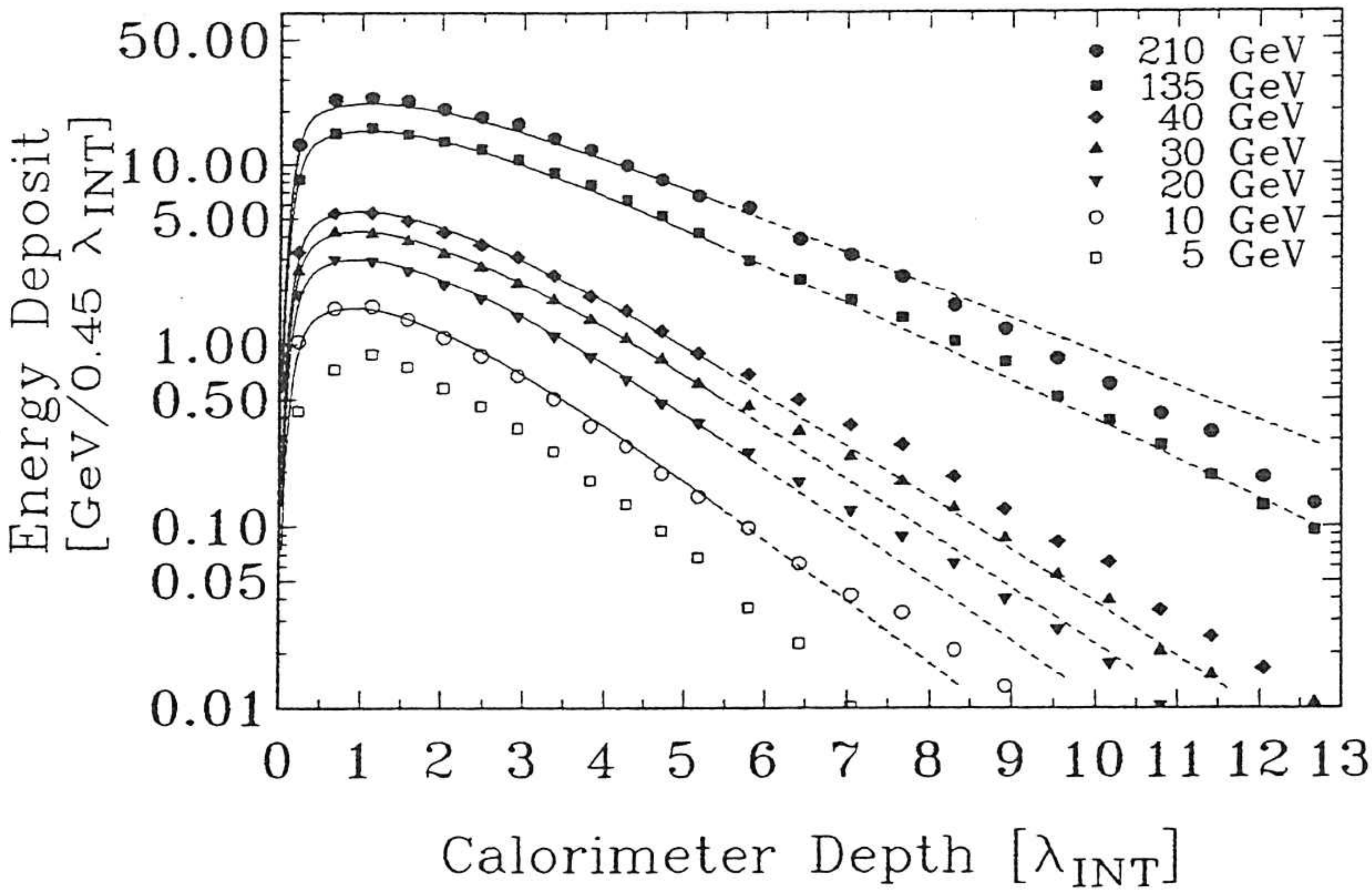

ZEUS
Uranium/Scint

Lateral Scaling with Material

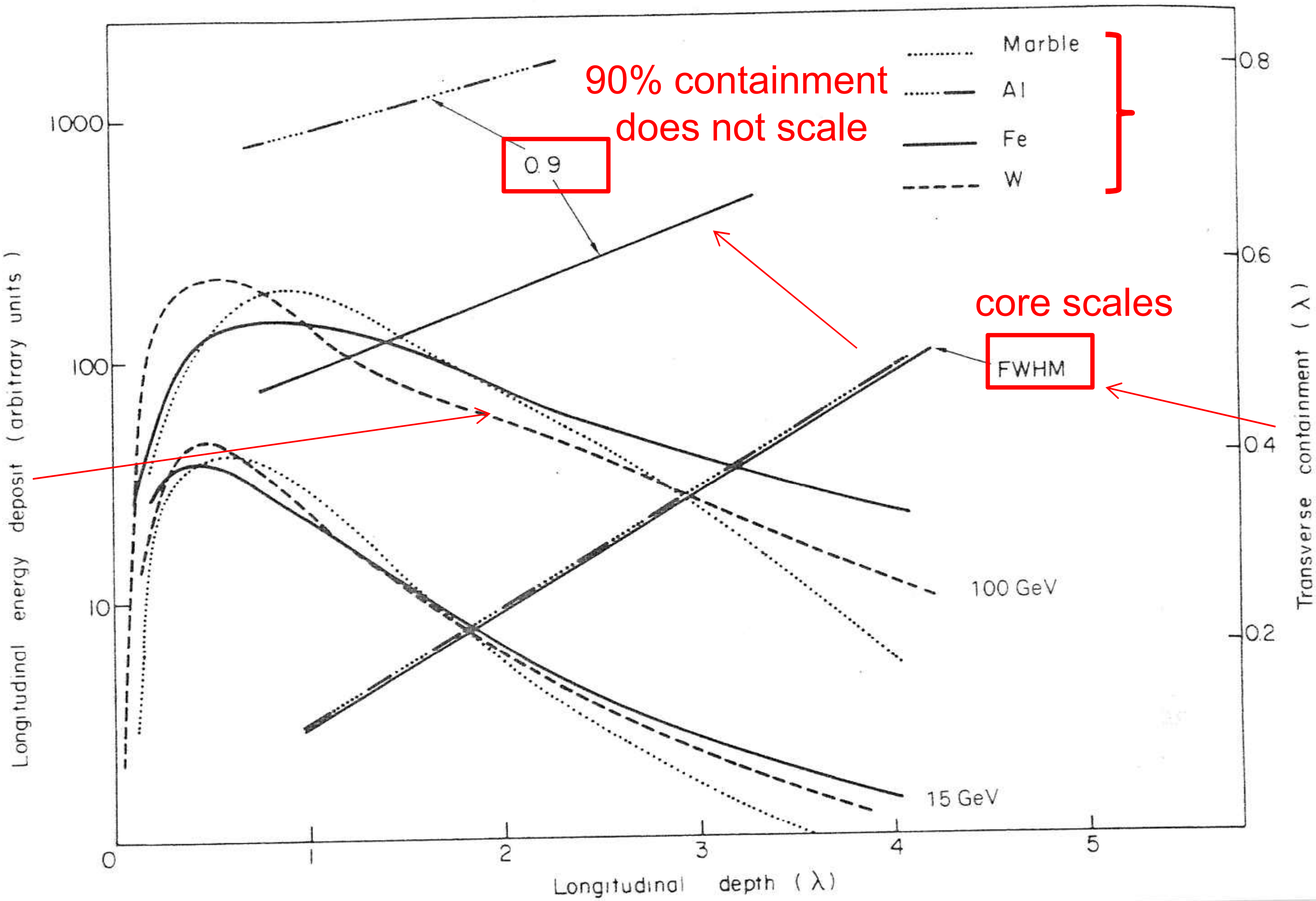

Calorimeter Energy Resolution

$$\left(\frac{\sigma}{E}\right)^2 = \left(\frac{A_0}{\sqrt{E}}\right)^2 + \left(\frac{A_1}{\sqrt{E}}\right)^2 + \left(A_2 \ln E\right)^2 + \left(\frac{A_3\sqrt{N}}{E}\right)^2 + A_4$$

$\frac{A_0}{\sqrt{E}}$ sampling and shower fluctuations

number of samples $N = \frac{E}{\Delta E}$

energy

energy deposited in a sampling step

$$\sigma_E = \sigma_N \cdot \Delta E = \sqrt{N} \cdot \Delta E$$

$$\frac{\sigma_E}{E} = \sqrt{N}\,\frac{\Delta E}{E}$$

$$\frac{\sigma_E}{E} = \frac{\sqrt{\Delta E}}{\sqrt{E}}$$

stochastic term $A_0 \sim \sqrt{\Delta E}$

Calorimeter Energy Resolution

$$\left(\frac{\sigma}{E}\right)^2 = \left(\frac{A_0}{\sqrt{E}}\right)^2 + \left(\frac{A_1}{\sqrt{E}}\right)^2 + \left(A_2 \ln E\right)^2 + \left(\frac{A_3\sqrt{N}}{E}\right)^2 + A_4$$

$\frac{A_1}{\sqrt{E}}$ counting statics in sensor system

e.g. # of photo-electrons in PM, ion pairs in liquid argon

$$N = \bar{n} \cdot E$$

mean # of photo-electrons in PM per unit of incident energy

$$\sigma_E = \frac{\sigma_N}{\bar{n}} = \frac{\sqrt{N}}{\bar{n}} = \frac{\sqrt{\bar{n} \cdot E}}{\bar{n}}$$

$$\frac{\sigma_E}{E} = \frac{1}{\sqrt{\bar{n}}} \cdot \frac{1}{\sqrt{E}}$$

$A_1 = \frac{1}{\sqrt{\bar{n}}}$ this term is usually negligible

A_2 shower leakage fluctuations – make calorimeter as deep as $$ allow

Calorimeter Energy Resolution

$$\left(\frac{\sigma}{E}\right)^2 = \left(\frac{A_0}{\sqrt{E}}\right)^2 + \left(\frac{A_1}{\sqrt{E}}\right)^2 + \left(A_2 \ln E\right)^2 + \left(\frac{A_3\sqrt{N}}{E}\right)^2 + A_4$$

A_3 noise - detector or electronics
- important for low level signal
- liquid argon electronics
- detector capacitance

N channels with some intrinsic noise $\Sigma \rightarrow N \cdot \Delta E$ noise (energy)

$$\frac{\sigma_E}{E} = N\frac{\Delta E}{E}$$

deposited energy

$\frac{1}{E}$ behaviour

$A_3 \simeq \Delta E \cdot N$ increases with number of channels summed over

Calorimeter Energy Resolution

$$\left(\frac{\sigma}{E}\right)^2 = \left(\frac{A_0}{\sqrt{E}}\right)^2 + \left(\frac{A_1}{\sqrt{E}}\right)^2 + \left(A_2 \ln E\right)^2 + \left(\frac{A_3\sqrt{N}}{E}\right)^2 + A_4$$

A_4 inter - calibration uncertainty of channels - constant in E

- fractional channel to channel gain uncertainty
- spatial in-homogeneity of detector energy response
- dead space
- temperature variation
- radiation damage
- all these influence spatial variation of effective energy response

$$\sigma = k \cdot E$$

$$\frac{\sigma_E}{E} = k$$ constant

The em energy resolution of the ATLAS calorimeter

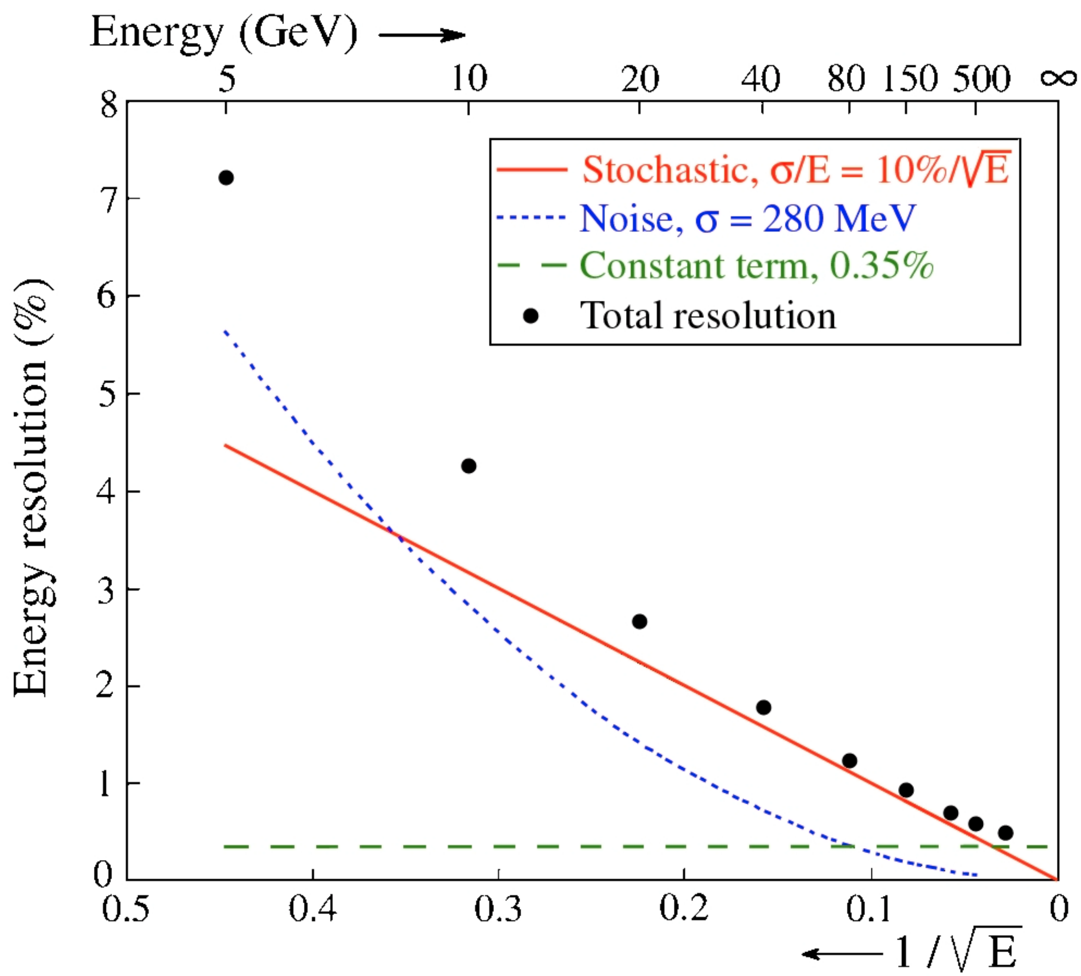

FIG. 9.30. The em energy resolution and the separate contributions to it, for the em barrel calorimeter, at $\eta = 0.28$ [Gin 95].

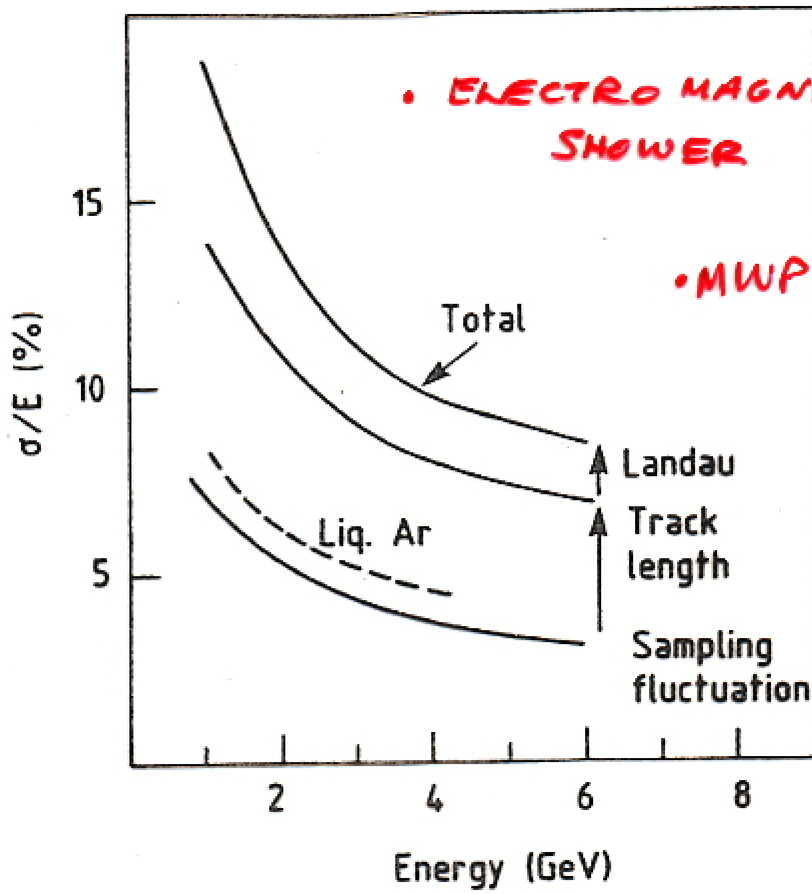

- ELECTRO MAGNETIC SHOWER

Pb +

- MWPC READOUT

- EFFECT OF SAMPLING + SHOWER TRACK LENGTH FLUCTUATIONS IN ELECTROMAGNETIC SHOWER

MONTE CARLO SIMULATION

• SEE EFFECTS MOST CLEARLY FOR ELECTROMAGNETIC SHOWERS

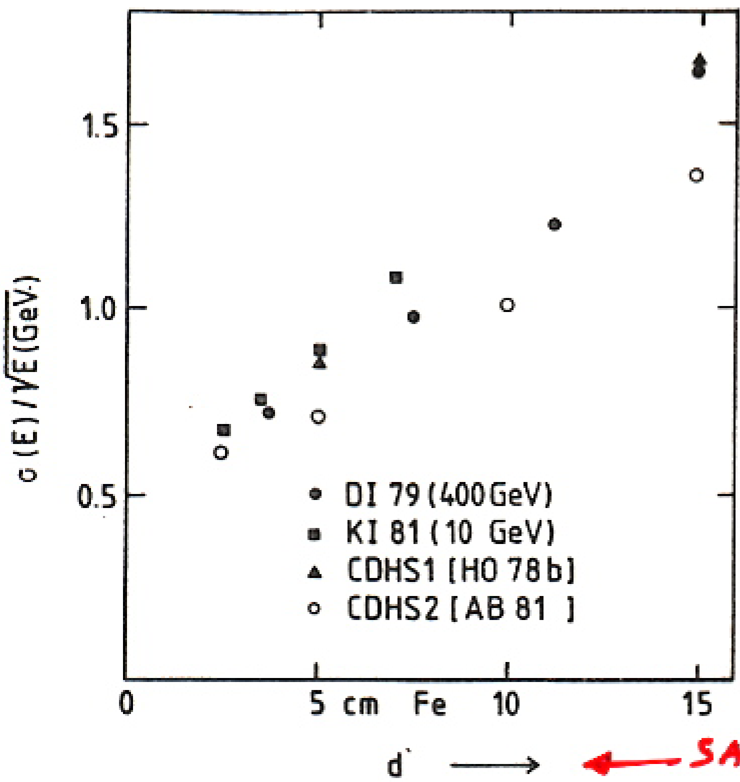

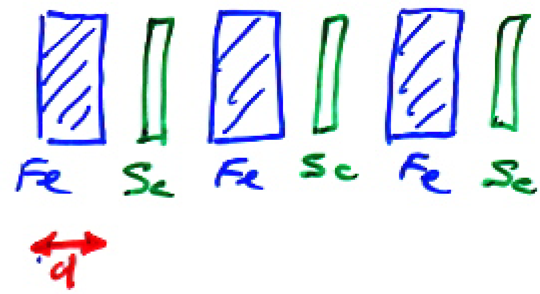

• INCREASING SAMPLING FREQUENCY, REDUCES EFFECT OF SAMPLING FLUCTUATIONS

• IMPROVES ENERGY RESOLUTION

← SAMPLING FREQUENCY

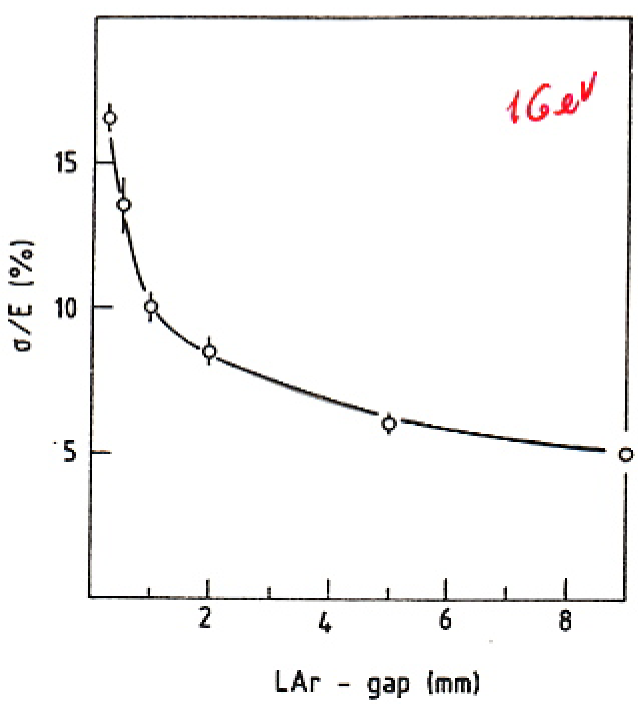

← INCREASING FRACTION OF SHOWER SAMPLED

Sampling fluctuations in em and hadronic showers

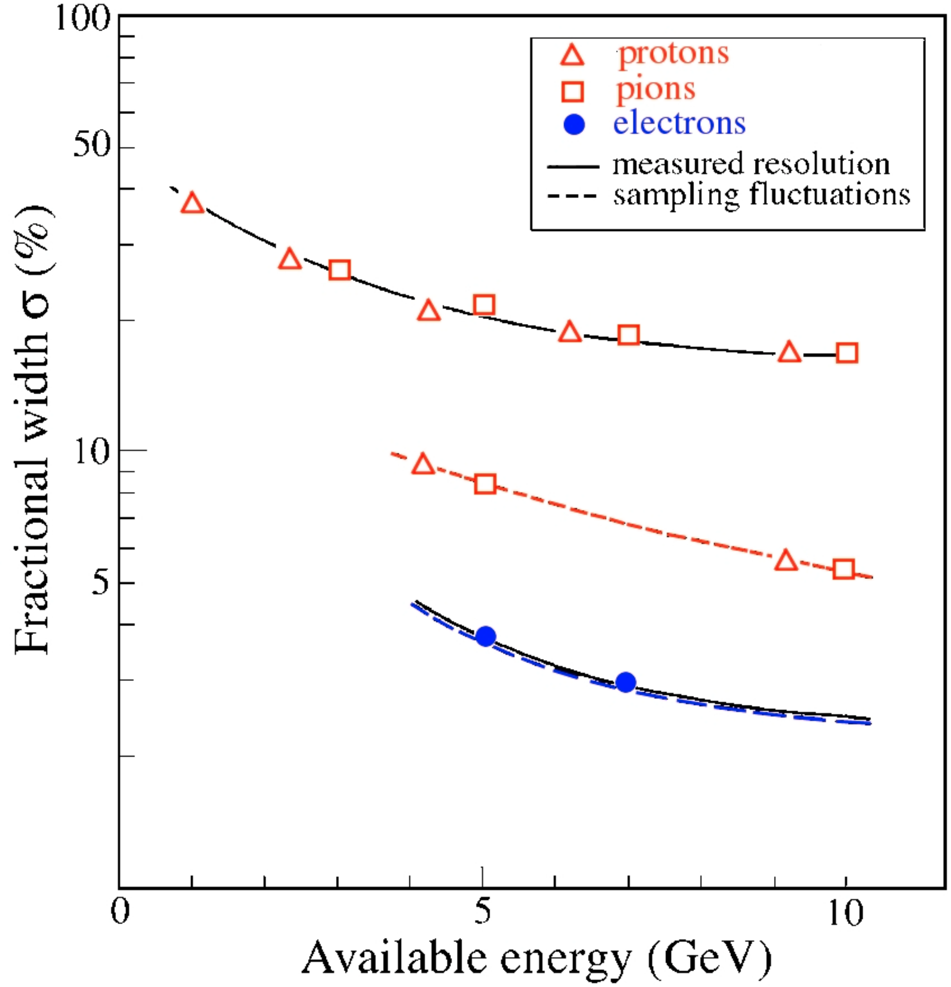

FIG. 4.15. The energy resolution and the contribution from sampling fluctuations to this resolution measured for electrons and hadrons, in a calorimeter consisting of 1.5 mm thick iron plates separated by 2 mm gaps filled with liquid argon. From [Fab 77].

Sampling fluctuations in em calorimeters
Determined by sampling fraction and sampling frequency

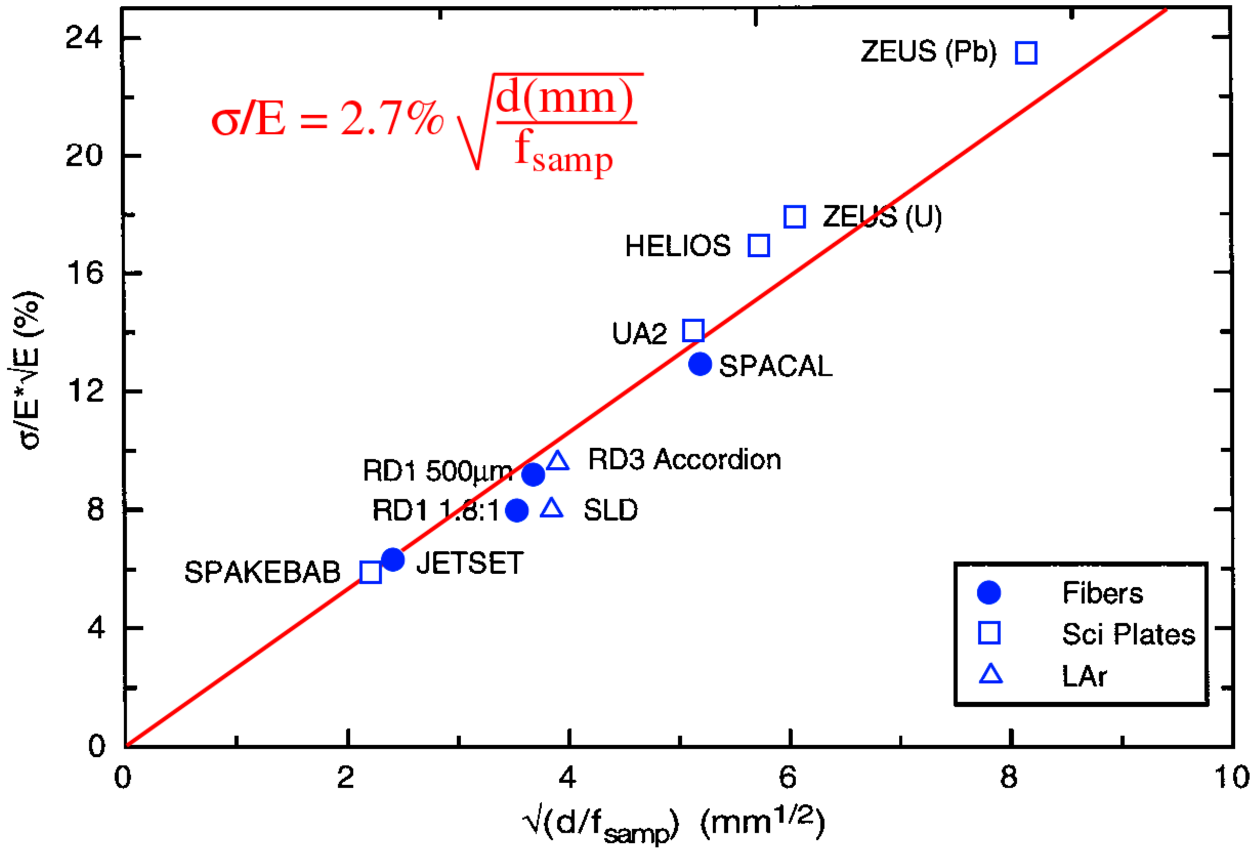

FIG. 4.8. The em energy resolution of sampling calorimeters as a function of the parameter $(d/f_{\text{samp}})^{1/2}$, in which d is the thickness of an active sampling layer (*e.g.* the diameter of a fiber or the thickness of a scintillator plate or a liquid-argon gap), and f_{samp} is the sampling fraction for mips [Liv 95].

How to measure the effects of sampling fluctuations (2)

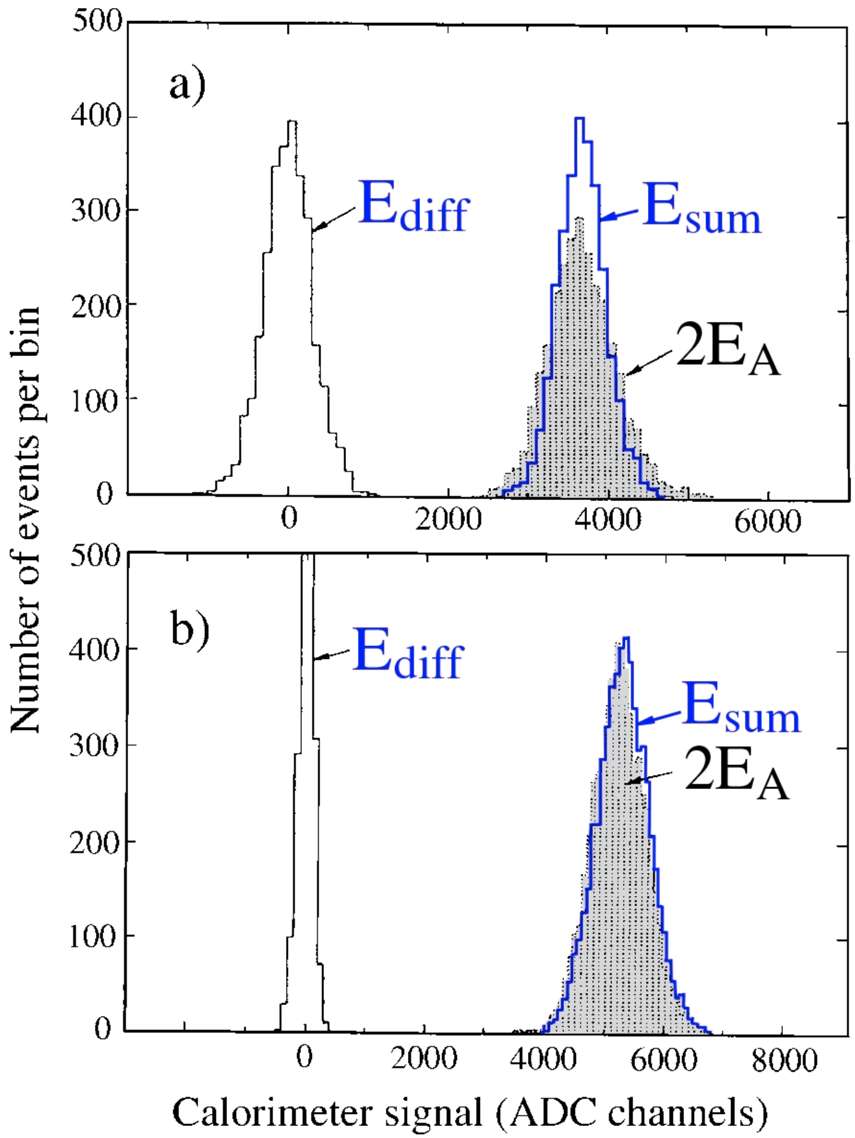

BLACK TAPE

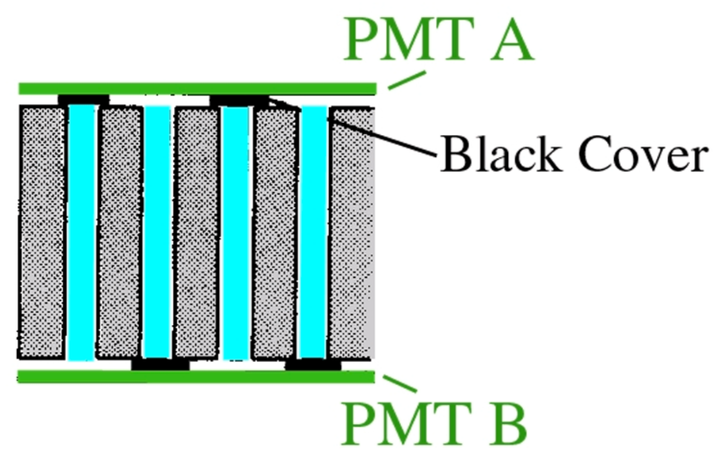

NO BLACK TAPE

FIG. 4.14. Pulse height distributions for 30 GeV hadrons obtained with the ZEUS lead/plastic-scintillator prototype calorimeter. Diagram a) shows the distributions of $E_{\rm sum}$, $E_{\rm diff}$ and $2E_{\rm A}$, measured in the configuration depicted in Figure 4.13b. Diagram b) shows the same distributions measured in the same configuration, but with the black tape removed. See text for details. From [Dre 90].

I DID THESE MEASUREMENTS

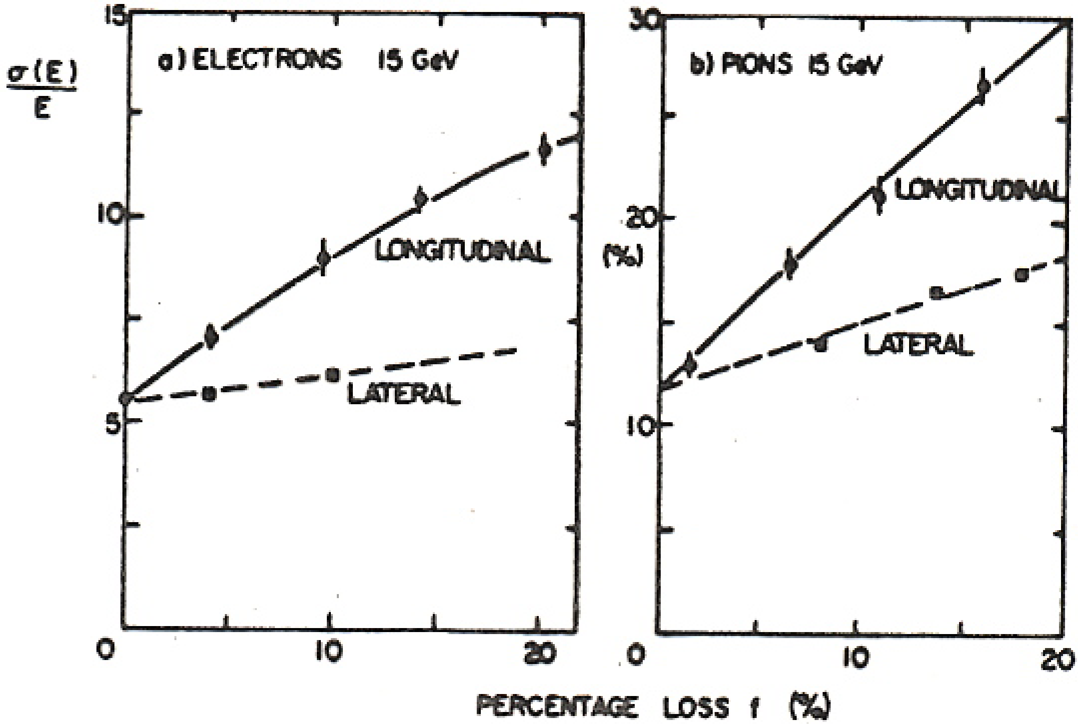

- ENERGY RESOLUTION DEGRADATION DUE TO LONGITUDINAL OR LATERAL ENERGY LEAKAGE

MATERIAL?

- LONGITUDINAL $L_{95\%} = \cancel{9.4 \ln E + 39 \text{ cm}}$

  $\sim 6 \lambda_{INT}$

- LATERAL $R_{95\%} \sim 1 \lambda_{INT}$

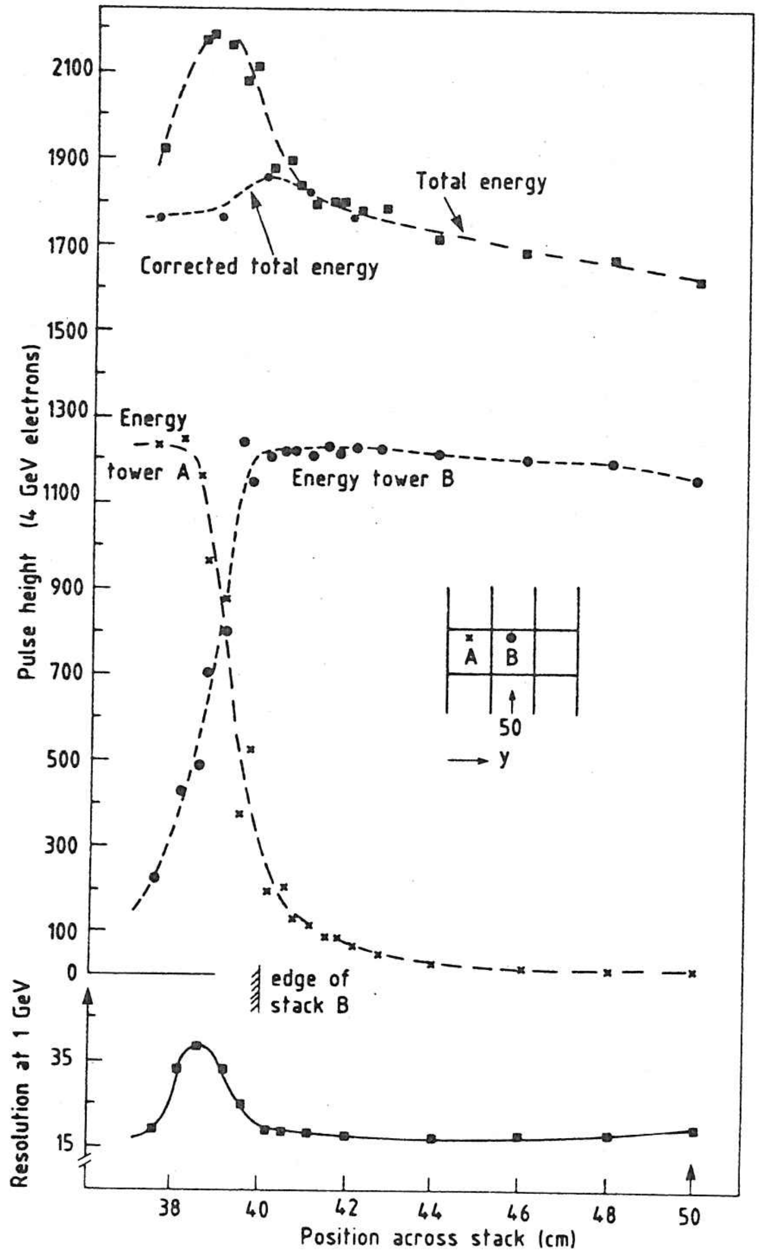

Calorimeter non-uniformity

Table 5: Principal Contributions to Energy Resolution in Electromagnetic and Hadronic Calorimeters

Mechanisms (add in quadrature)	Electromagnetic showers	Hadronic showers
Intrinsic shower fluctuations	Track-length fluctuations: $\sigma/E \gtrsim 0.005/\sqrt{E}$ (GeV).	Fluctuations in the energy loss: $\sigma/E \simeq 0.45/\sqrt{E}$ (GeV). Scaling weaker than $1/\sqrt{E}$ for high energies. With compensation for nuclea effects: $\sigma/E \simeq 0.22/\sqrt{E}$ (GeV).
Sampling fluctuations	$\sigma/E \simeq 0.04\sqrt{\Delta E/E}$. Nature of readout may augment sampling fluctuations.	$\sigma/E \simeq 0.09\sqrt{\Delta E/E}$
Instrumental effects	Noise and pedestal width: $\sigma/E \sim 1/E$ – determine minimum detectable signal; – limit low-energy performance. Calibration errors and non-uniformities: $\sigma/E \sim$ constant and therefore limits high-energy performance.	
Incomplete containment of shower	$\sigma/E \sim E^{-\alpha}$, $\alpha < 1/2$ (see subsec. 2.2, resp. 3.4). For leakage fraction $\geq$ few %: non-linear response and non-Gaussian 'tail'.	

it

Semi-empirical model of hadron shower development

$$\frac{dE}{dS} = E_{INC}\left\{\frac{Cx^{(\alpha_E - 1)}e^{-x}}{\Gamma(\alpha_E)}\right\} + E_{INC}(1-C)\left\{\frac{y^{(\alpha_H - 1)}e^{-y}}{\Gamma(\alpha_H)}\right\}$$

electromagnetic part

hadronic part

$$x \equiv \beta_E \frac{(S - S_0)}{\chi_0}$$

radiation length

$$y \equiv \beta_H \frac{(S - S_0)}{\lambda}$$

interaction length

$$\alpha_H = \alpha_E = 0.62 + 0.32 \ln E$$

$$\beta_H = 0.91 - 0.02 \ln E$$

$$\beta_E = 0.22$$

$$C = 0.46$$

$S_0 \neq 0$ - significant amount of material in front of calorimeter (magnet coil etc.)

More Rules of Thumb for the Hobbyist

- Shower maximum

$$t_{\max}(\lambda) \sim 0.2 \ln E(GeV) + 0.7$$

- 95% Longitudinal containment

$$L_{95\%}(\lambda) \sim t_{\max} + 2.5\lambda_{ATT}$$

$$\lambda_{ATT} \approx \lambda\left[E(GeV)\right]^{0.13}$$

- 95% Lateral containment

$$R_{95\%} \sim 1\lambda$$

- Mixtures in sampling calorimeters

active + passive material

$$\frac{1}{\chi_{eff}} = \sum_i \frac{f_i}{\chi_0^i}$$

FRACTION BY WEIGHT.

$$f_{act} = \frac{m_{act}}{m_{act} + m_{pass}}$$

$$\frac{\varepsilon_{eff}^{crit}}{\chi_{eff}} = \sum_i f_i \frac{\varepsilon_i^{crit}}{\chi_0^i}$$

$$\frac{E_{vis}}{E_{inc}} = f_{act} \frac{\varepsilon_{act}^{crit} / \chi_0^{act}}{\varepsilon_{eff}^{crit} / \chi_{eff}}$$

Typical Calorimeter Resolutions

- Homogeneous EM (crystal, glass)

$$\frac{0.5\%}{\sqrt{E}} \rightarrow \frac{3.0\%}{\sqrt{E}} \oplus 0.5\%$$

CLEO, Crystal Ball, Belle, CMS.....

- Sampling EM (Pb/Scint, Pb/LAr)

$$\frac{8\%}{\sqrt{E}} \rightarrow \frac{15\%}{\sqrt{E}} \oplus 1\%$$

CDF, ZEUS, ALEPH, ATLAS.....

- Non-compensating HAD (Fe/Scint, Fe/LAr)

$$\frac{70\%}{\sqrt{E}} \rightarrow \frac{110\%}{\sqrt{E}} \oplus 5\%$$

CDF,ATLAS,H1, LEP = everyone

- Compensating HAD (DU/Scint)

$$\frac{35\%}{\sqrt{E}} \oplus 1\%$$

ZEUS, HELIOS

Invisible Energy in Hadronic Showers

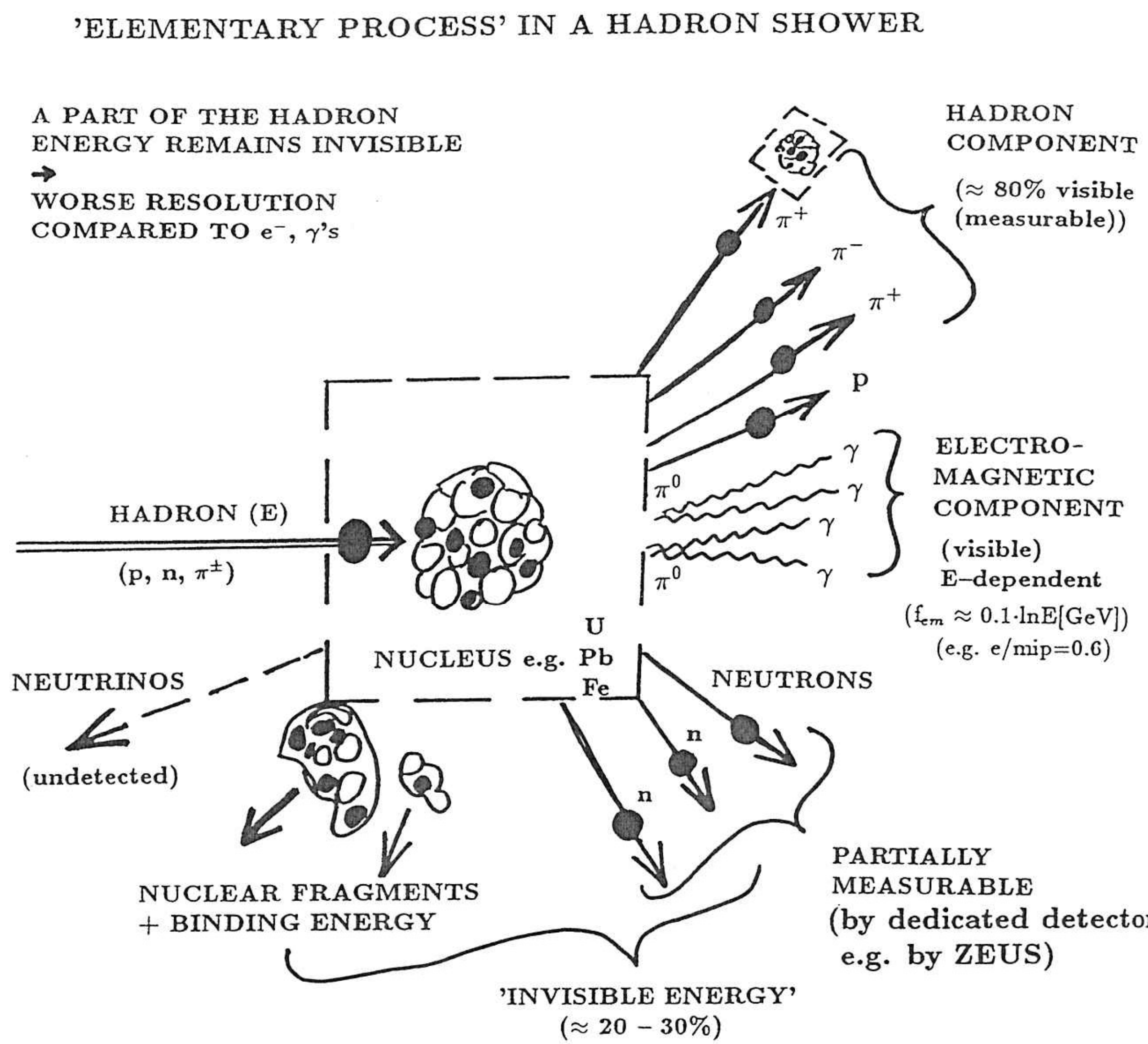

Fig. 3.6 'Elementary physical process' in a hadron shower.

Difference in Response to Electrons and Hadrons

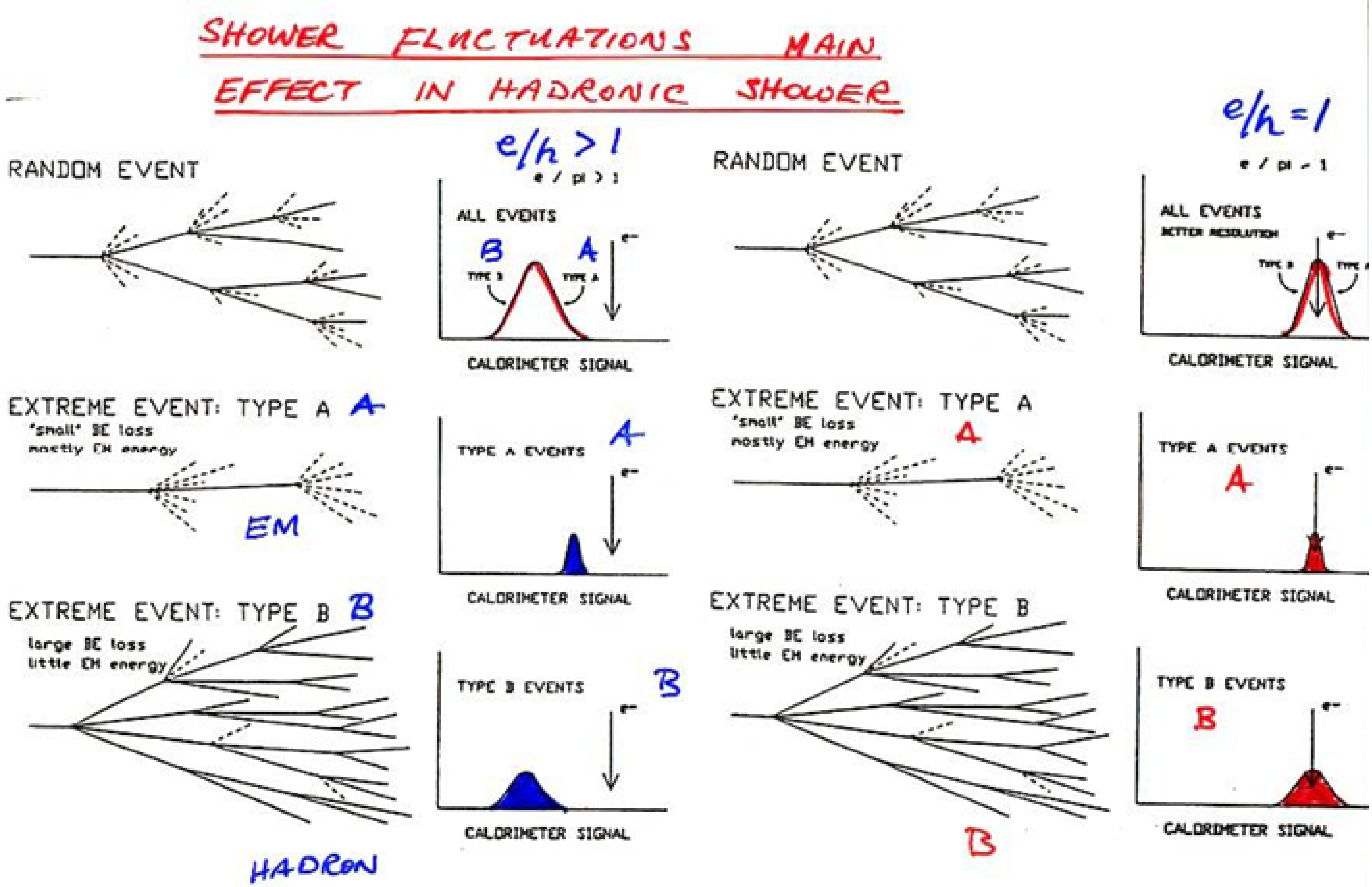

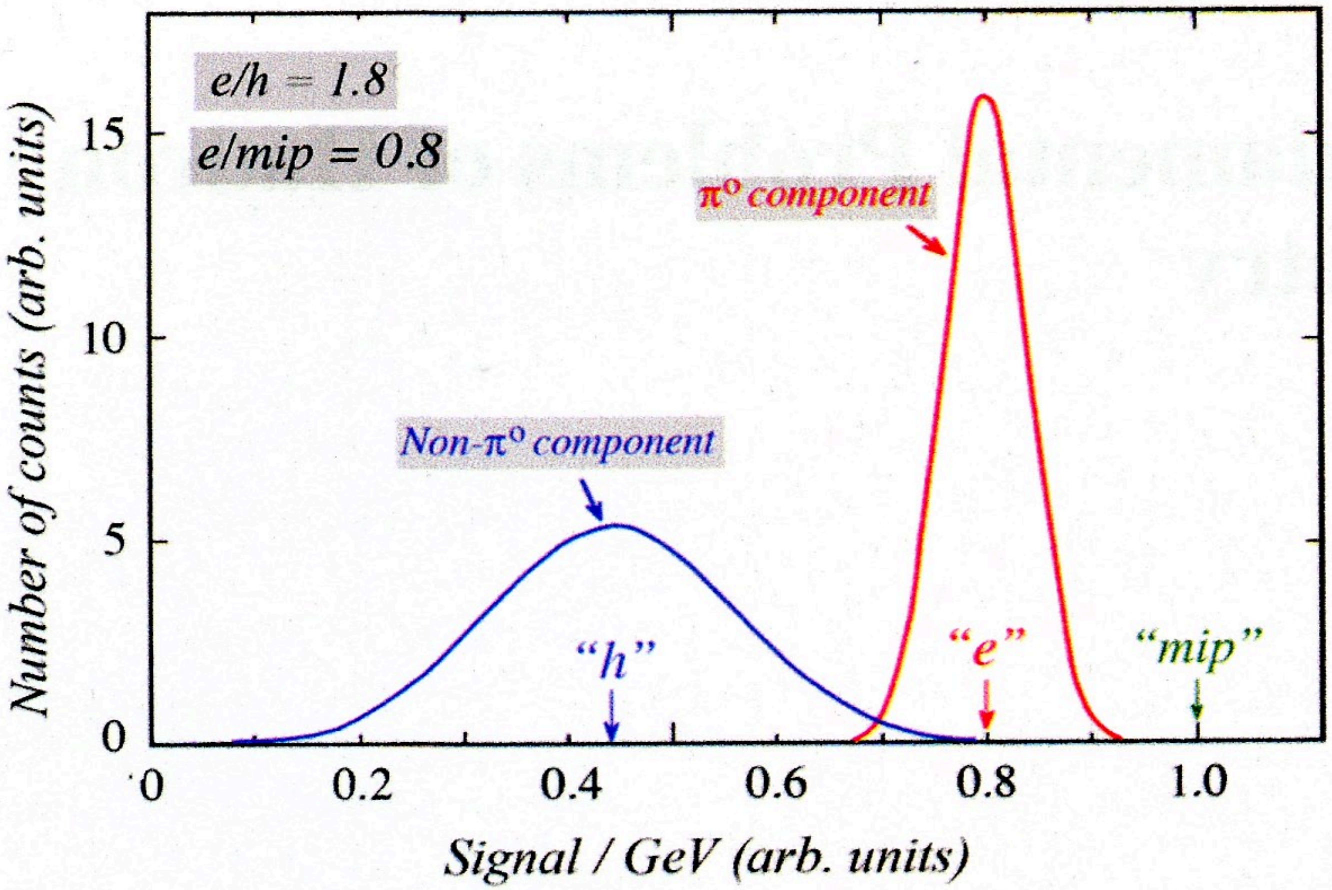

Fig. 7.1 Illustration of the meaning of the e/h and e/mip values of a calorimeter. Shown are distributions of the signal per unit deposited energy for the electromagnetic and non-em components of hadron showers. These distributions are normalized to the response for minimum ionizing particles ("mip"). The average values of the em and non-em distributions are the em response ("e") and non-em response ("h"), respectively [1]

The em shower fraction, f_{em} (1)

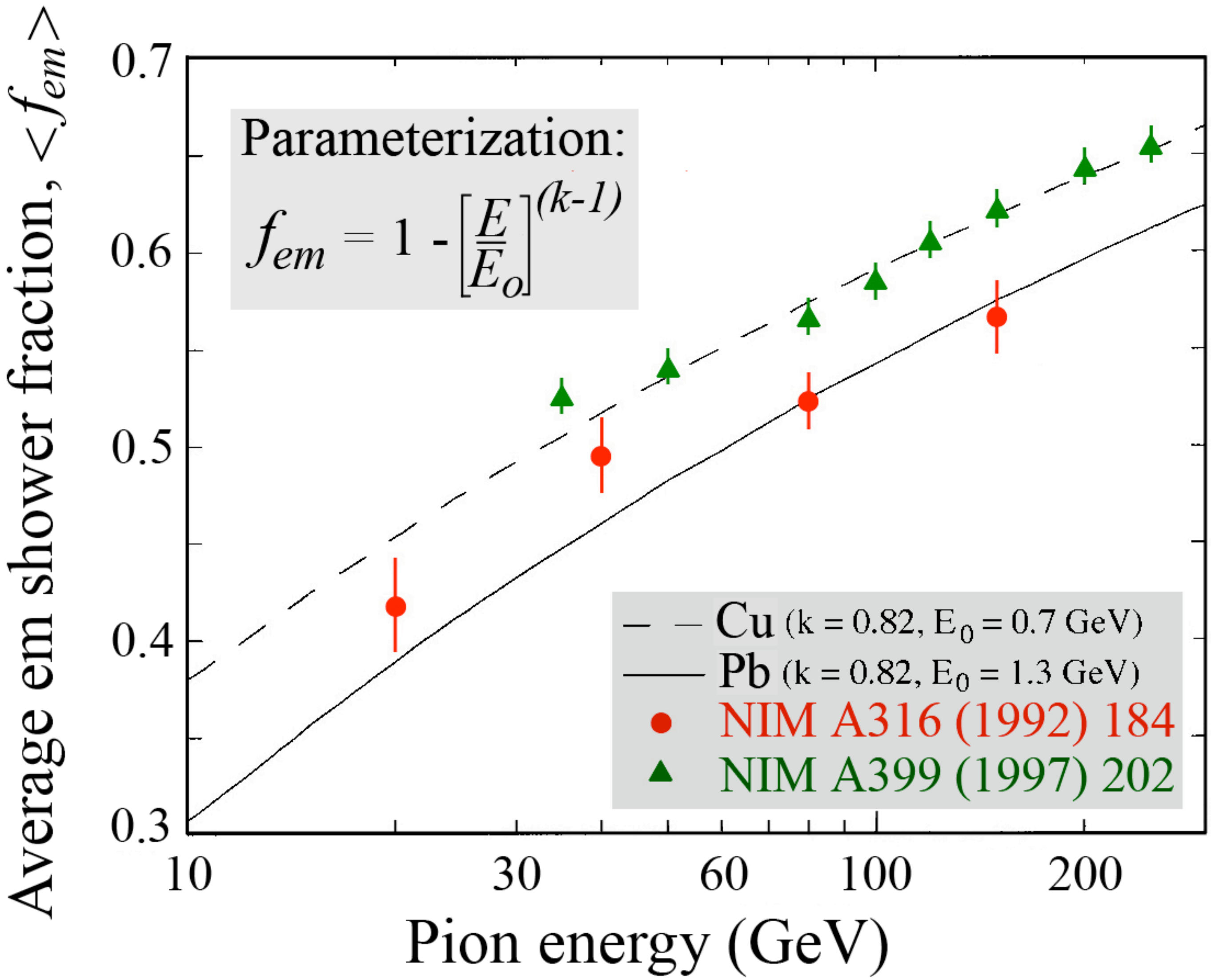

<f_{em}> is *large, energy dependent* and *material dependent*

The em shower fraction, f_{em} (2)

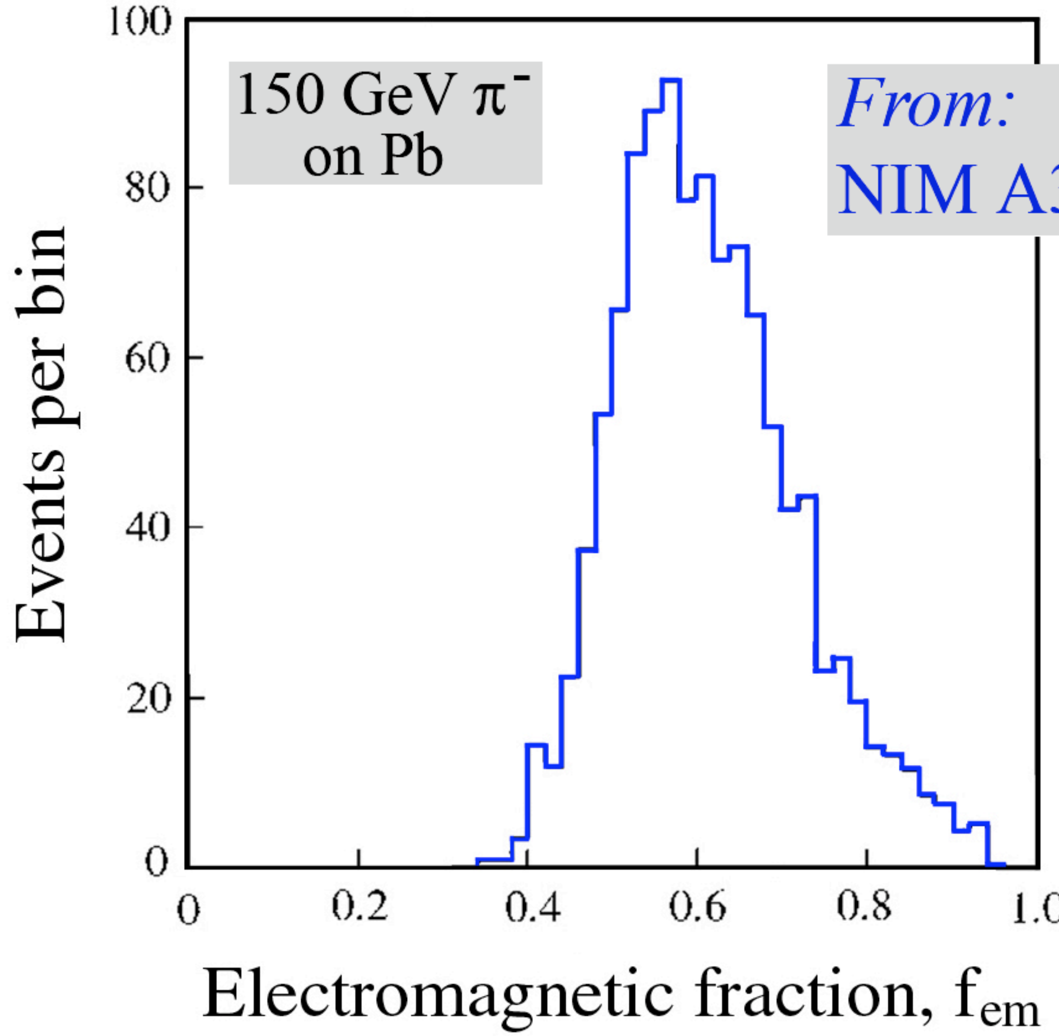

From:
NIM A316 (2002) 184

Fluctuations in f_{em} are *large and non-Poissonian*

The em shower fraction, f_{em} (4)

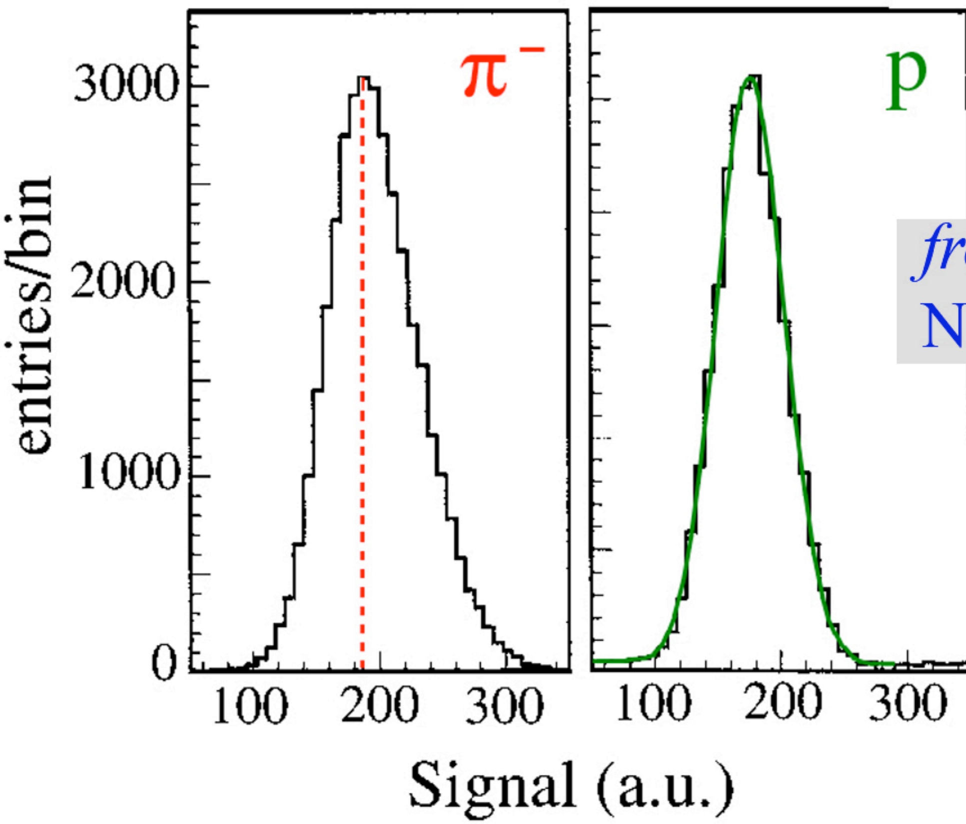

300 GeV showers in Cu

from:
NIM A408 (1998) 380

f_{em} fluctuations are different in π- and *p*-induced showers

Calibration problems for hadronic shower detection

π^o production may take place anywhere in the absorber

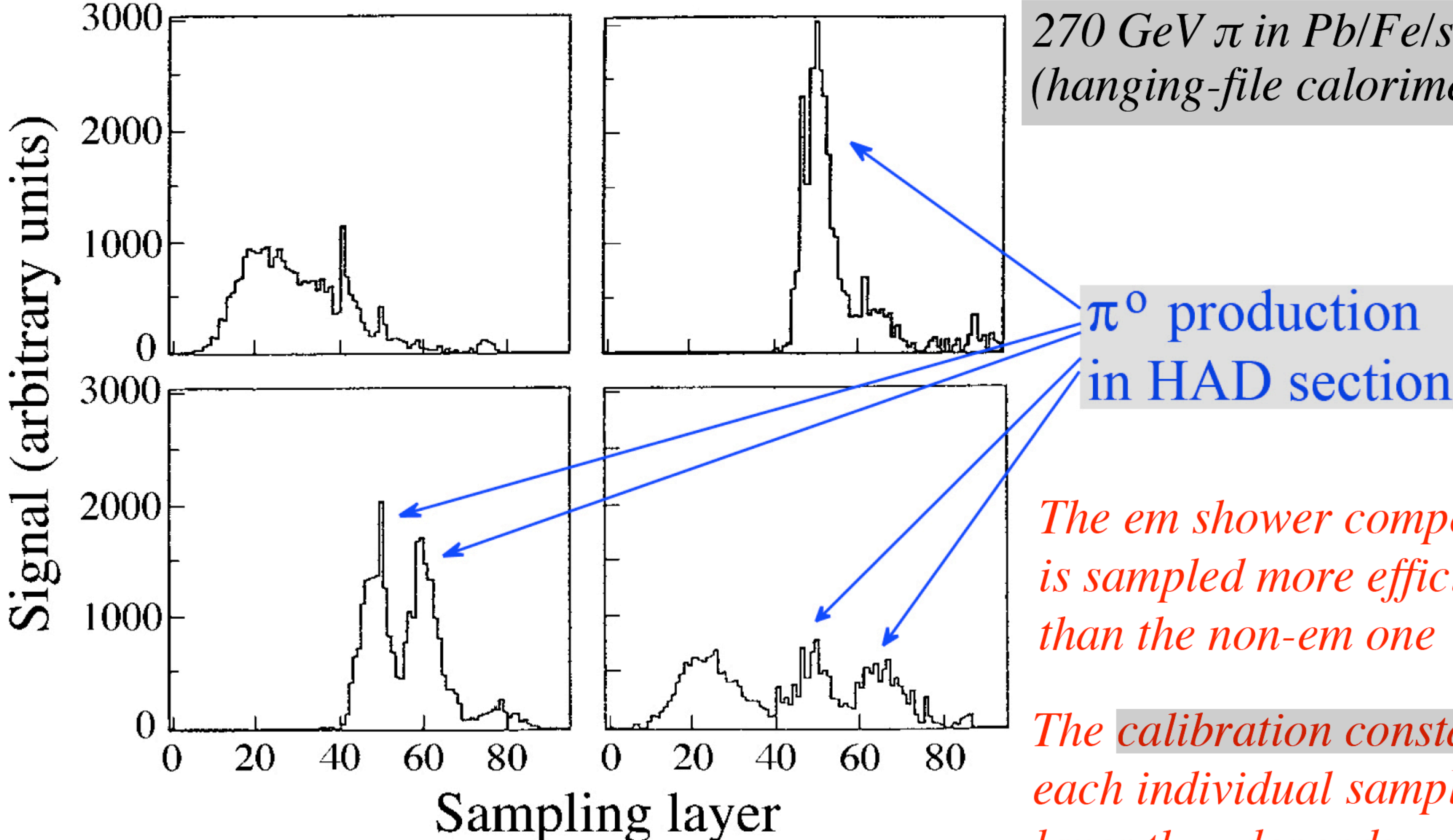

- depth (0-6 λ)→

270 GeV π in Pb/Fe/scint.
(hanging-file calorimeter)

The em shower component is sampled more efficiently than the non-em one

The calibration constant of each individual sampling layer thus depends on the type of event.

Hadronic shower response and the *e/h* ratio

- *The hadronic response is **not constant***

  $f_{\rm em}$, and therefore e/π signal ratio is a function of energy

  ➡ If calorimeter is linear for electrons, it is *non-linear* for hadrons

- Energy-independent way to characterize hadron calorimeters: *e/h*

  $e =$ response to the em shower component

  $h =$ response to the non-em shower component

  $\rightarrow$ Response to showers initiated by pions:

$$R_\pi = f_{\rm em}\, e \; + \; \left[1 - f_{\rm em}\right] h \quad \rightarrow \quad \boxed{e/\pi = \frac{e/h}{1 - f_{\rm em}\left[1 - e/h\right]}}$$

  e/h is inferred from e/π measured at several energies ($f_{\rm em}$ values)

- Calorimeters can be *Undercompensating* ($e/h > 1$)

  Overcompensating ($e/h < 1$)

  Compensating ($e/h = 1$)

Hadron showers: e/h and the e/π signal ratio

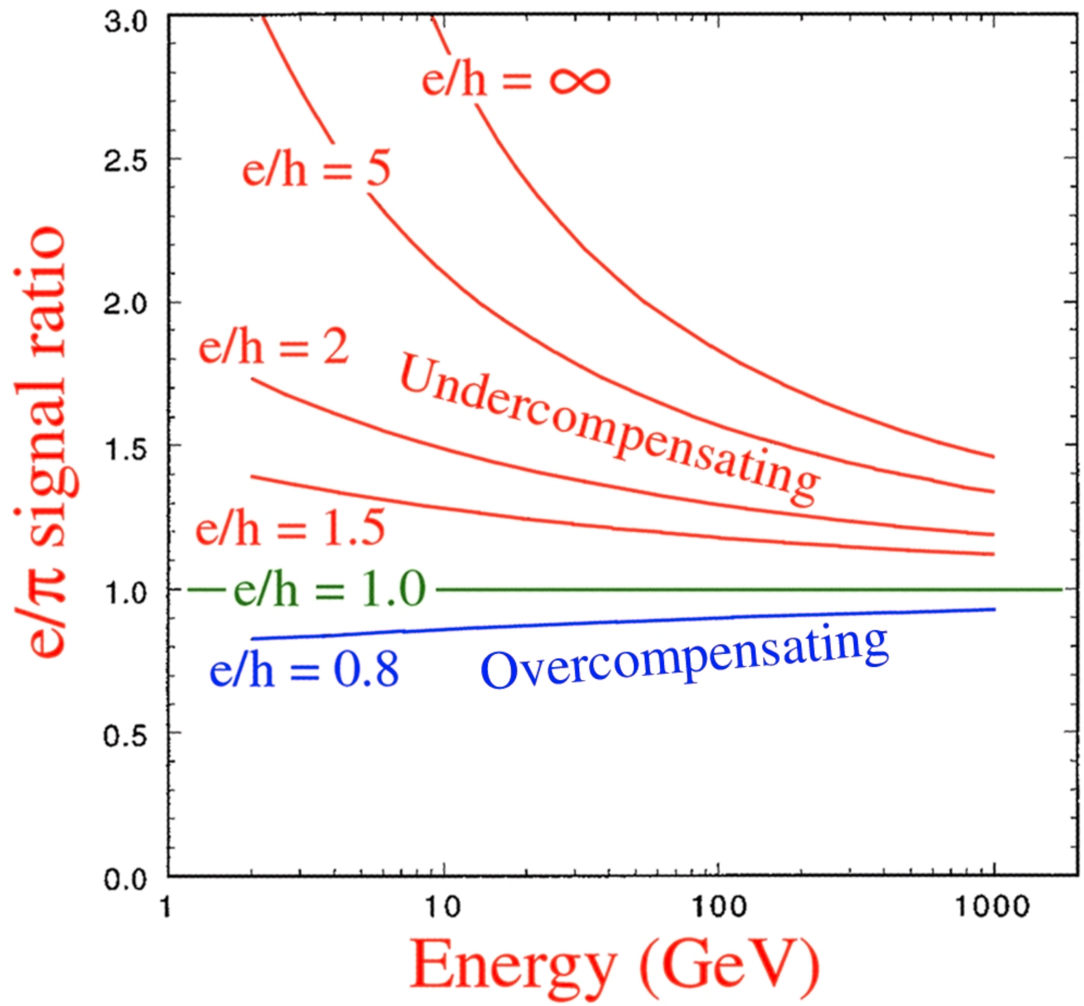

FIG. 3.4. The relation between the calorimeter response ratio to em and non-em energy deposition, e/h, and the measured e/π signal ratios. See text for details.

Effect of e/h on Energy Resolution

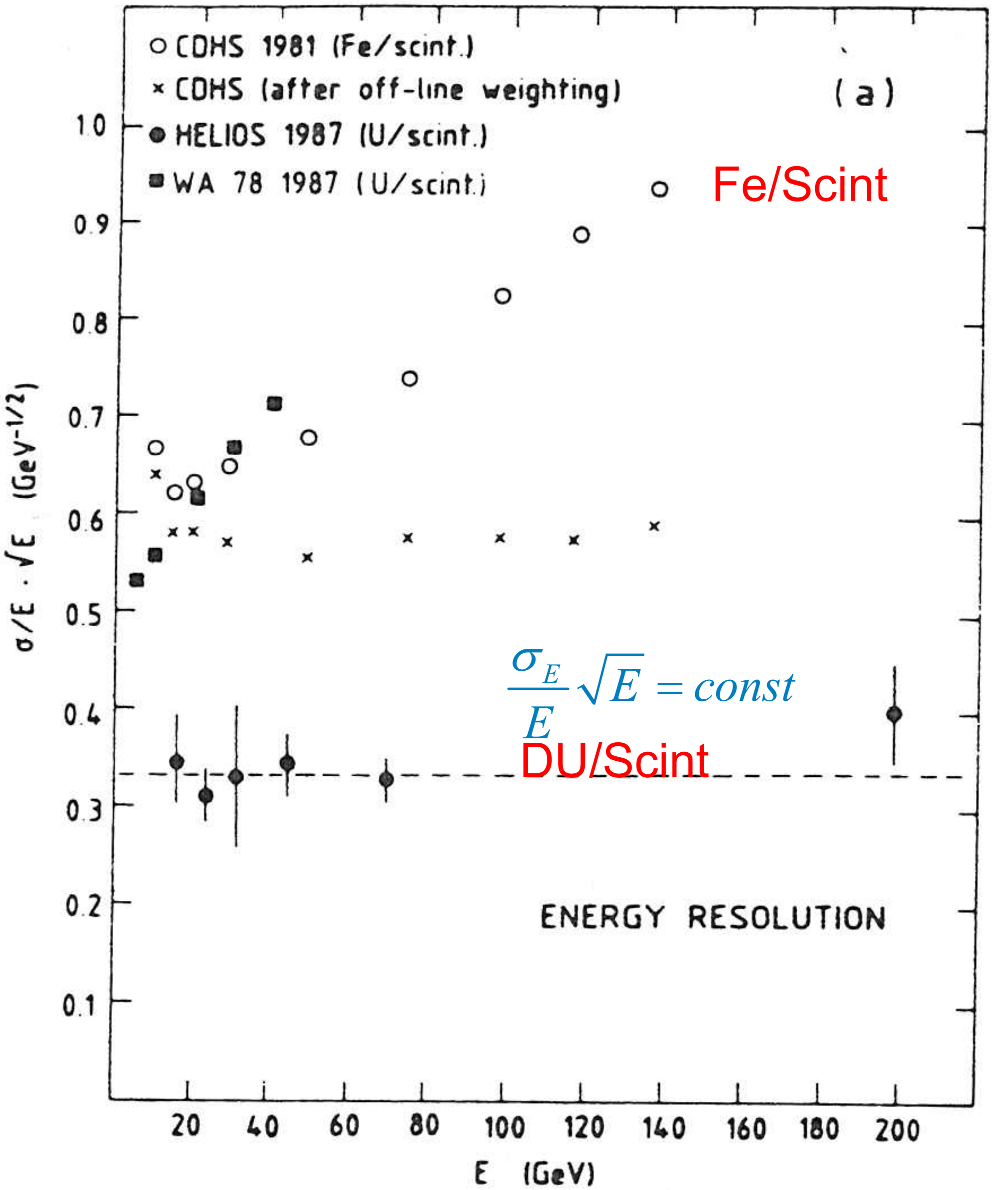

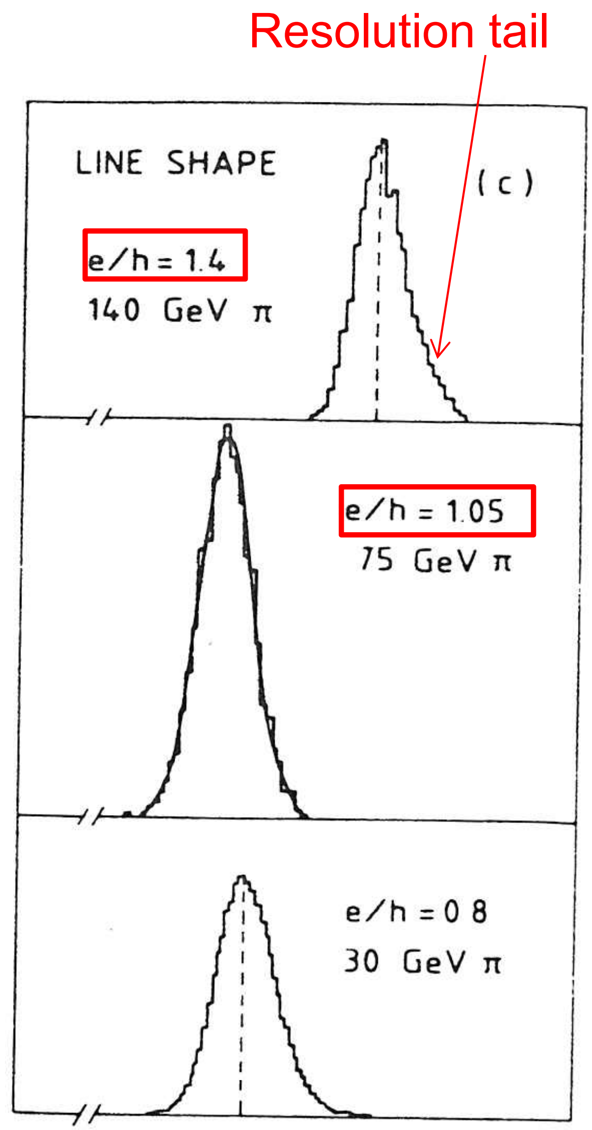

Effect of e/h on Linearity

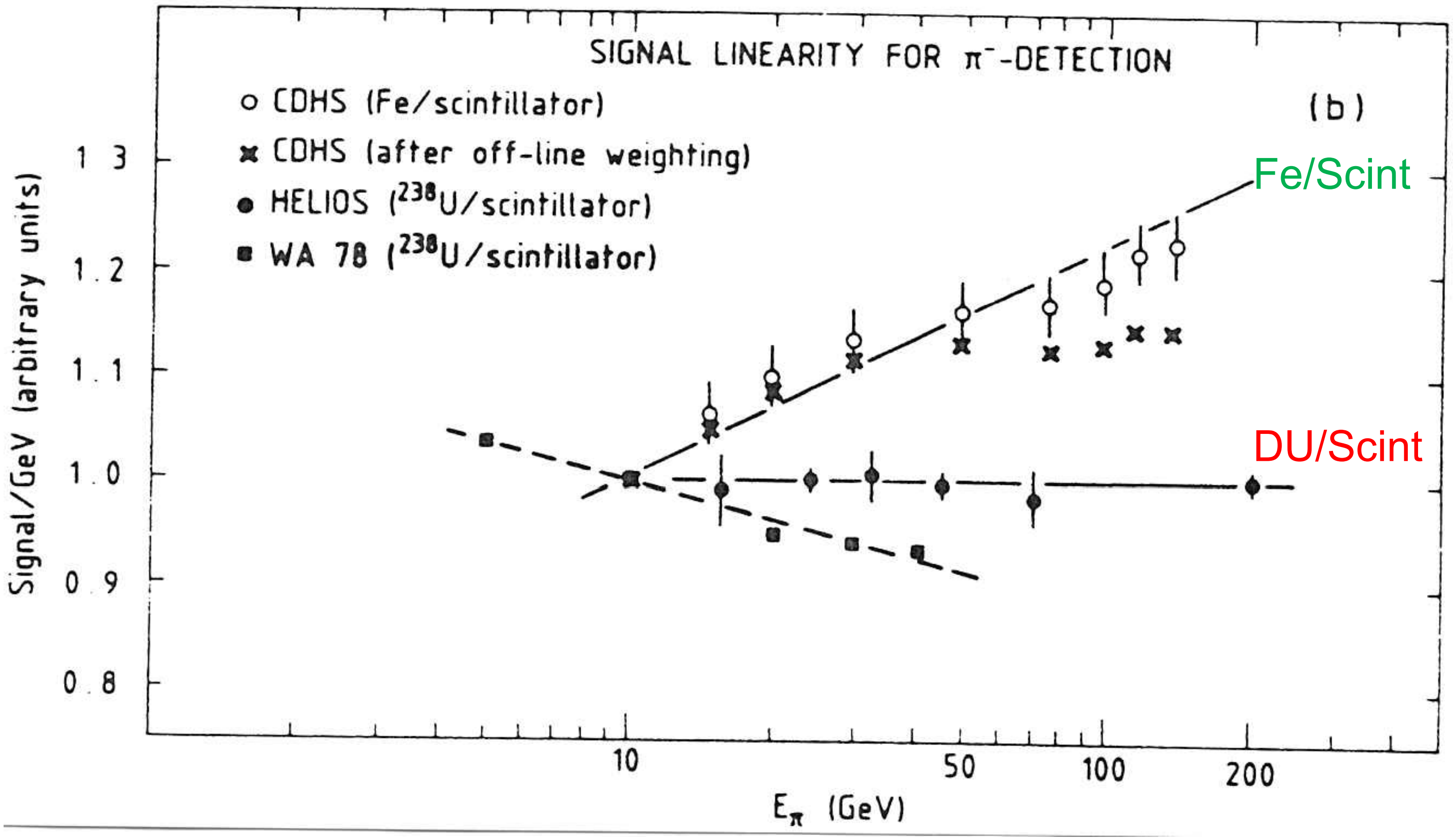

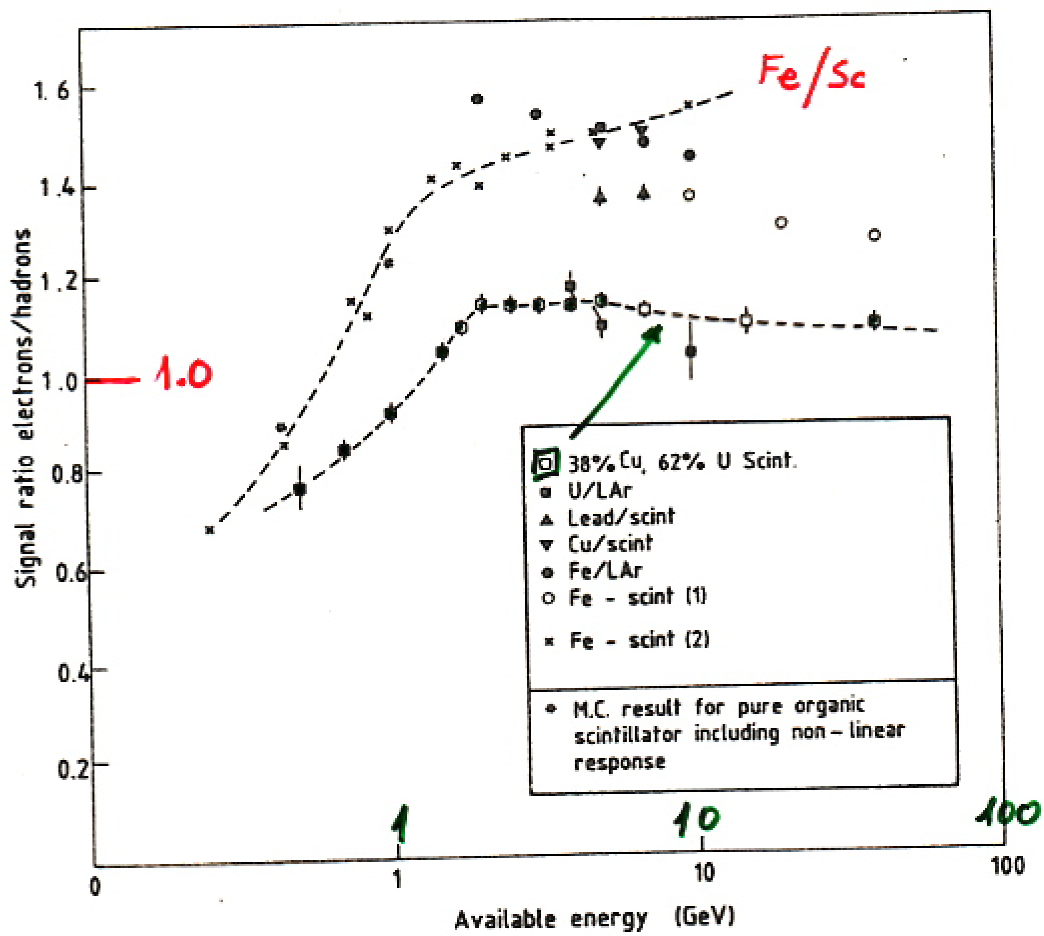

LINEARITY IN Cu / Scint / U

HELIOS ⇒ FIRST COMPENSATING CALORIMETER

Pb / Scint   Du / Scint

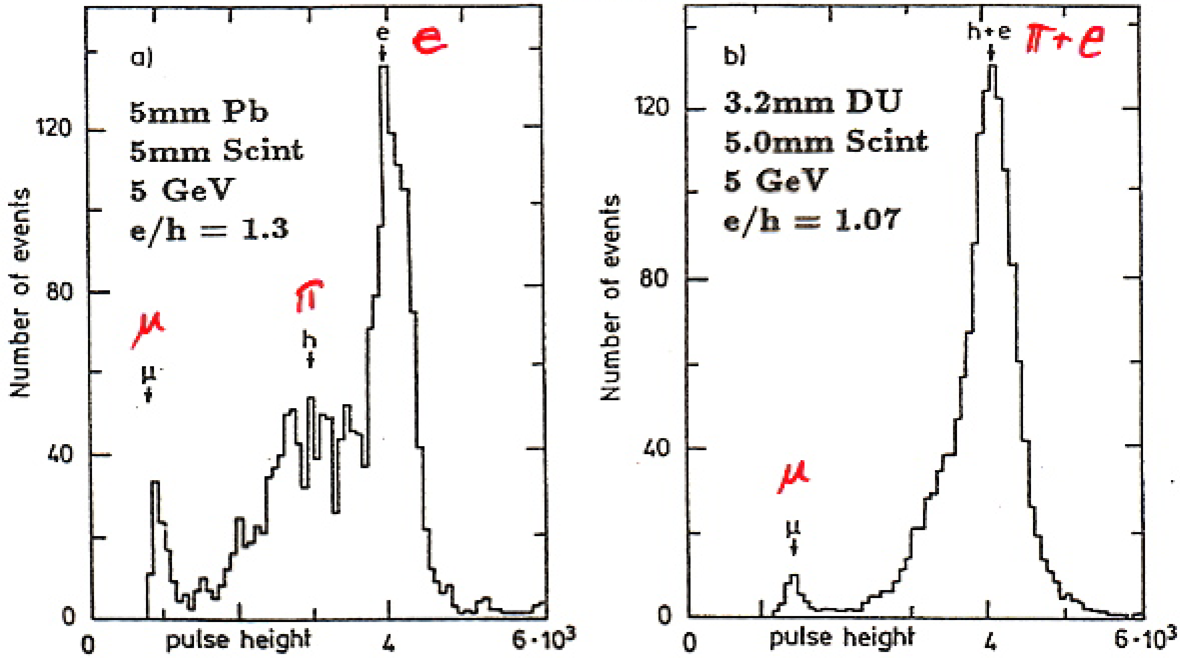

3.14 Pulse height distributions of 5 GeV electrons, hadrons and muons measured with a lead scintillator (5mm Pb, 5mm Scint) calorimeter (a), and a depleted–uranium scintillator (3.2mm DU, 5mm Scint) calorimeter (b) (ZEUS).

- DEMONSTRATION OF $e/h = 1$ FOR ZEUS DU / Scint

- NB ph → ENERGY CALIBRATED BY μ line

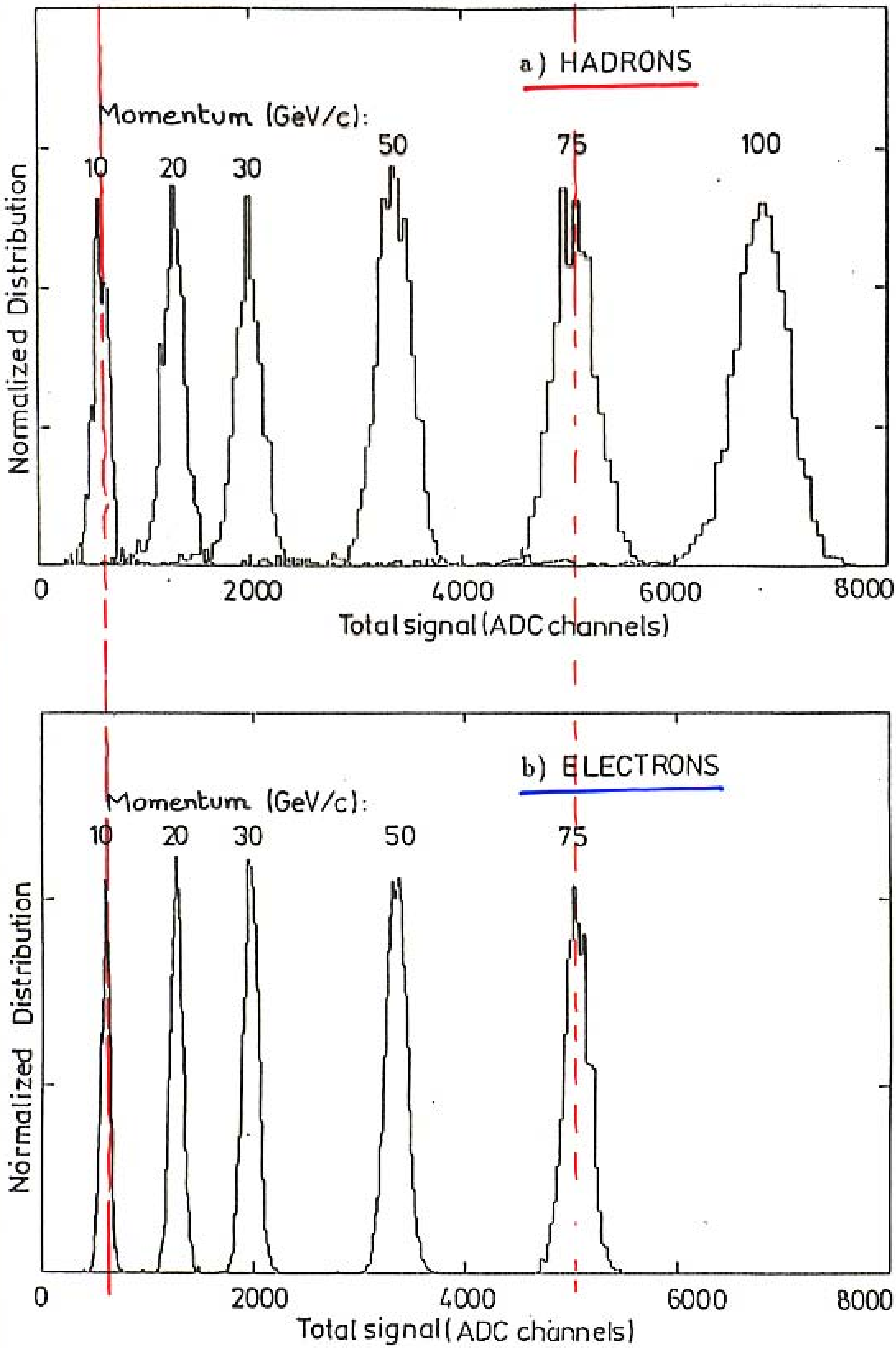

$$\frac{\sigma_E}{E} = \frac{35\%}{\sqrt{E}}$$

FOR HADRONS

$$\frac{e}{h} = 1 \pm .02$$

2 - 100 Ge

$$\frac{\sigma_E}{E} = \frac{18\%}{\sqrt{E}}$$

FOR ELECTRON

14.27 a) Hadron and b) electron energy distributions measured at the SPS, 10 - 100

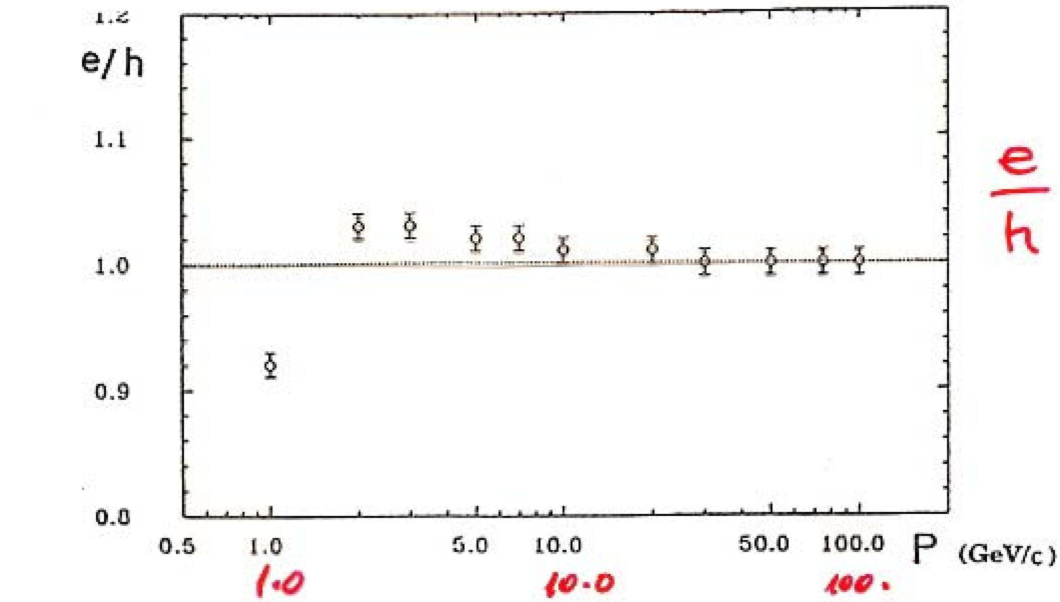

Fig. 3.26 The e/h-ratio versus beam momentum measured with the ZEUS prototype calorimeter at CERN.

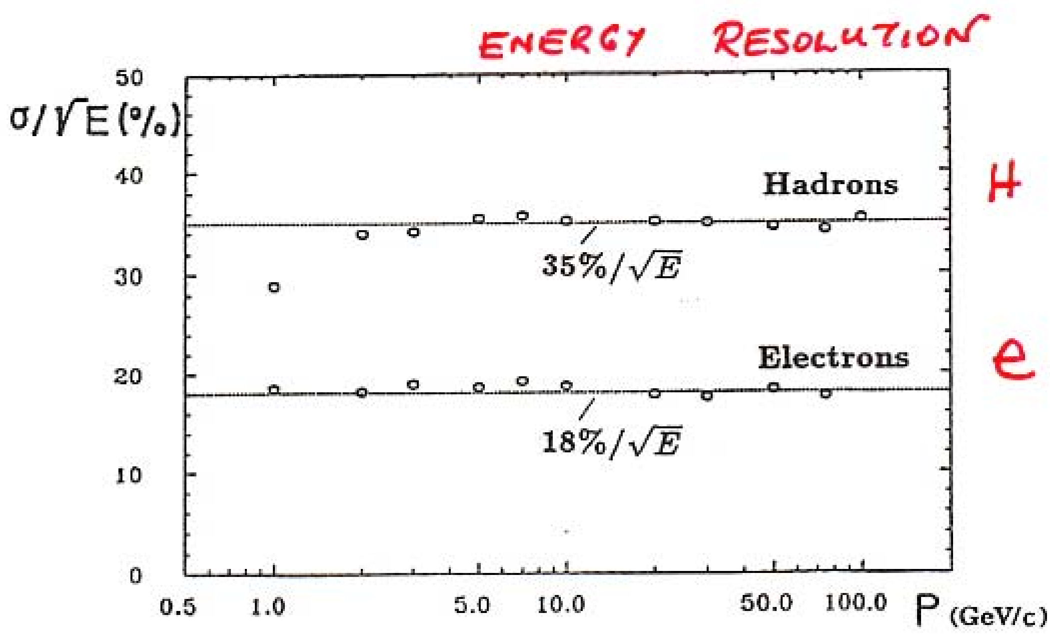

Fig. 3.27 The energy resolution versus beam momentum for electrons and hadrons measured with the ZEUS prototype calorimeter at CERN.

Physics of Sampling Calorimetry

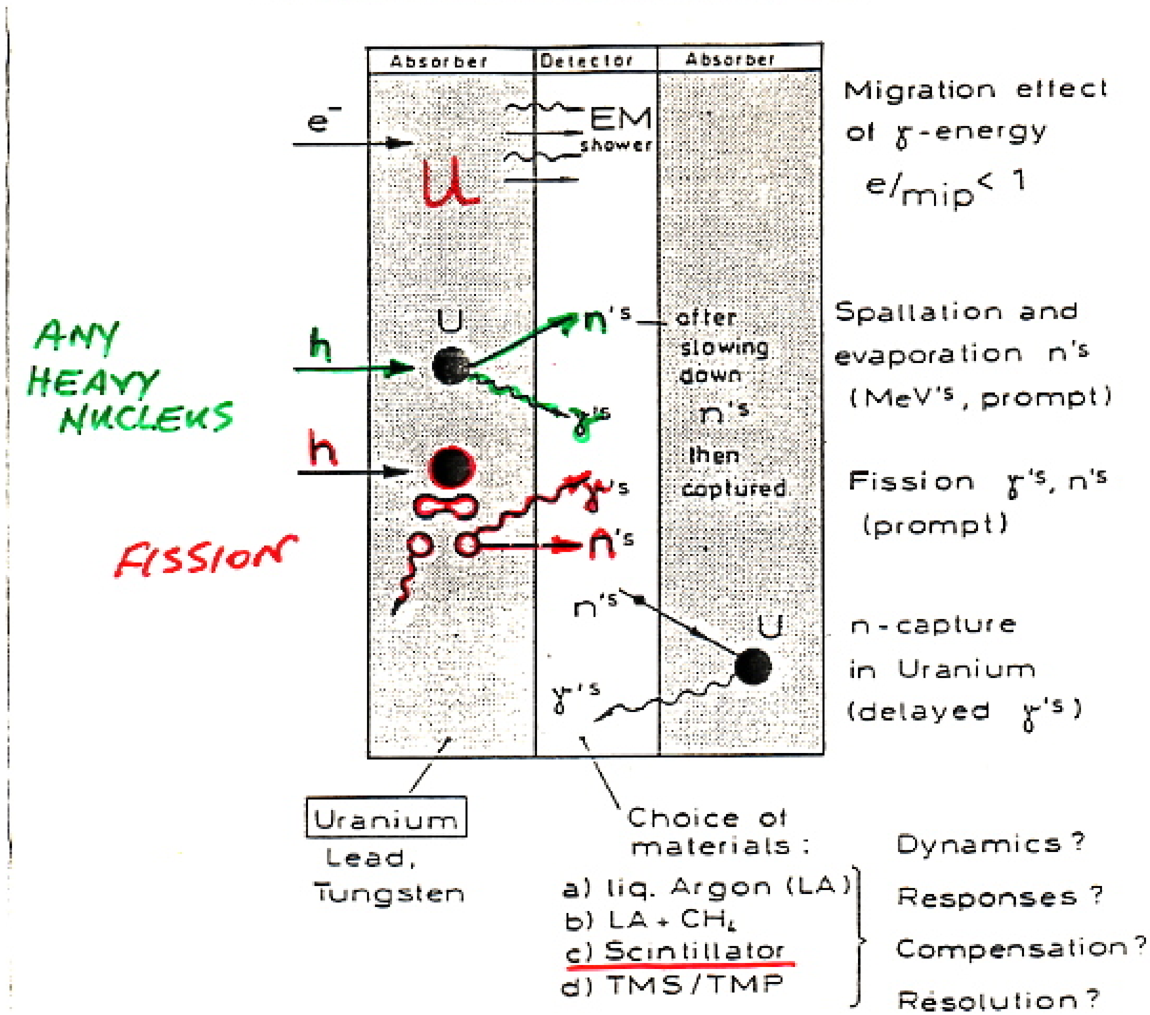

- BOOST HADRONIC RESPONSE

URANIUM → γ, n

The compensation puzzle solved!

The e/h value is not determined by the absorber, but by active medium

and in particular by its H-content!

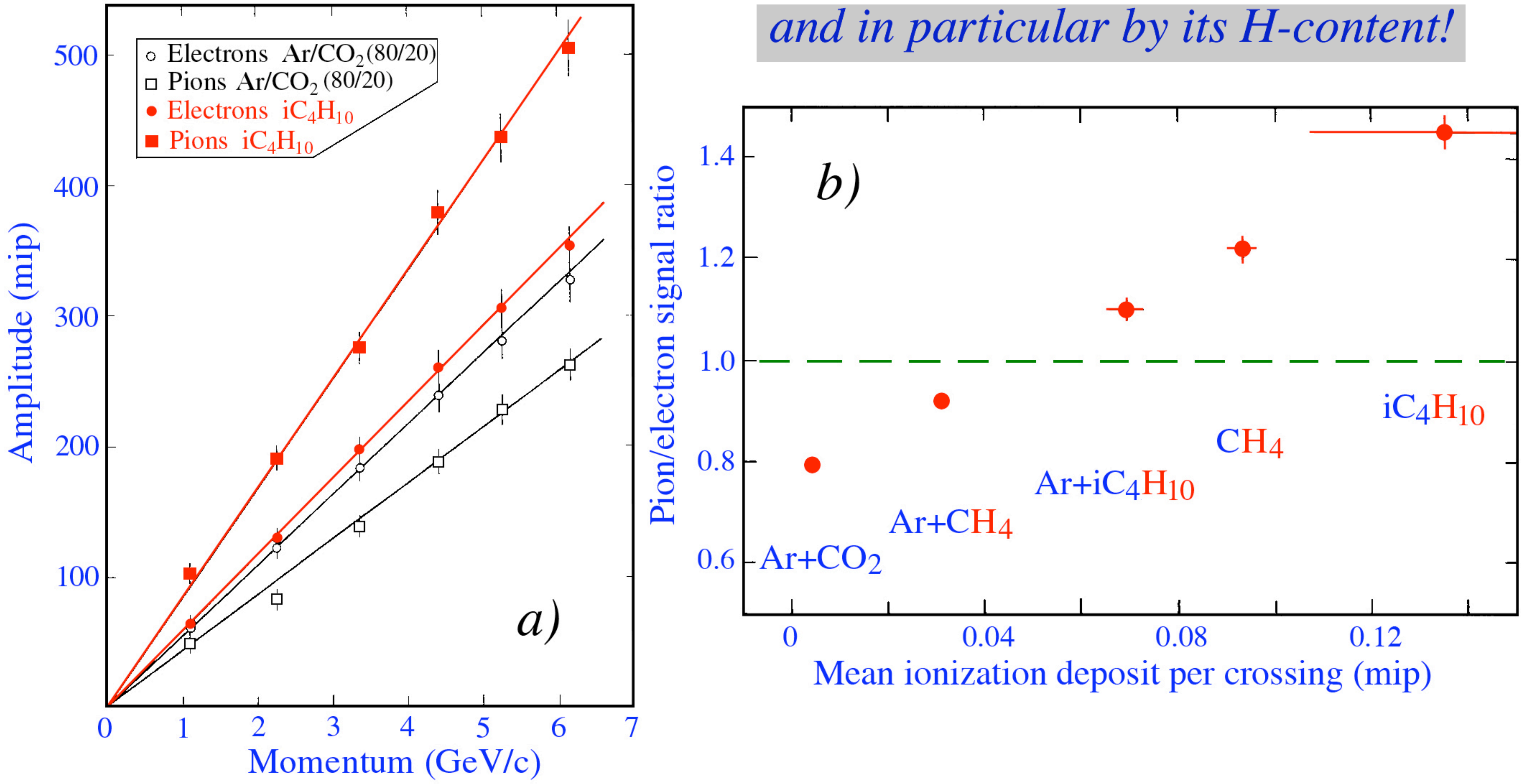

Compensation in practice: Pb/scintillator calorimeters

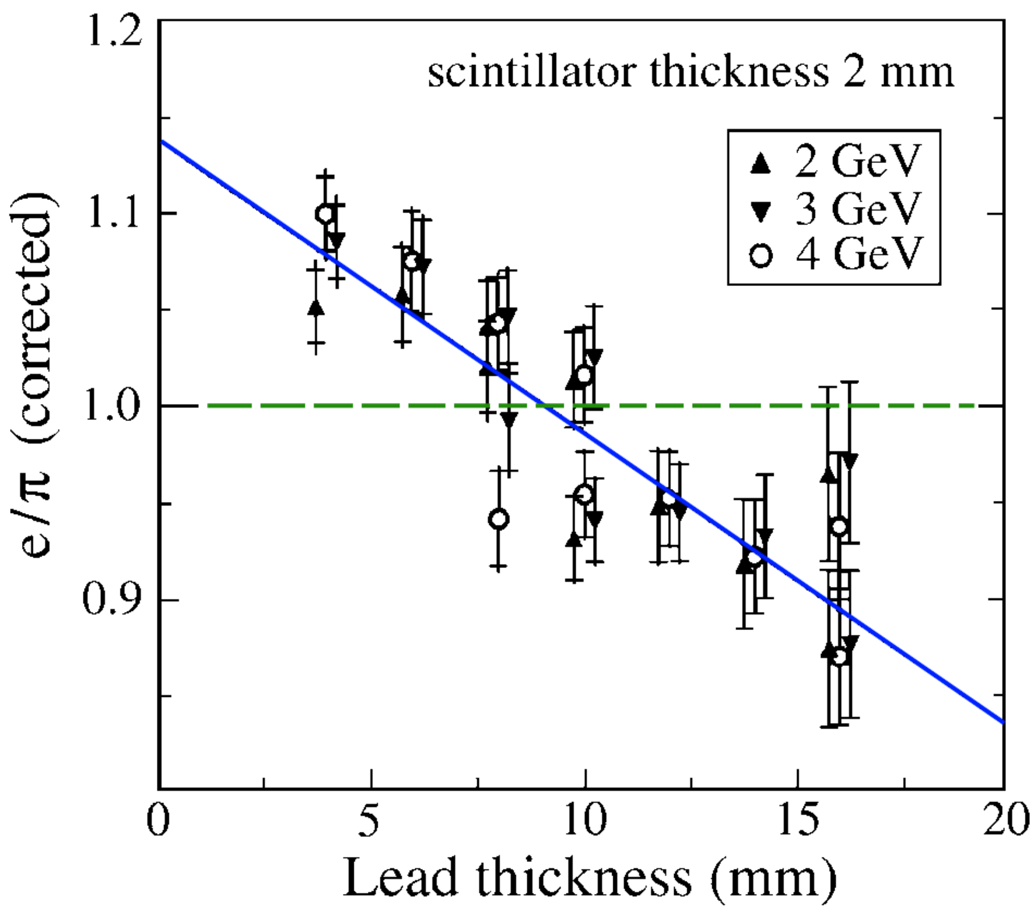

FIG. 3.35. The e/π signal ratio, corrected for the effects of shower leakage, for lead/polystyrene-scintillator calorimeters, as a function of the thickness of the lead plates, for 2 mm thick scintillator plates. The inner (outer) error bars show the combined systematic and statistical uncertainty without (with) the shower leakage corrections. The line in the plot is a result of a linear fit to the experimental data [Suz 99].

Compensation in Fe/scintillator calorimeters?

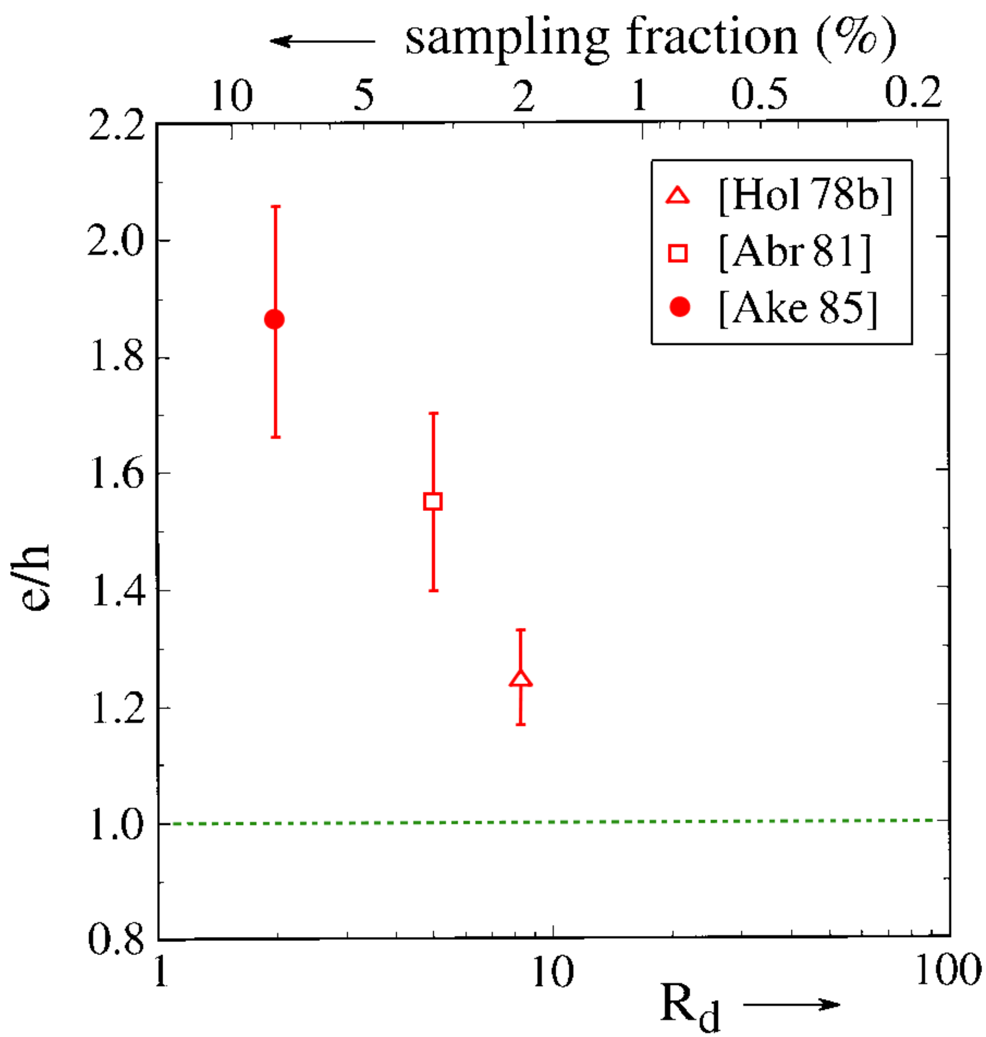

FIG. 3.36. The e/h value for iron/plastic-scintillator calorimeters, as a function of the sampling fraction for mips (top horizontal scale), or the volume ratio of the amounts of passive and active material (bottom horizontal scale).

Compensation: Effect of slow neutrons on the signals

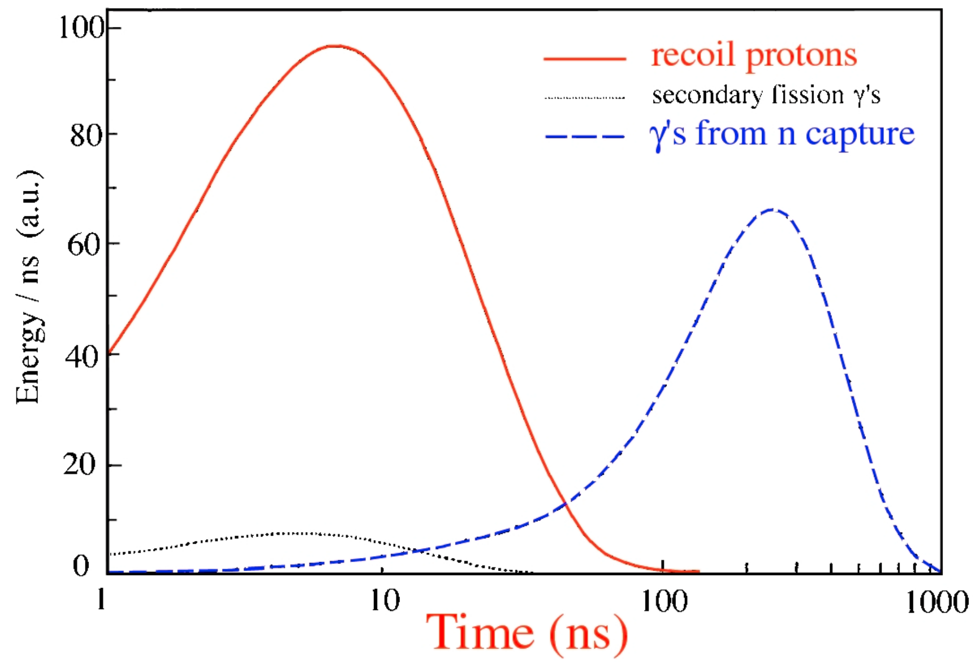

FIG. 3.22. Time structure of various contributions from neutron-induced processes to the hadronic signals of the ZEUS uranium/plastic-scintillator calorimeter [Bru 88].

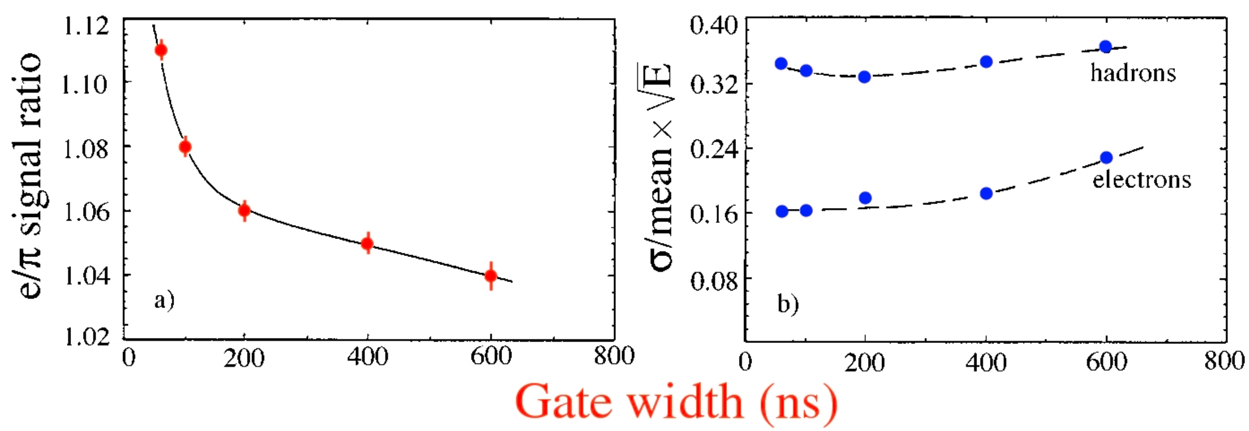

FIG. 3.23. The ratio of the average ZEUS calorimeter signals from 5 GeV/c electrons and pions (a) and the energy resolutions for detecting these particles (b), as a function of the charge integration time [Kru 92].

Weighting to Correct for e/h

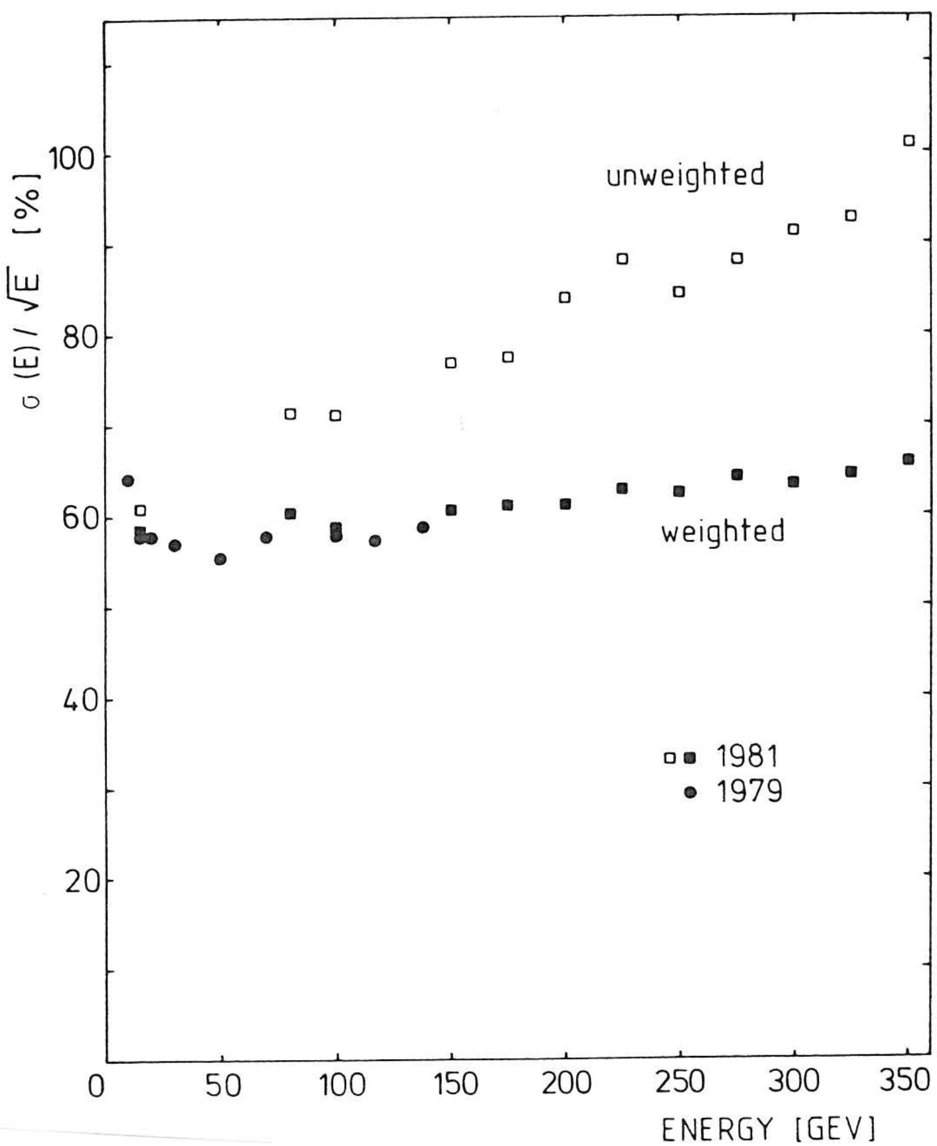

Energy resolution does not improve

$$\frac{1}{\sqrt{E}} \quad \frac{e}{h} \neq 1$$

$$\frac{e}{h} > 1$$

Weight down EM part of shower

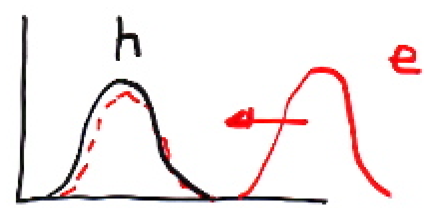

$$E_k^{'} = E_k \left(1 - c \cdot E_k\right)$$

tune

Jet Energy Resolution

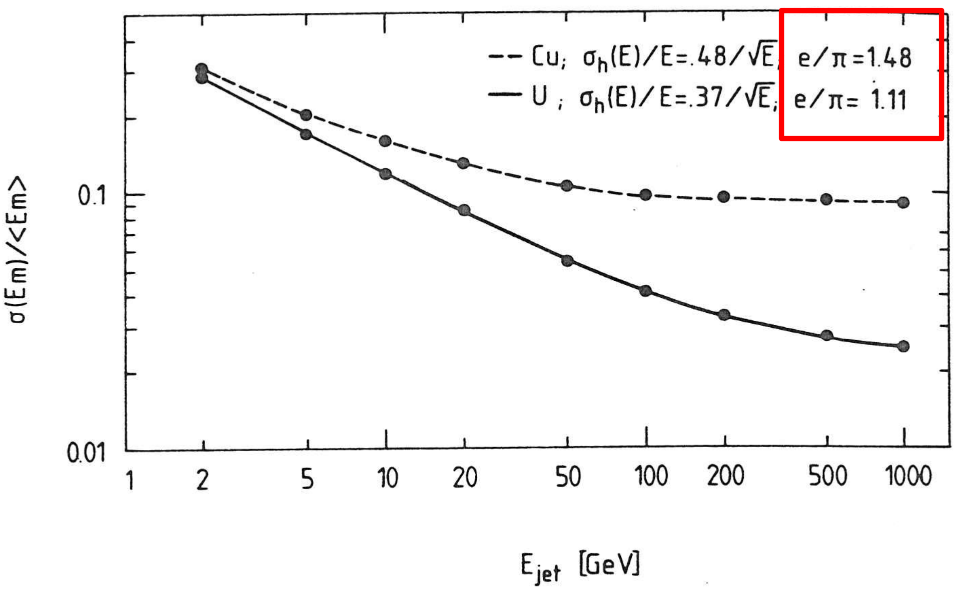

Fluctuations between EM and Hadronic component in jets will degrade the energy resolution for jets

Jet-jet Mass Resolution

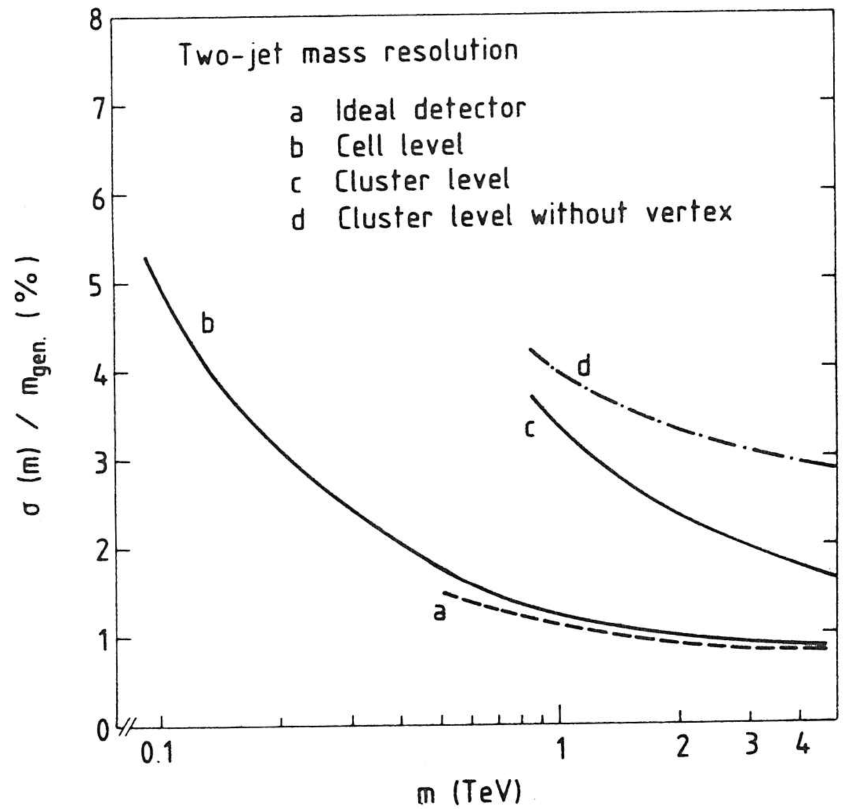

Effects other than e/h dominate the 2-jet mass resoluton

TYPICAL JET-JET MASS RESOLUTIONS

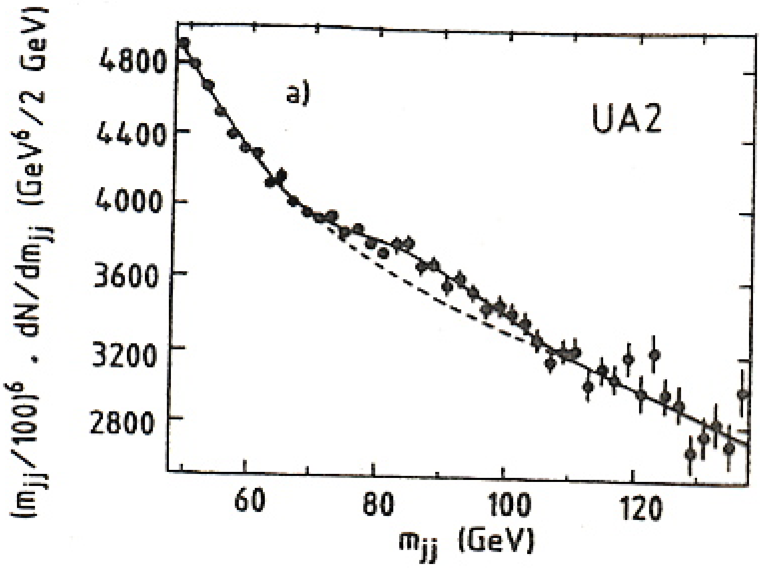

DISCOVERY OF W

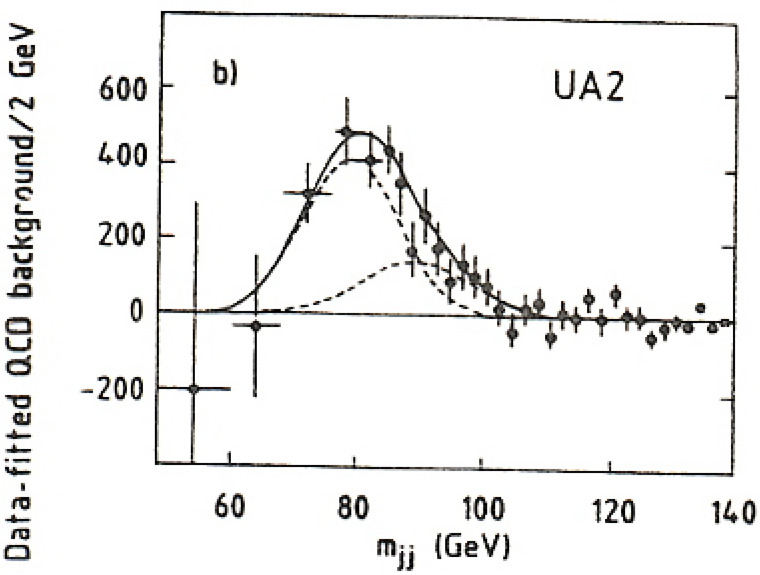

eg CLUSTERING

TURNS OUT THAT INSTRUMENTAL EFFECTS OTHER THAN $\frac{\sigma_E}{E}$ DOMINATE

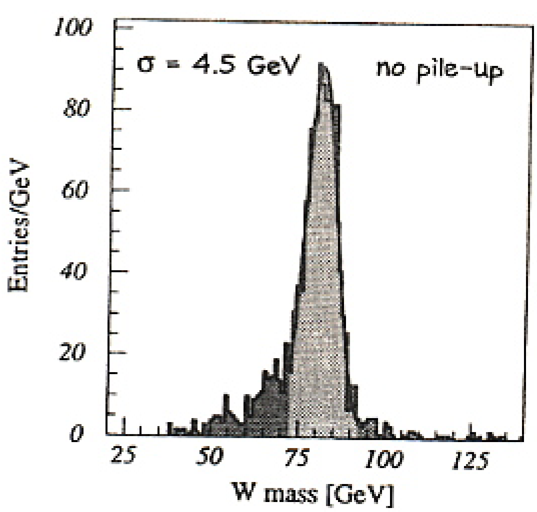

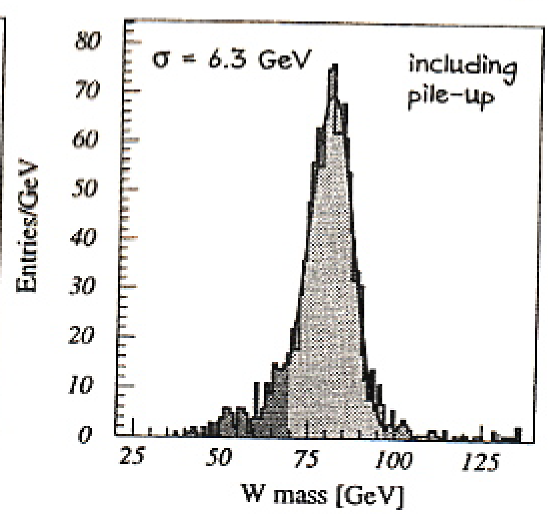

ATLAS

NON COMPENSATING

Jet-Jet Mass Resolutions

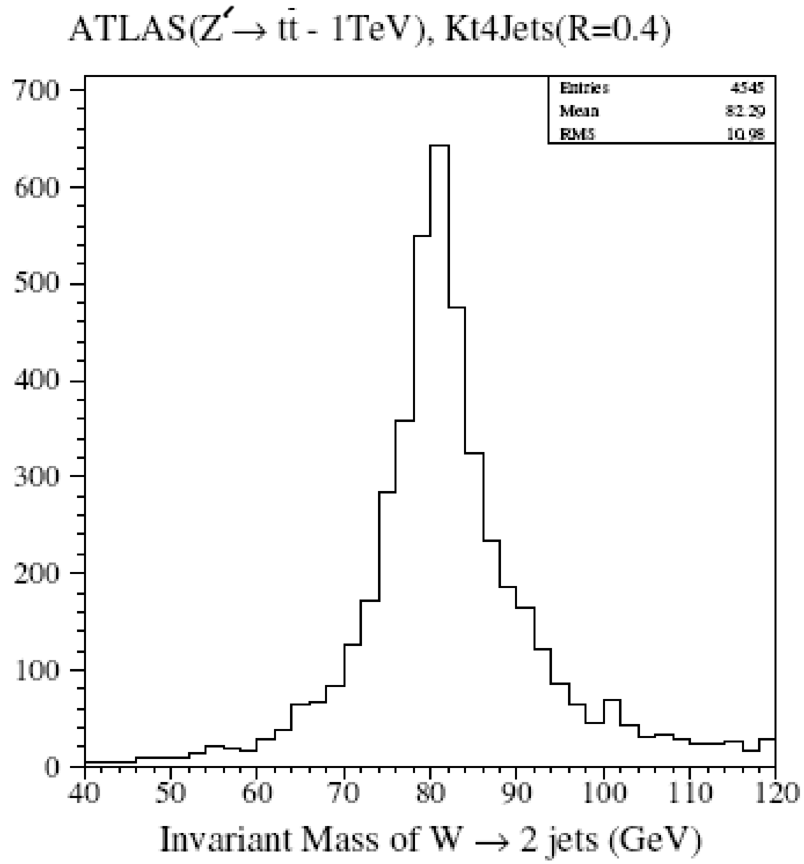

MONTE CARLO

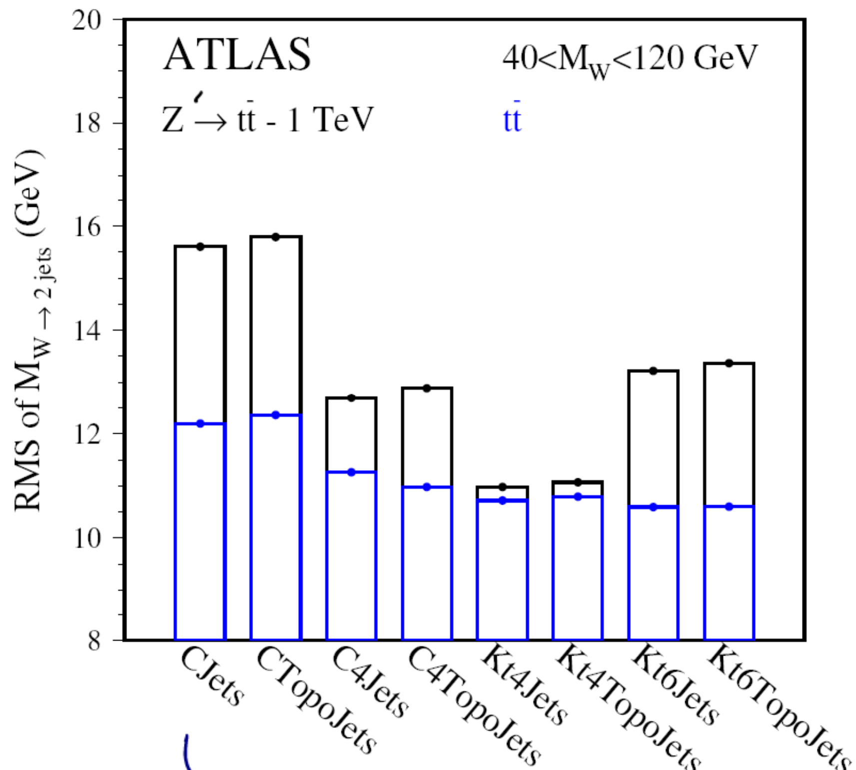

JET ALGORITHMS

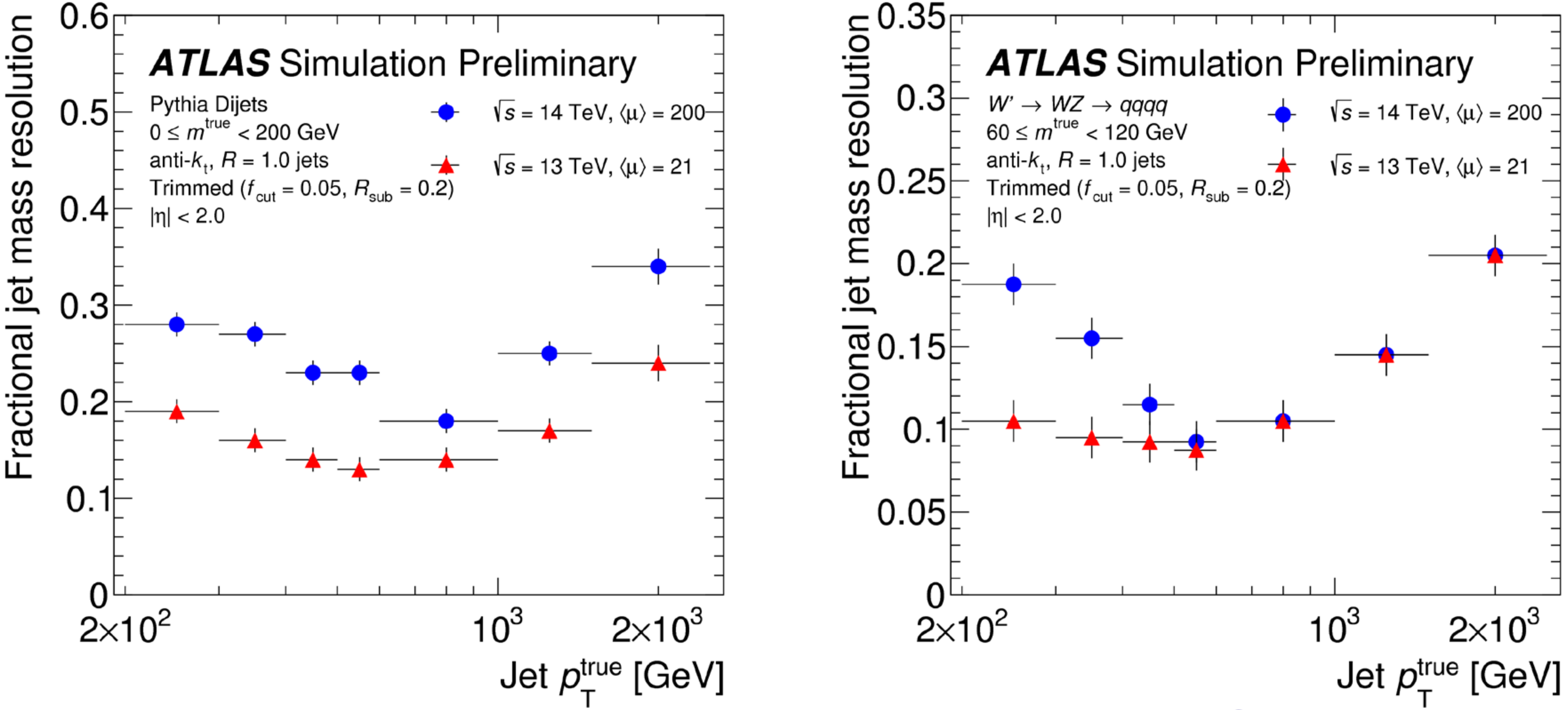

RECONSTRUCT SINGLE JET MASS FROM JET AREA → IMPORTANT FOR HIGH BOOST

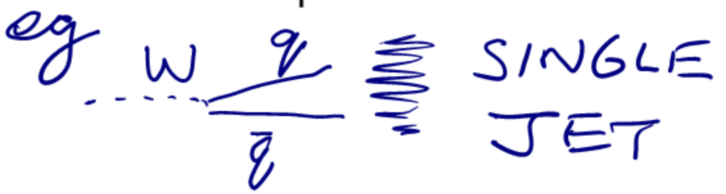

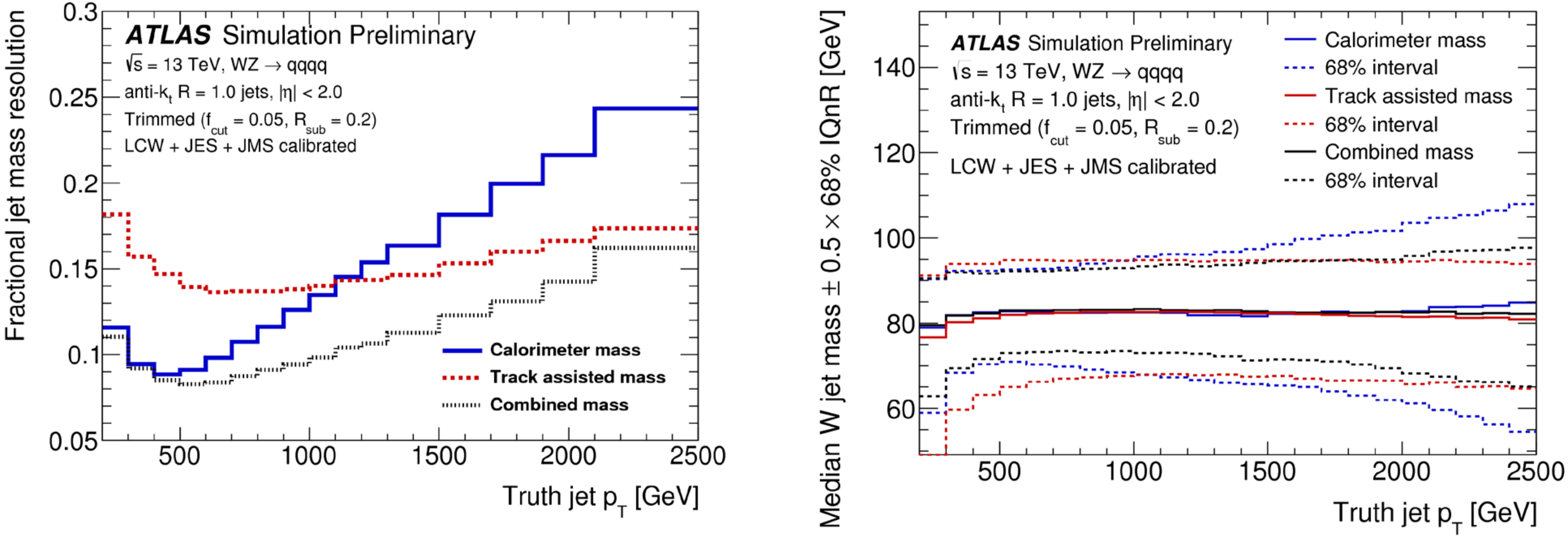

HIGH $P_\perp$ SINGLE JET MASS RESOLUTION
FOR W RECONSTRUCTION IN $W' \to WZ$

Conceptual Readout Schemes

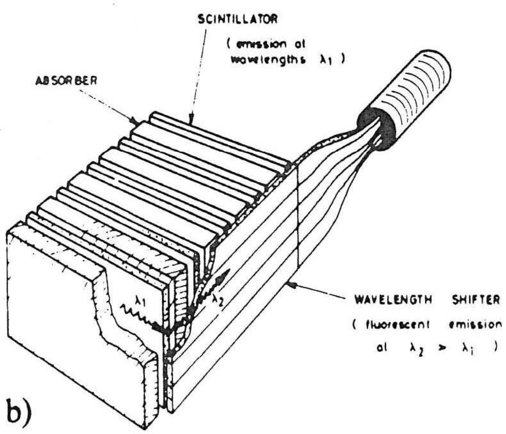

b)

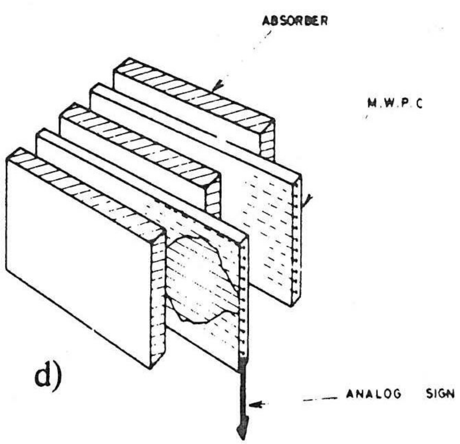

d)

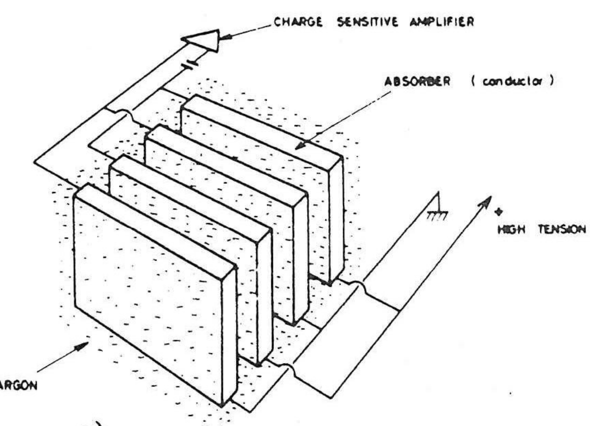

c)

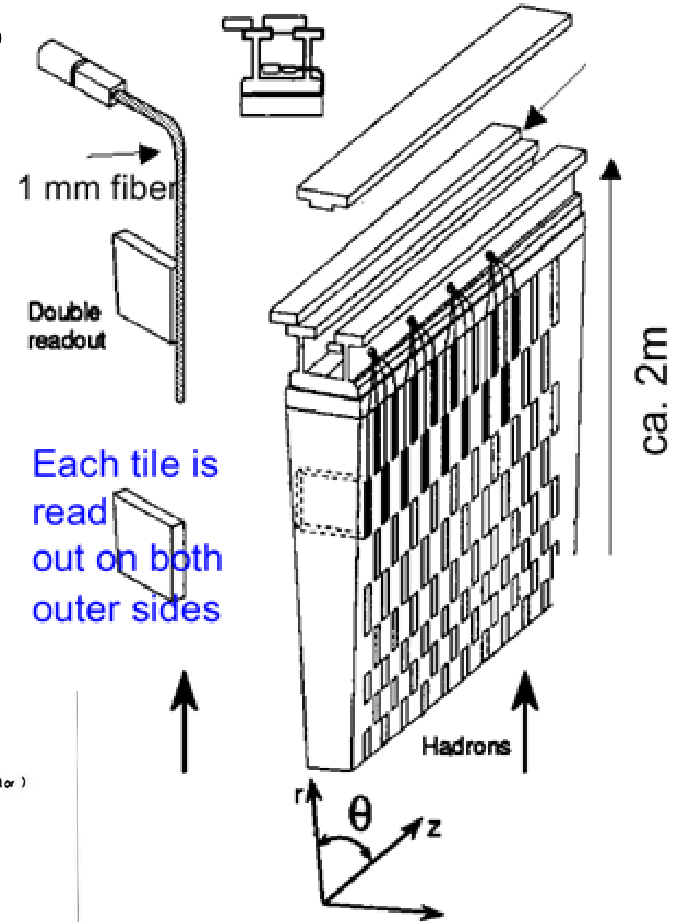

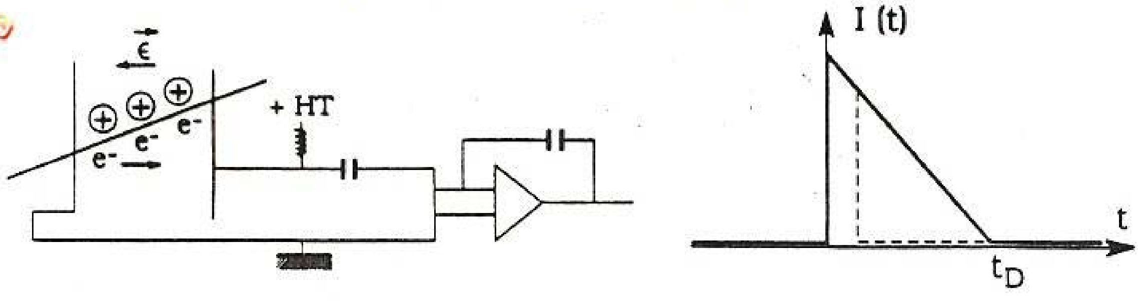

a b

Fig.8 a: Principle of operation of an ionization chamber. 8 b:current pulse shape in the ionization chamber(solid line). Dashed line : after clipping.

• ACCORDION GEOMETRY

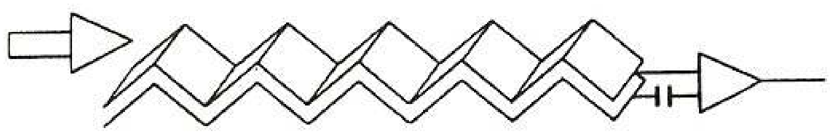

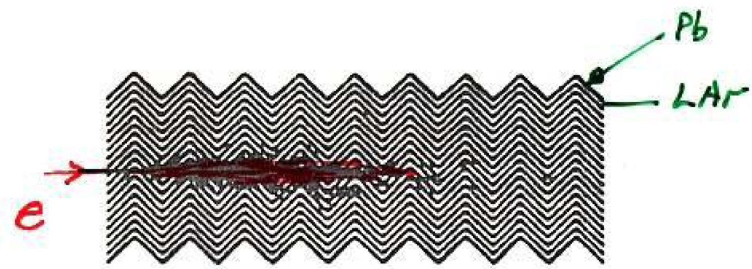

ZEUS Forward Calorimeter

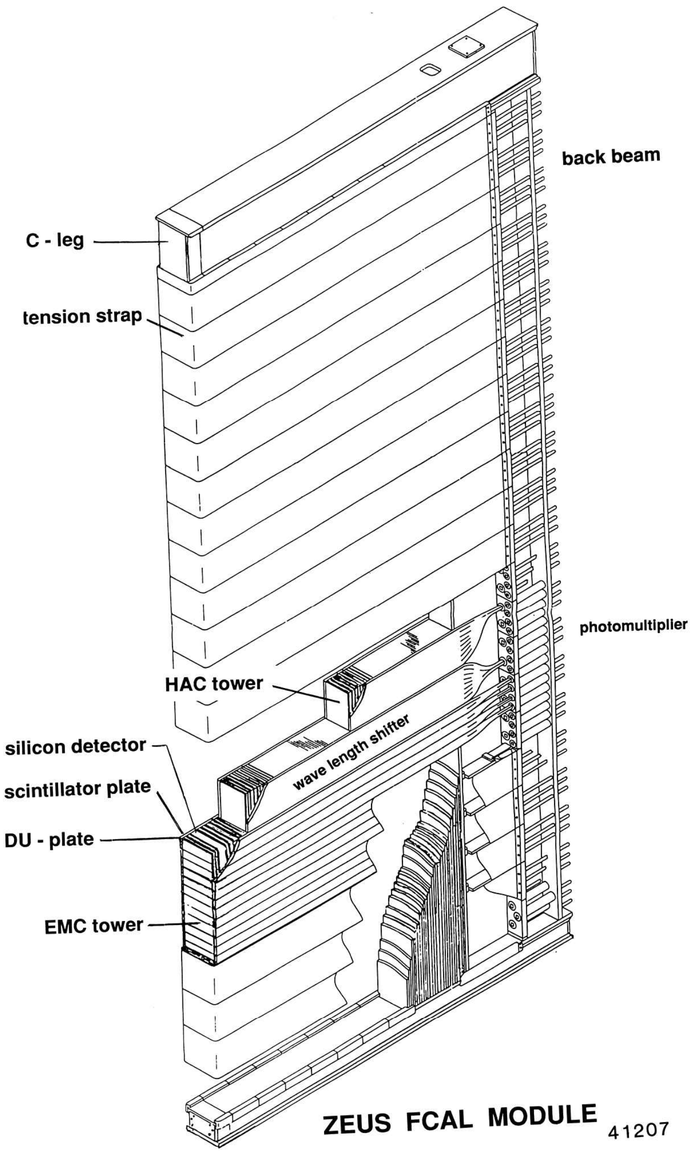

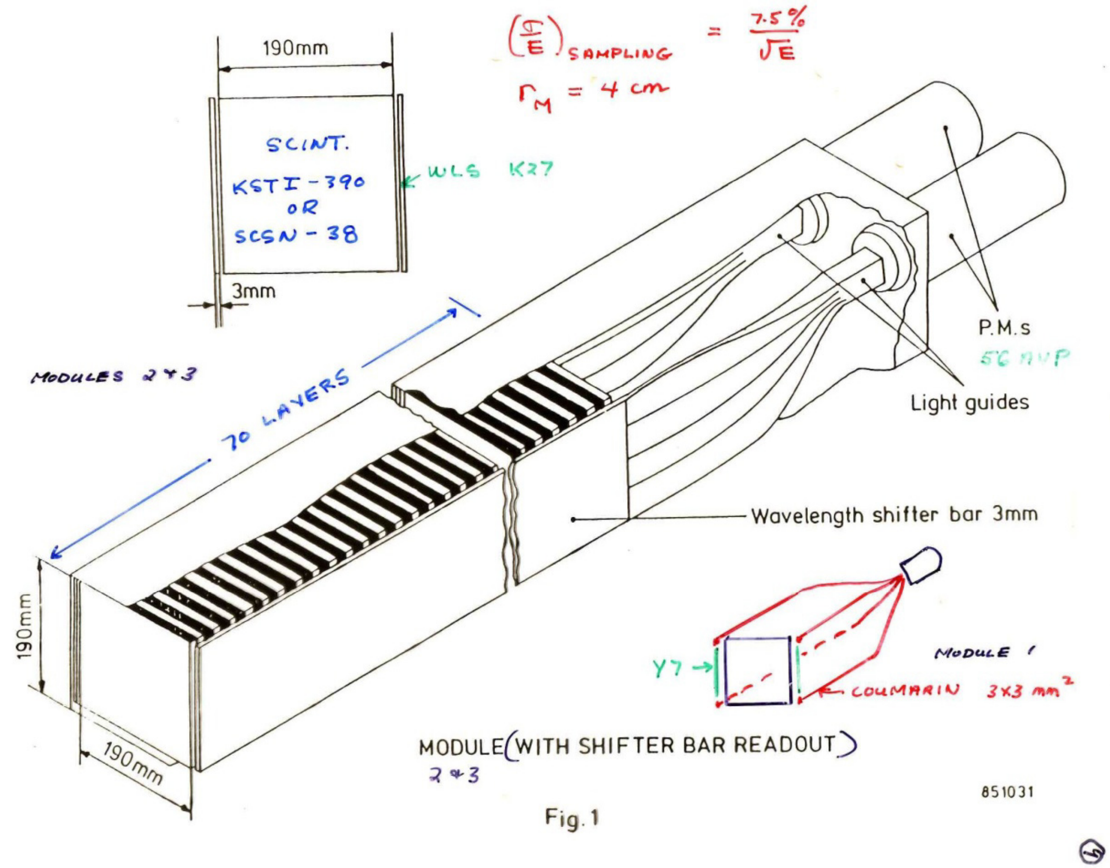

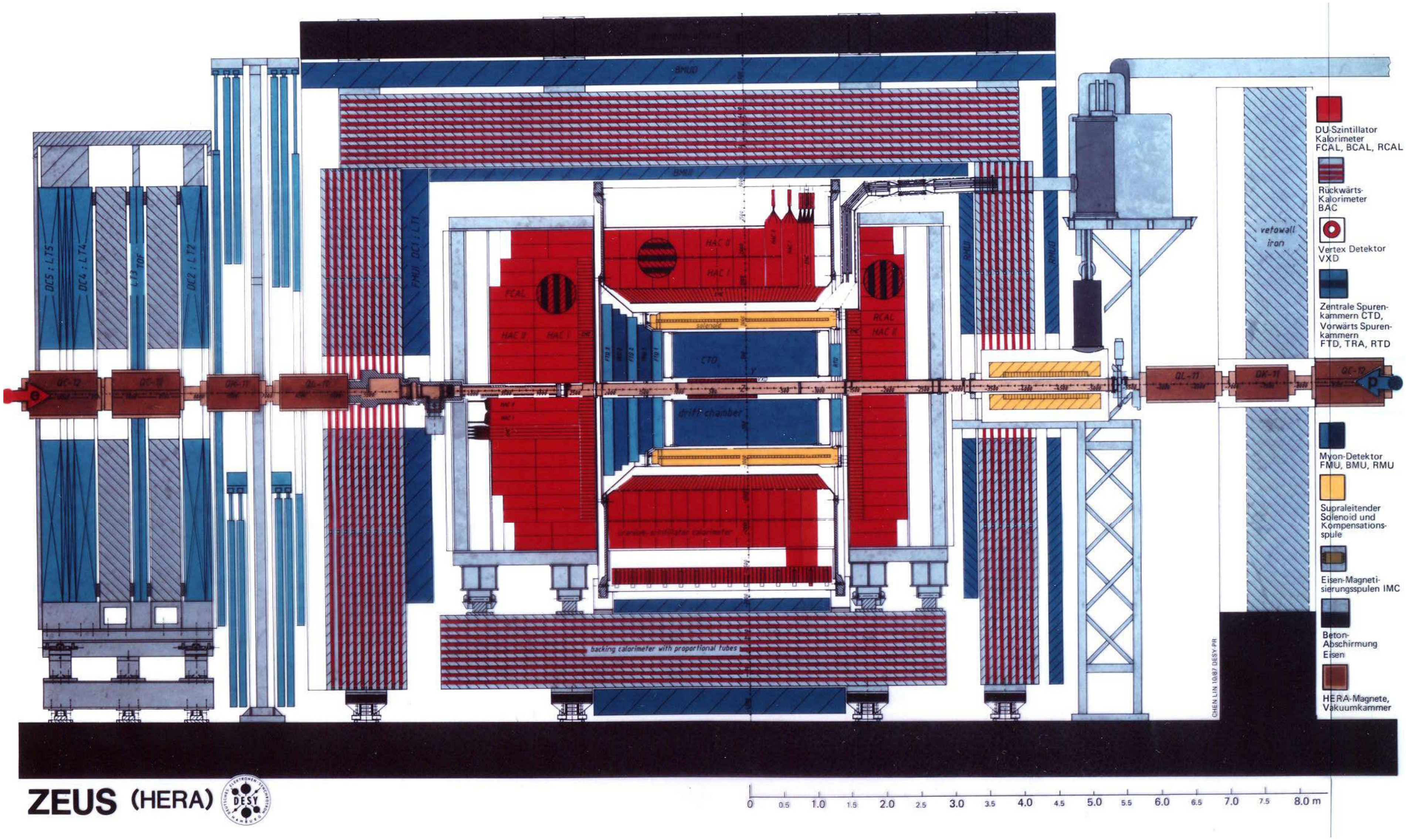

DU-Szintillator Kalorimeter FCAL, BCAL, RCAL
Rückwärts-Kalorimeter BAC
Vertex Detektor VXD
Zentrale Spurenkammern CTD, Vorwärts Spurenkammern FTD, TRA, RTD
Myon-Detektor FMU, BMU, RMU
Supraleitender Solenoid und Kompensationsspule
Eisen-Magnetisierungsspulen IMC
Beton-Abschirmung Eisen
HERA-Magnete, Vakuumkammer
FCAL
RCAL
CTD
driff chamber
backing calorimeter with proportional tubes
vetowall iron
ZEUS (HERA)
0 0.5 1.0 1.5 2.0 2.5 3.0 3.5 4.0 4.5 5.0 5.5 6.0 6.5 7.0 7.5 8.0 m

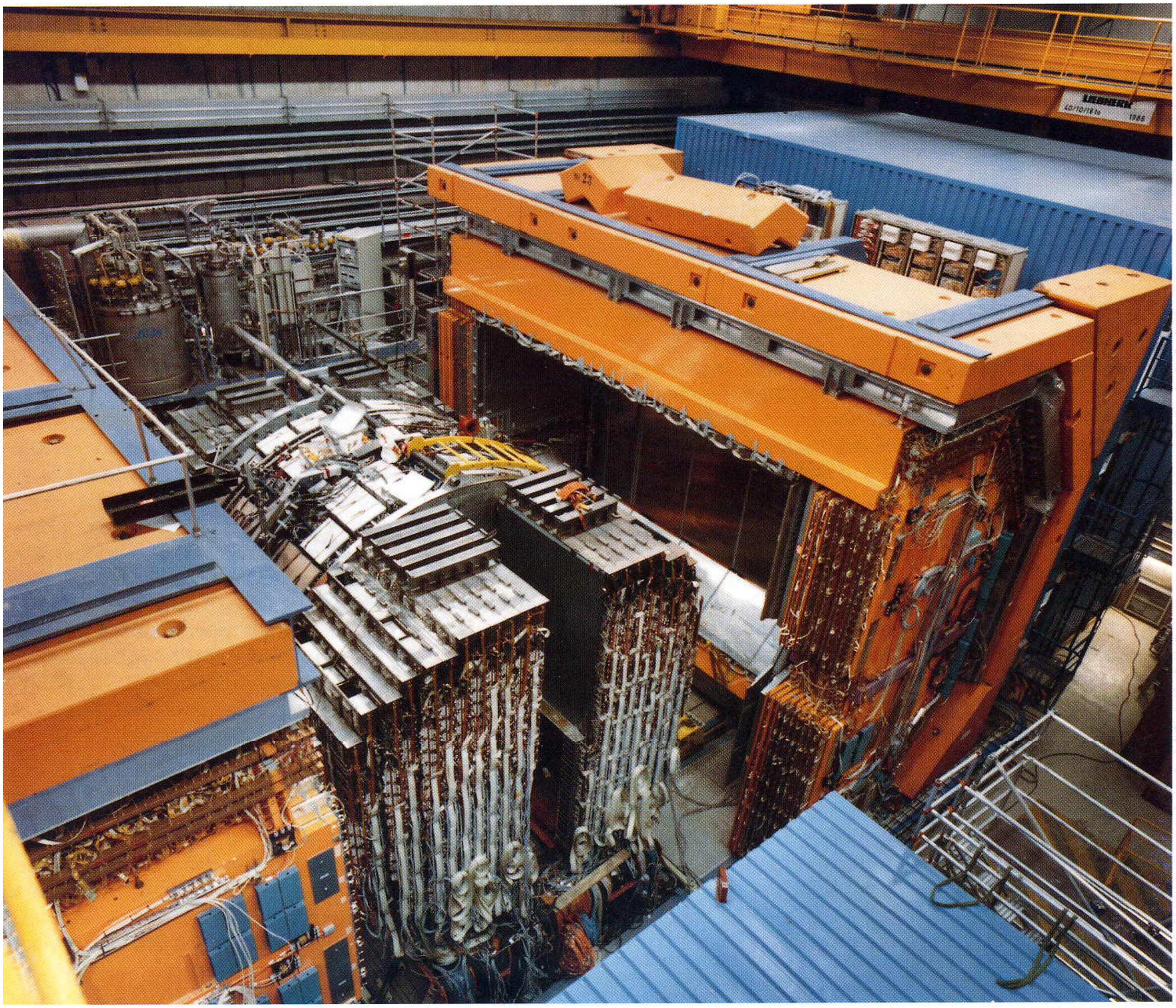

ɔint

LAr Calorimetry

- Five different detector technologies
- Calorimetry coverage to

$|\eta| \simeq 5$

SM Higgs Discovery Potential

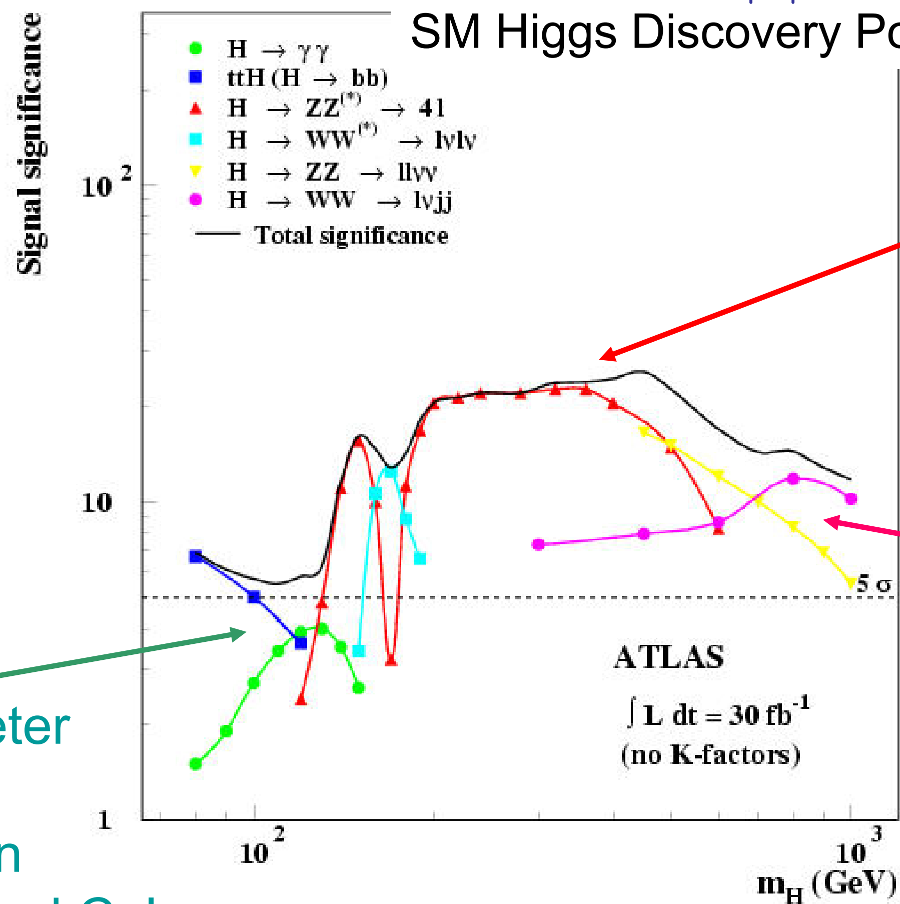

$H \to 4l$

EM Calorimeter

$H \to ZZ$ & $H \to WW$

Hadronic & Forward Calorimeters

$H \to \gamma\gamma$

EM Calorimeter

WW Fusion

Tag jets in Forward Cal

LAr Calorimeter Technology Overview

Design Goals ➡ Technology

- **EM Calorimeters** ($0 \le |\eta| \le 3.2$) and Presampler ($0 \le |\eta| \le 1.8$)

$$\frac{\sigma}{E} \le \frac{10\%}{\sqrt{E(\mathrm{GeV})}} \oplus 0.7\% \oplus \frac{0.27}{E(\mathrm{GeV})} \qquad \sigma_\theta \le \frac{40\ \mathrm{mrad}}{\sqrt{E(\mathrm{GeV})}} \qquad \sigma_{\vec{r}} \le \frac{8\ \mathrm{mm}}{\sqrt{E(\mathrm{GeV})}}$$

⇨ Lead/Copper-Kapton/Liquid Argon *Accordion* Structure

- **Hadronic Endcap** ($1.5 \le |\eta| \le 3.2$)

$$\frac{50\%}{\sqrt{E(\mathrm{GeV})}} \oplus 3\% \le \frac{\sigma}{E}(\mathrm{jets}) \le \frac{100\%}{\sqrt{E(\mathrm{GeV})}} \oplus 10\%$$

⇨ Copper/Copper-Kapton/Liquid Argon *Plate* Structure

- **Forward Calorimeter** ($3 \le |\eta| \le 5$)

$$\frac{\sigma}{E}(\mathrm{jets}) \le \frac{100\%}{\sqrt{E(\mathrm{GeV})}} \oplus 10\%$$

⇨ Tungsten/Copper/Liquid Argon *Paraxial Rod* Structure

LAr and Tile Calorimeters

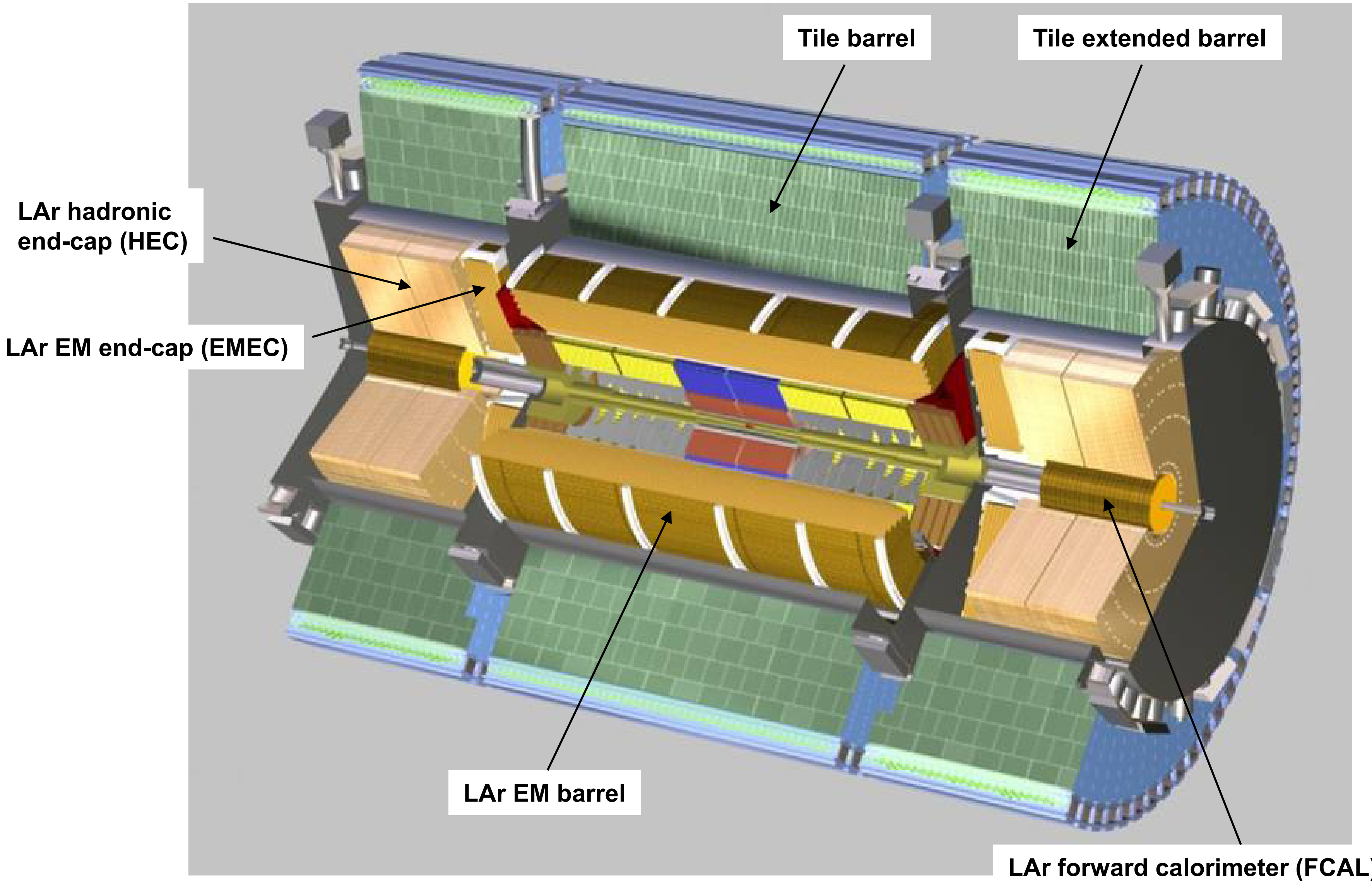

Electromagnetic Barrel

$0 < \eta < 1.4$

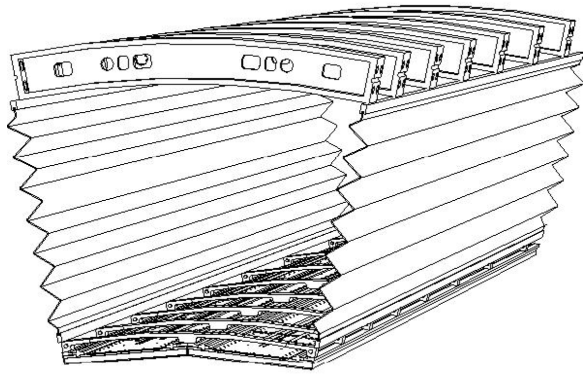

Barrel Module Schematic
with presampler

- 64 gaps /module
- 2.1 mm gap
- 2x3100 mm long

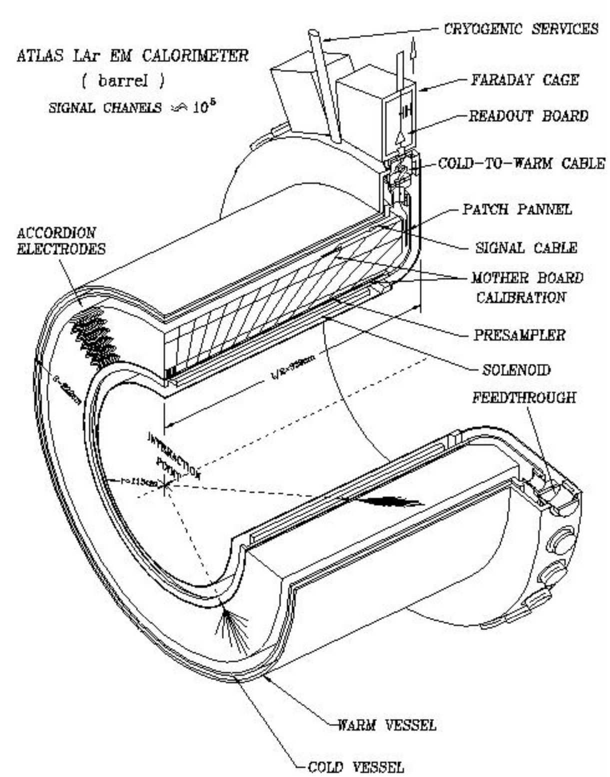

Half Barrel Assembly

- 2x16 modules
- I.R/O.R 1470/2000 mm
- 22 - 33 X_0
- 3 longitudinal samples
- $\Delta\eta \times \Delta\varphi \quad 0.025 \times 0.025$
- presampler $|\eta| < 1.8$

Electromagnetic Endcap

$1.4 < \eta < 3.2$

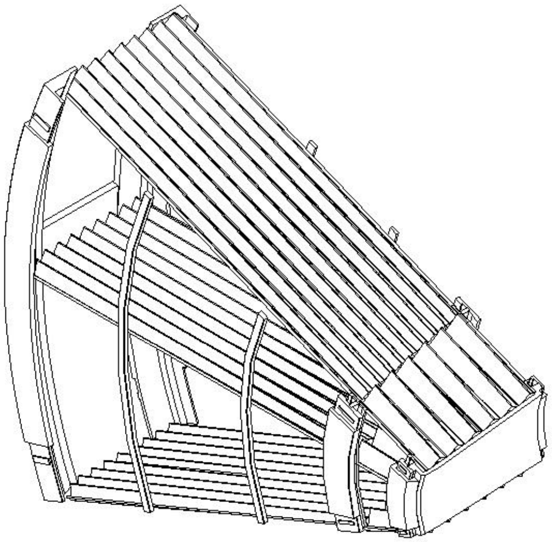

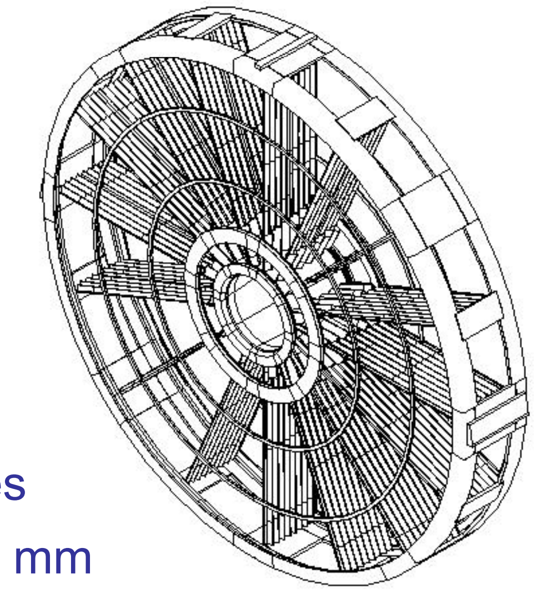

- 2x8 modules
- Diam. 4000 mm
- 22 - 37 X_0
- 3 longitudinal samples
- $\Delta\eta \times \Delta\varphi \quad 0.025 \times 0.025$
  $|\eta| > 2.5 \rightarrow 0.1 \times 0.1$
- Front sampling of 6 X_0
  for $|\eta| < 2.5$, η - strips.

- 96 gaps /module outer wheel
  32 gaps/module inner wheel
- 2.8 - 0.9 mm gap outer
  3.1-1.8 mm inner

Accordion Structure

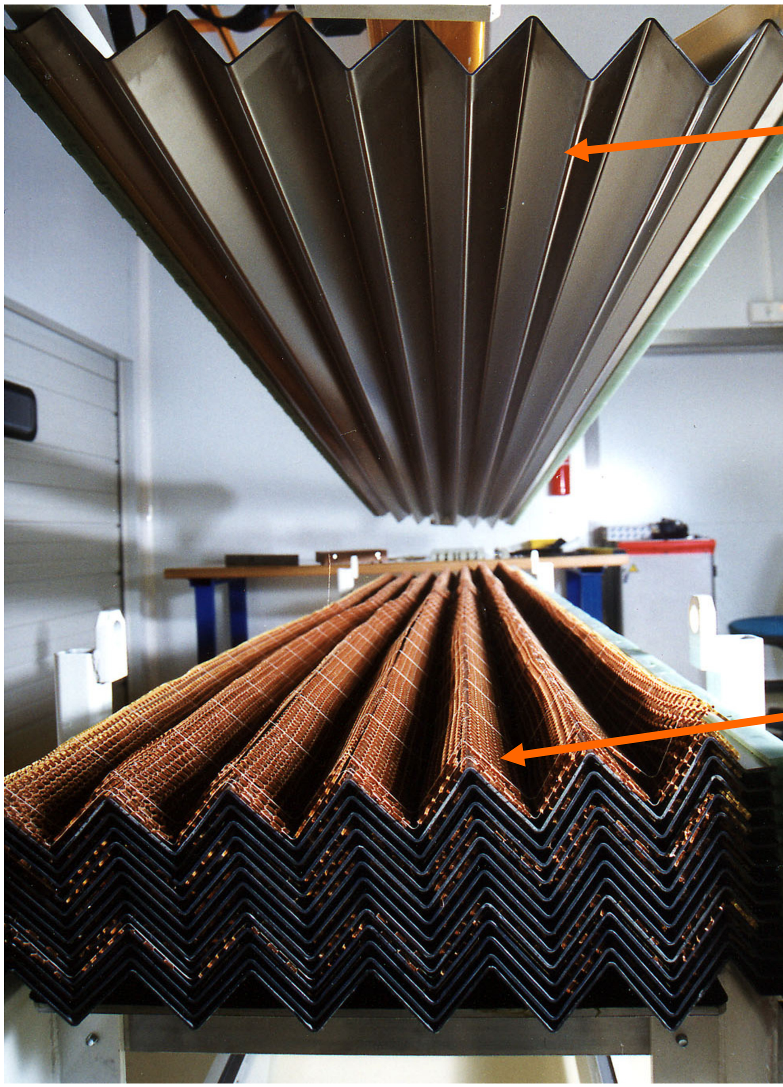

Pb Absorber

• Honeycomb spacer

&

• Cu/Kapton electrode

Prototype of EM endcap

Detail of Kaptons

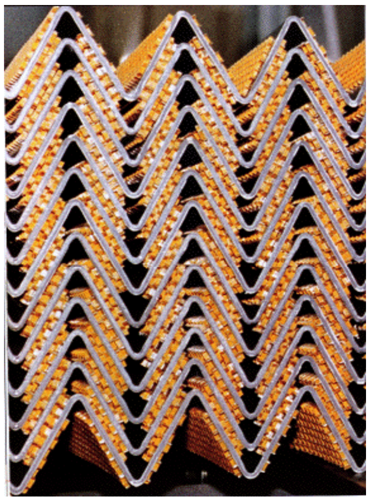

ATLAS FCAL

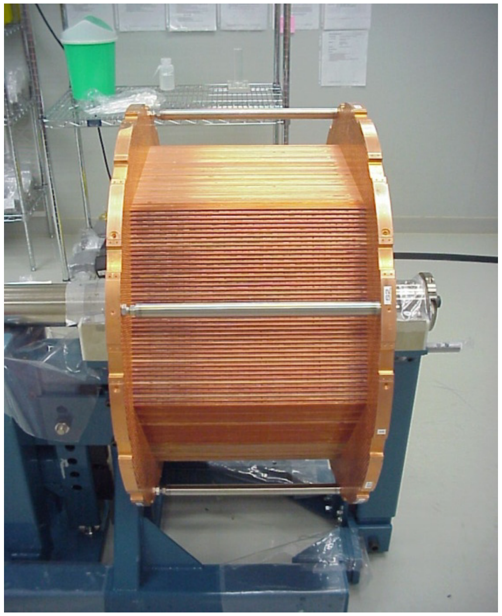

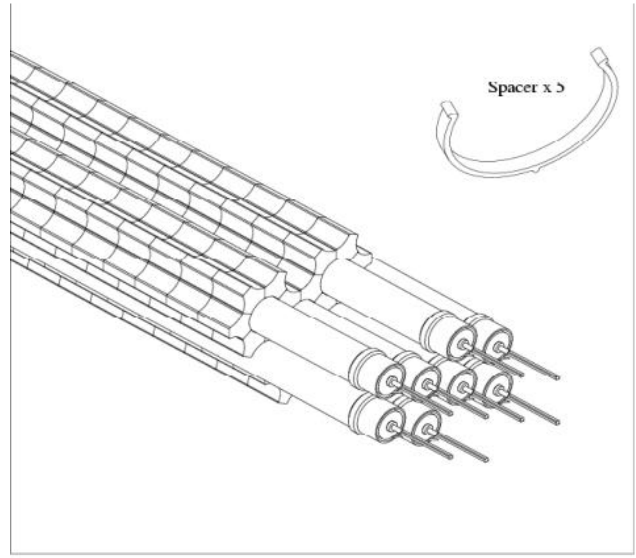

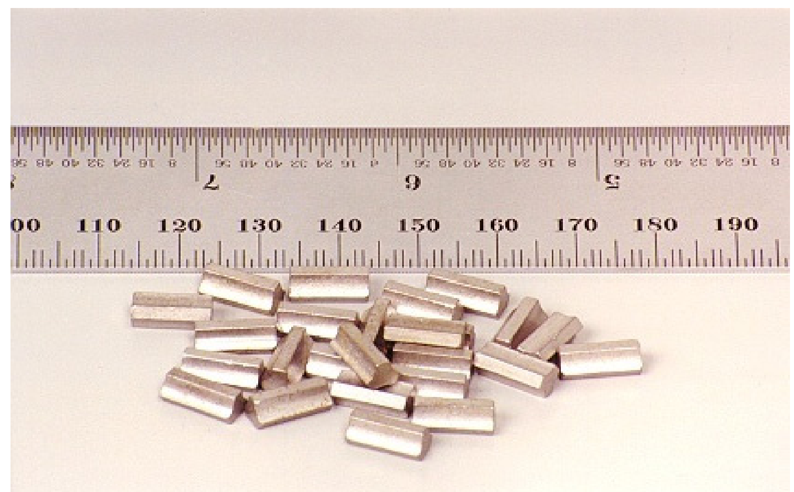

Pictures of assembly process

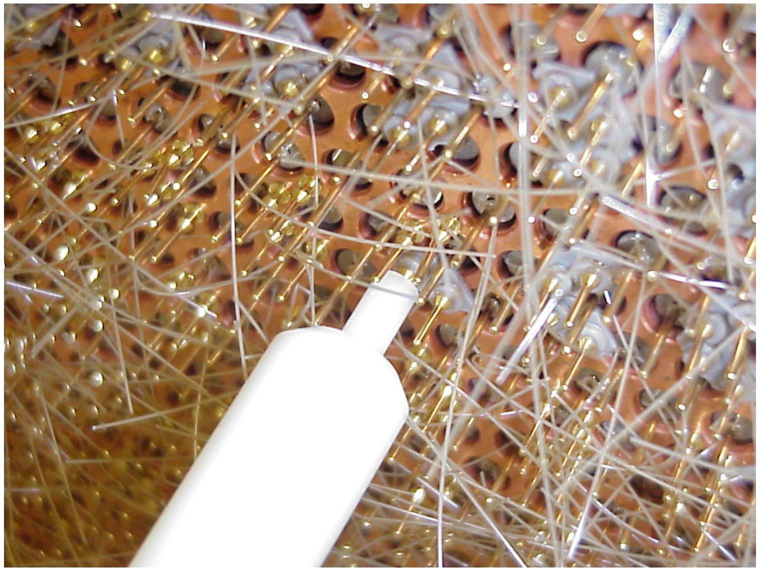
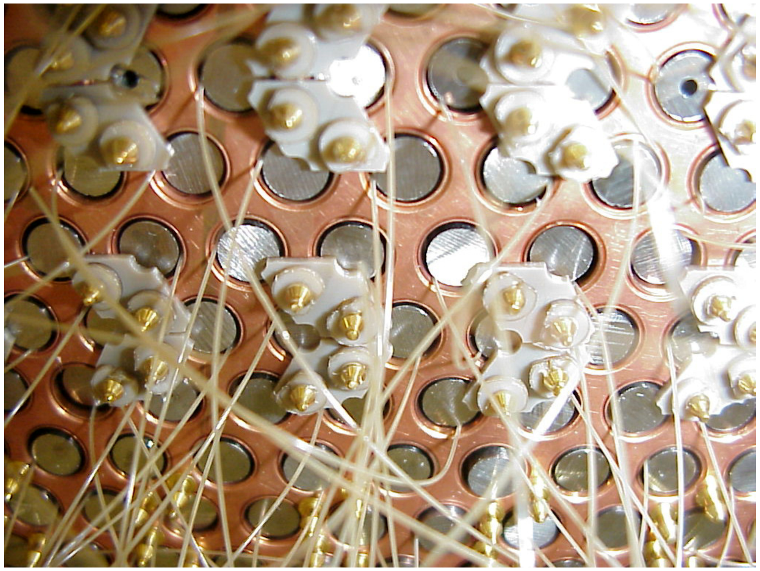
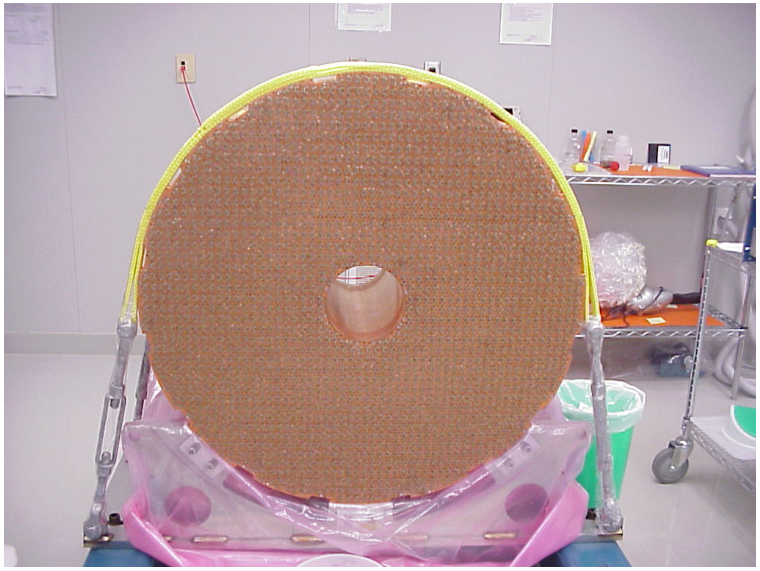


LAr Forward Calorimeters

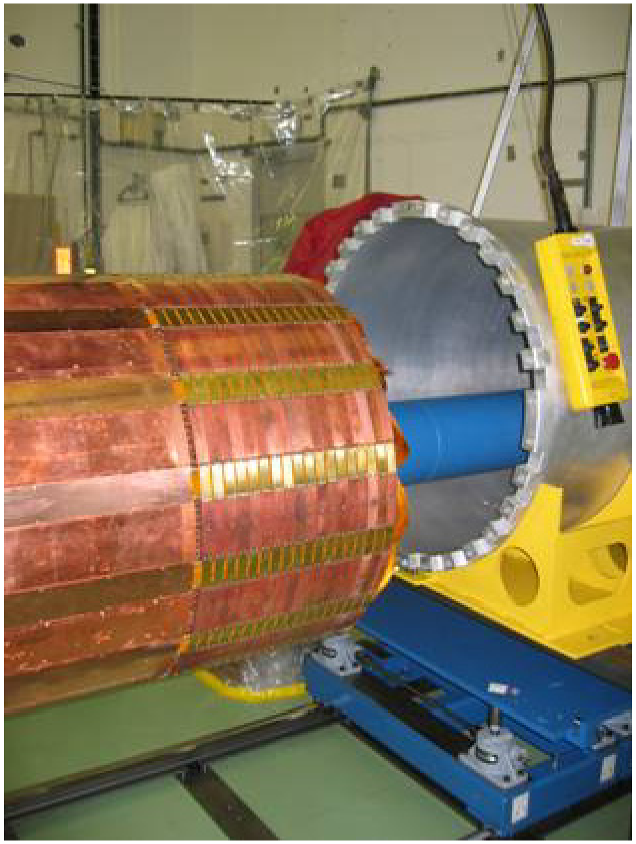

- FCAL C assembly into tube – Fall 2003

Liquid Argon Gap

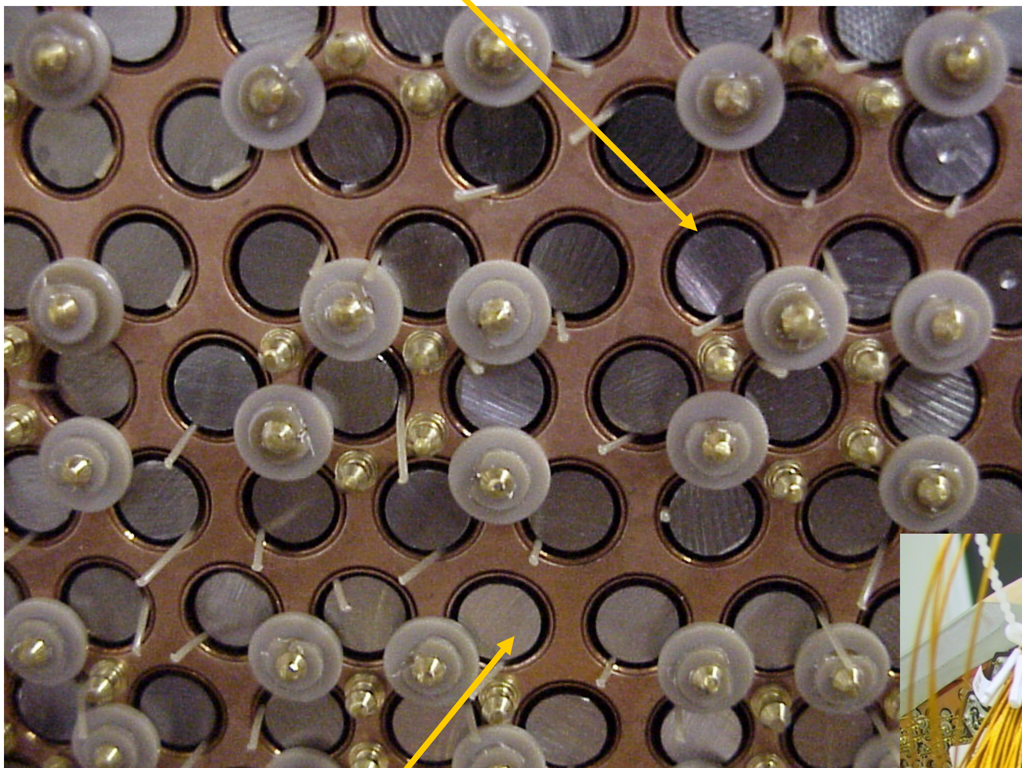

Tungsten Rod

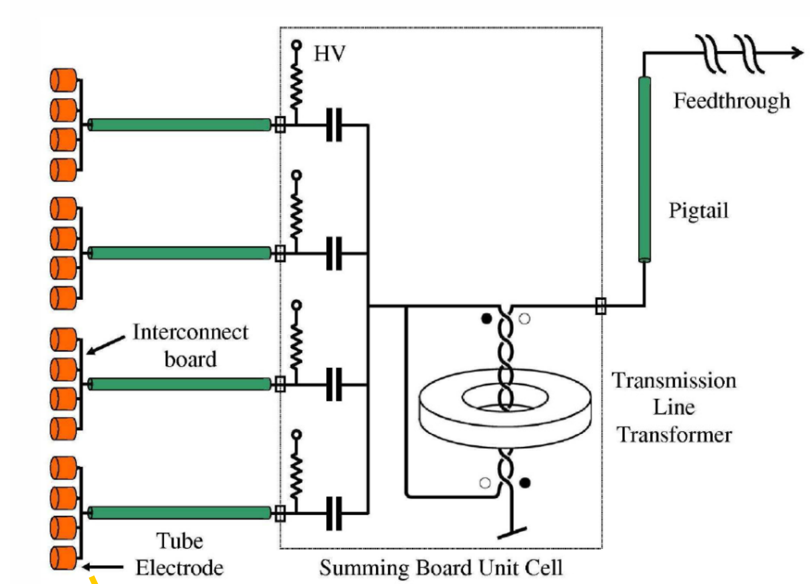

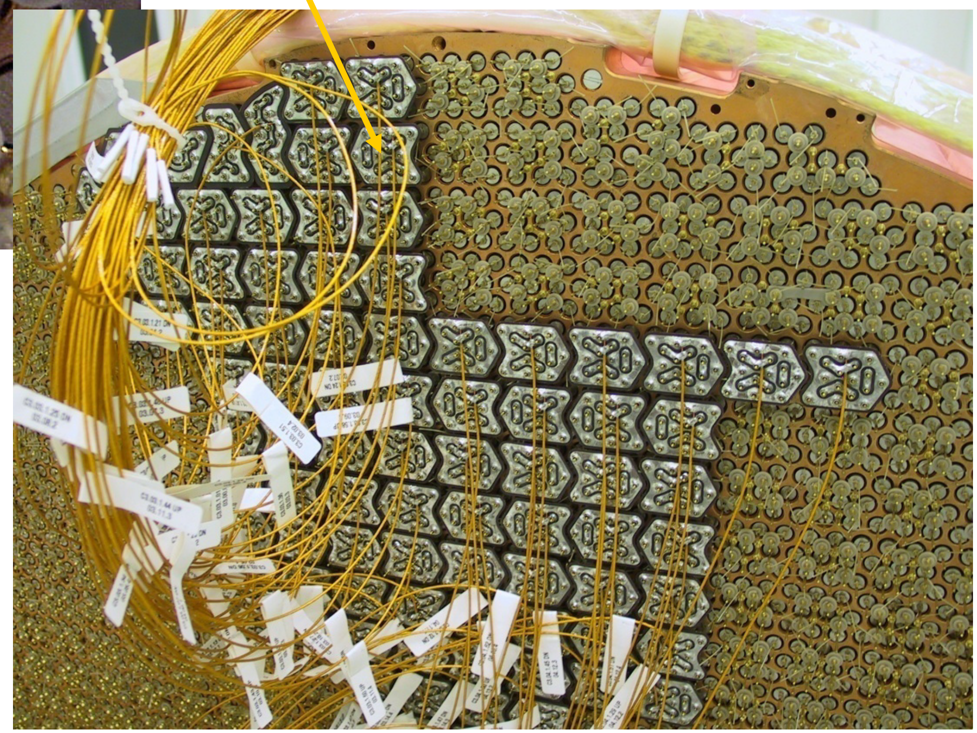

ATLAS HEC Structure

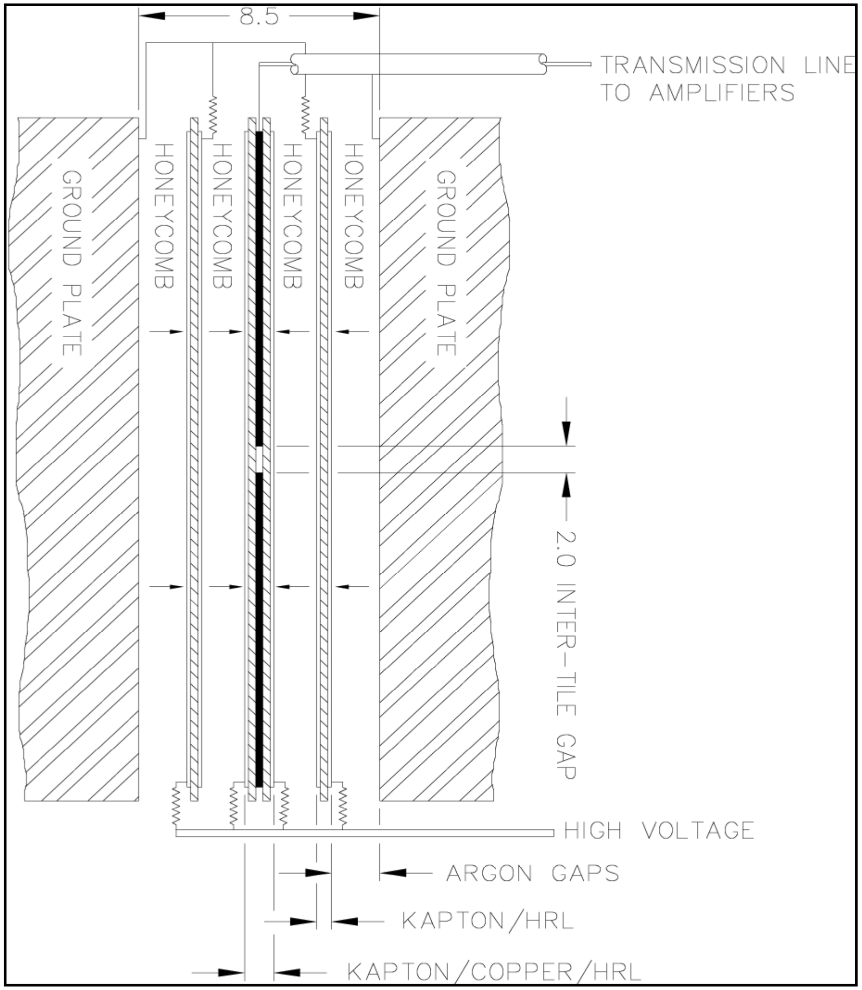

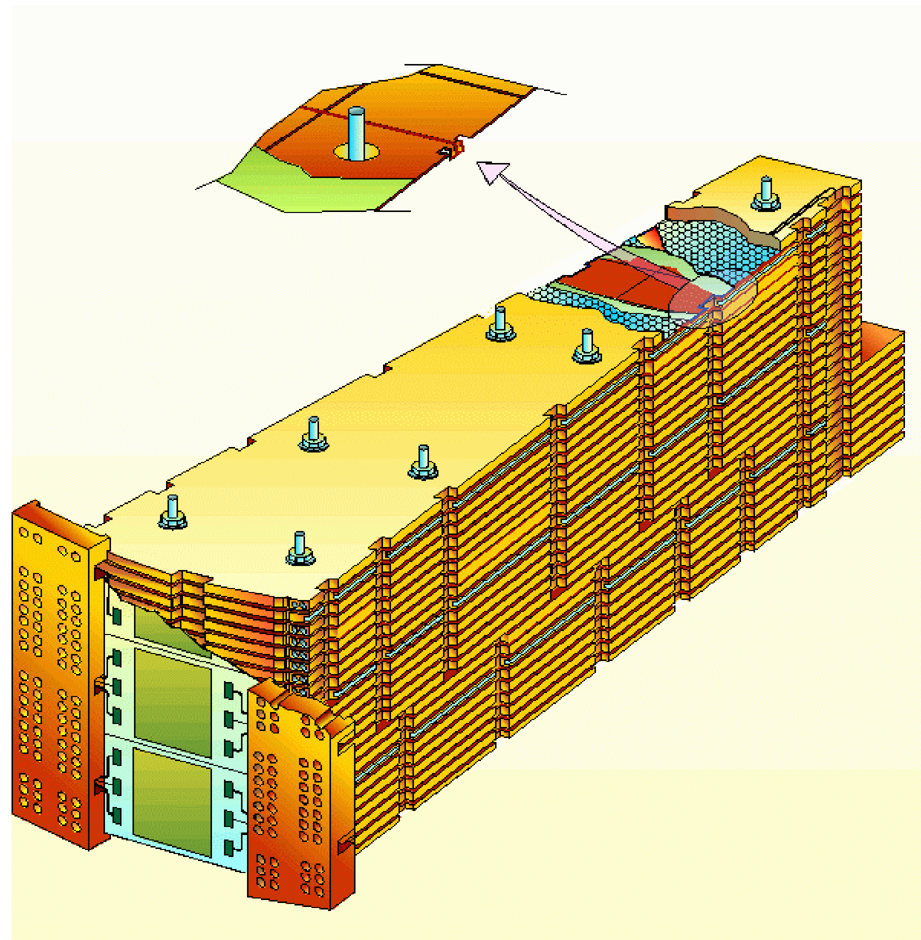

ELECTROSTATIC TRANSFORMER

- MATCHES CAL → PREAMP CAPACITANCE
- REDUCES EFFECTIVE CAPACITANCE

CHARGE TRANSFER TIME

NOISE

- Transformer matching
- Does not work in magnetic field. Long readout cables slow down signal
- Large capacitance, large noise

584 *J. Colas et al. / The electrostatic transformer*

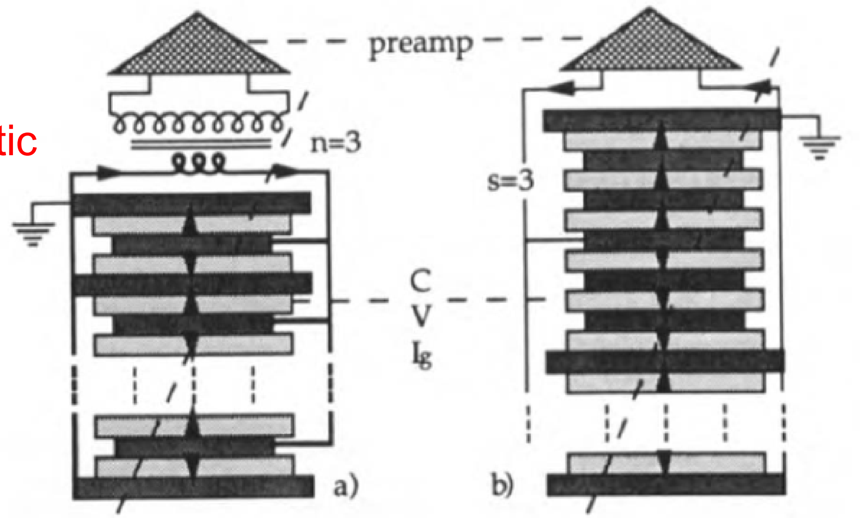

Fig. 1. Schematic representation of capacitance matching for a hadronic tower. High voltage connections are not shown. I_g is the ionization current in the gth gap. V and C are the dc voltage and capacitance per gap, respectively. The arrows show the directions of current flow. In (a) all N gaps are connected in parallel; matching is achieved with a ferrite-core transformer with turns ratio $n = 3$. (b) shows an electrostatic transformer with P parallel subtowers of $S = 3$ gaps in series ($N = SP$).

- EST
- Works in magnetic field
- Low capacitance

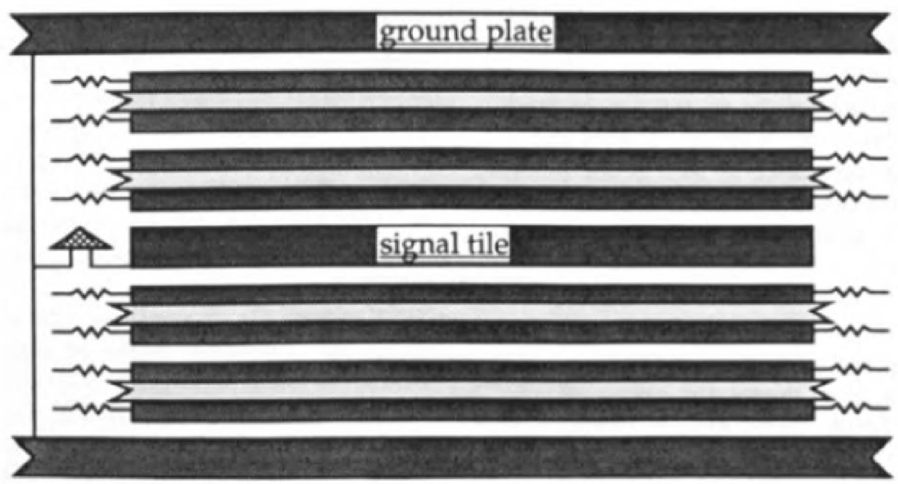

Fig. 2. Schematic view of two subsections of the tower with an electrostatic transformer of ratio $S = 3$. The absorbing signal tile is at dc ground. High voltages, decoupled by large resistances, are supplied to the half tiles, which are separated by thin insulating layers.

Hadronic Endcap Calorimeter (HEC)

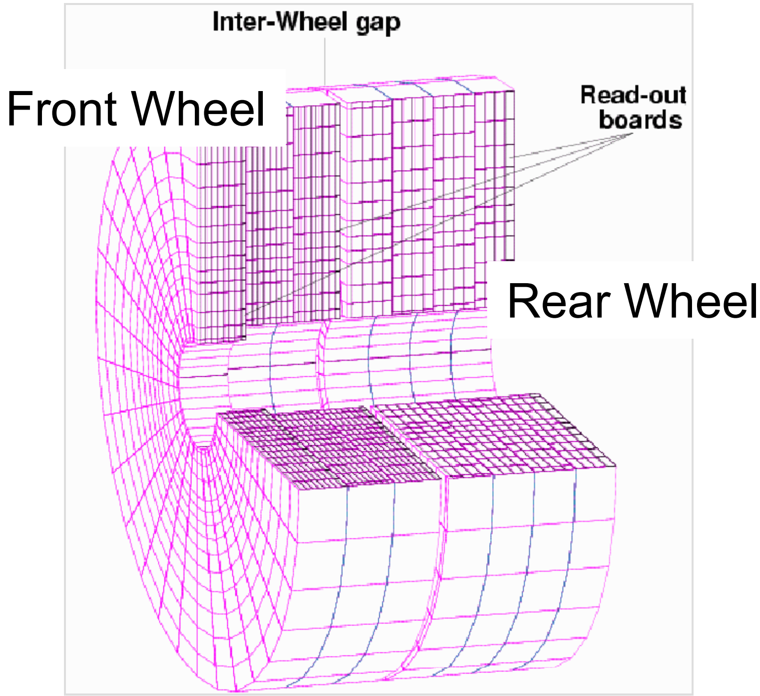

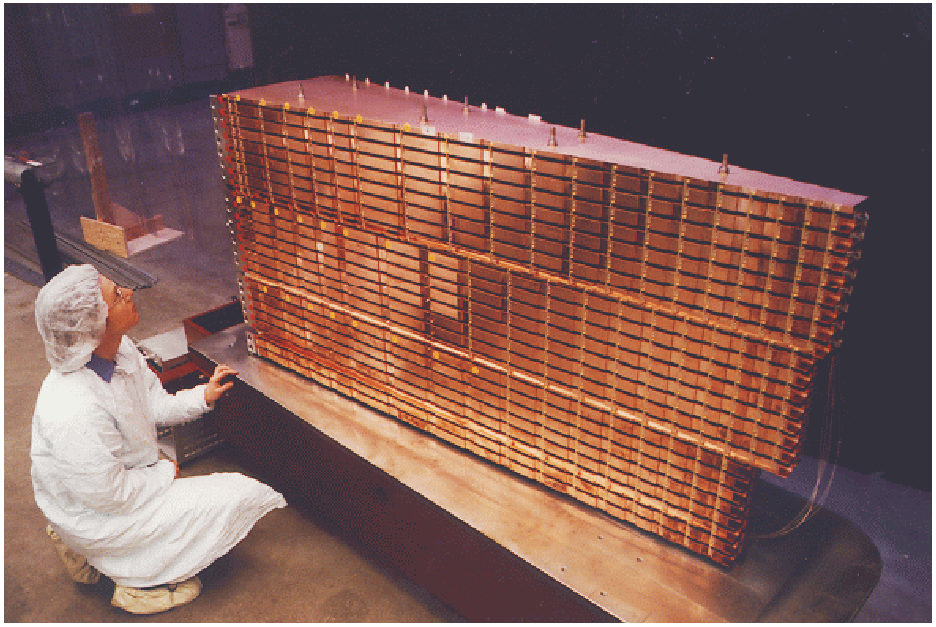

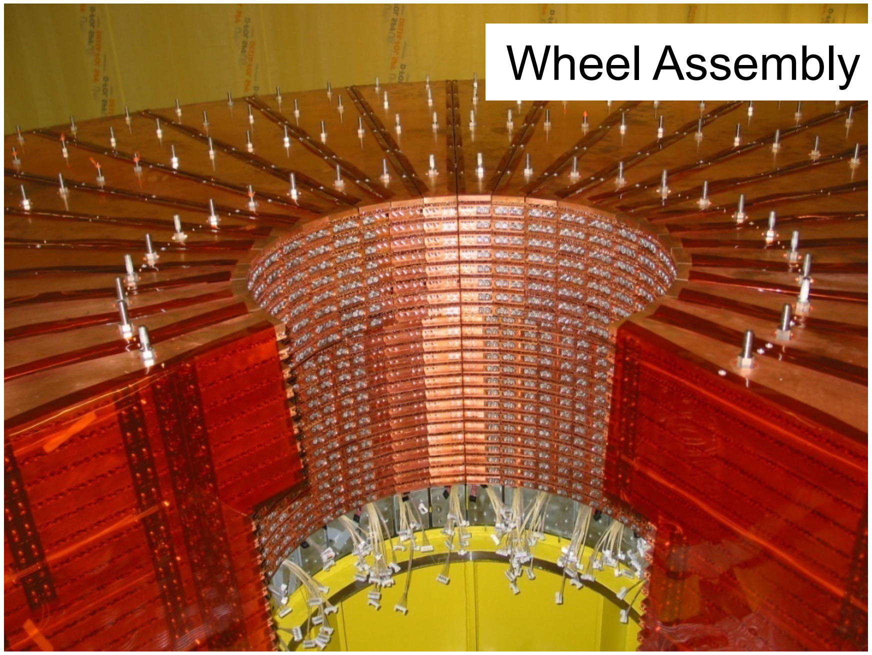

Composed of 2 wheels per end
Front wheel: 67 t 25 mm Cu plates
Back wheel: 90 t 50 mm Cu plates

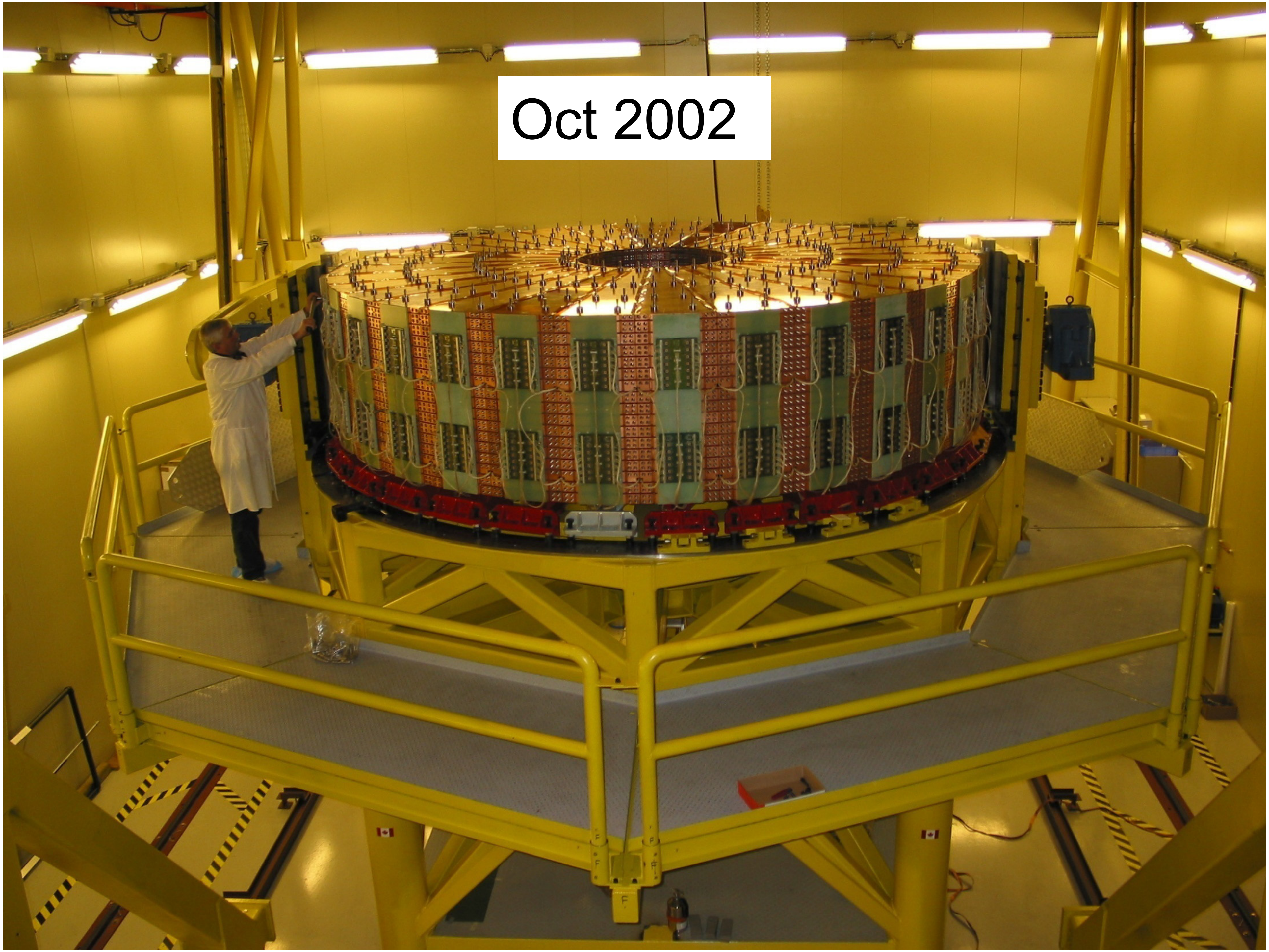
Oct 2002

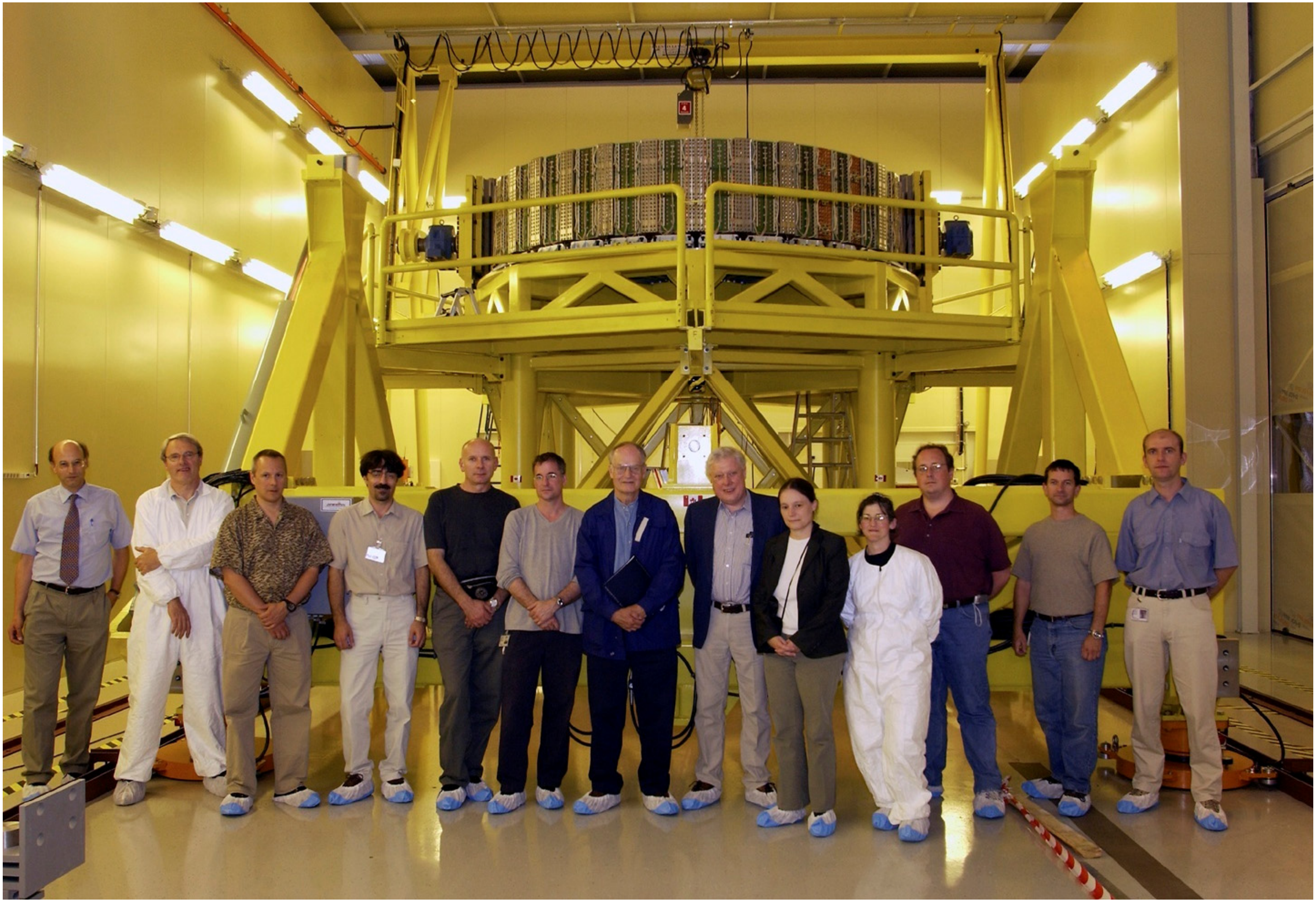

Electromagnetic Endcap

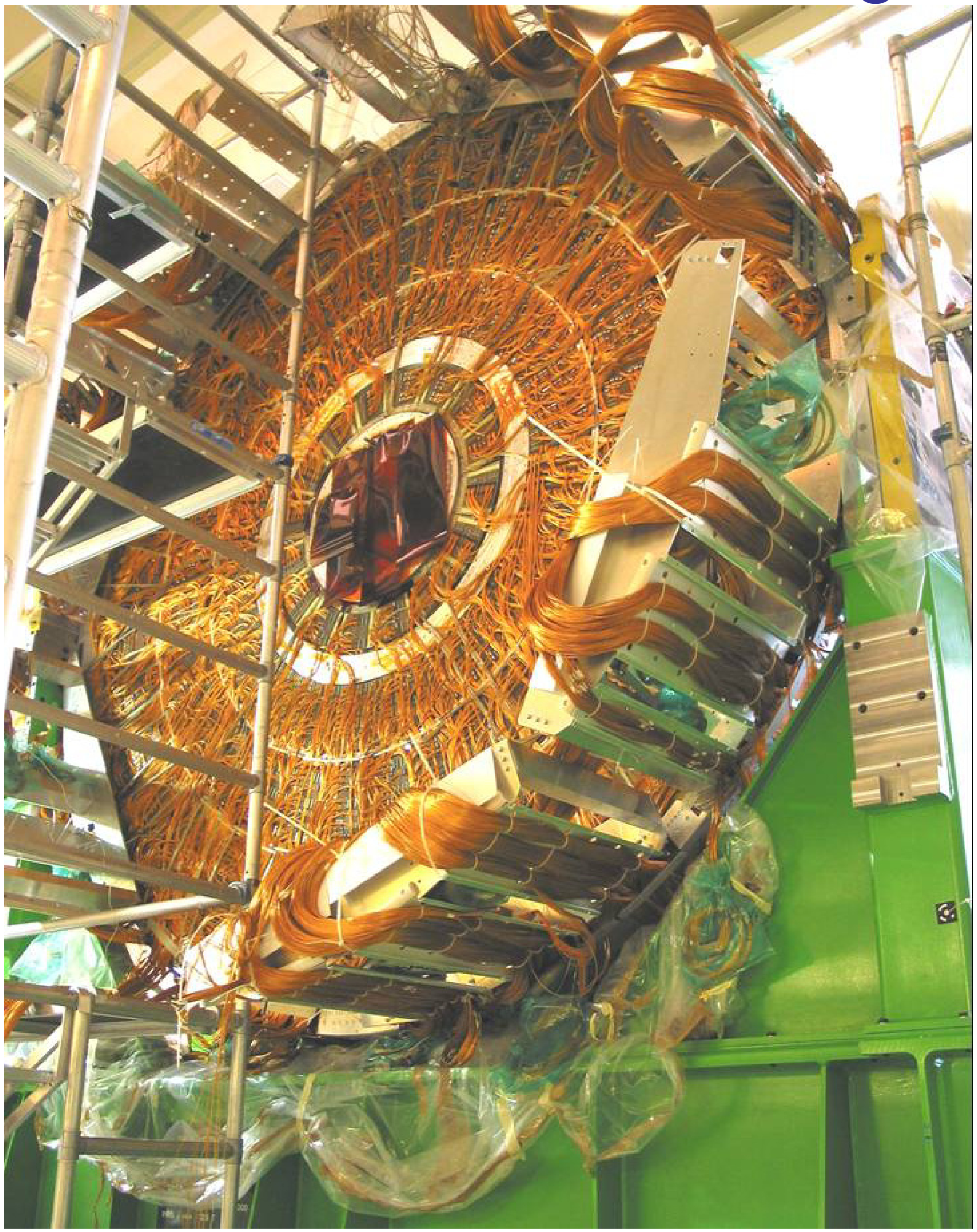

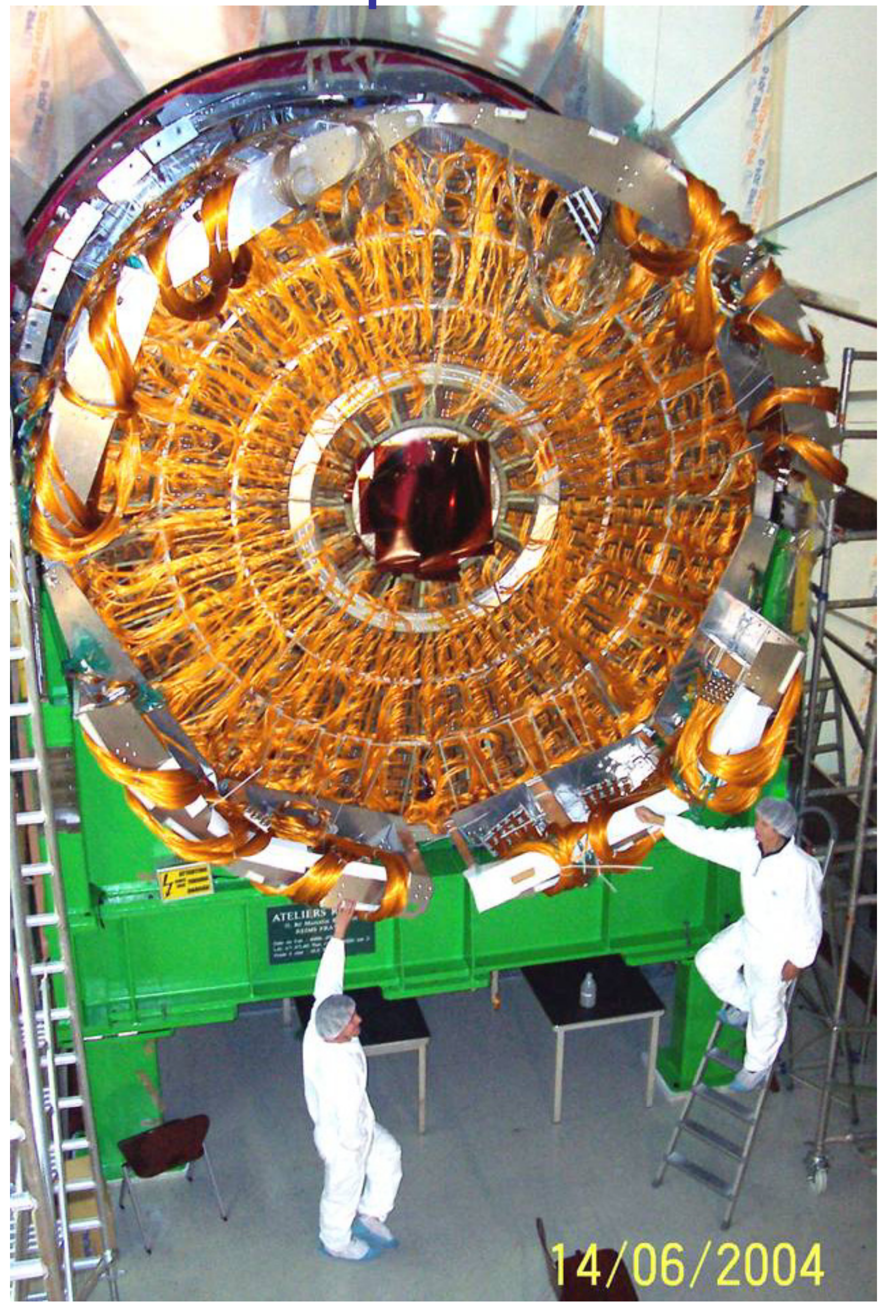

Hadronic Endcap

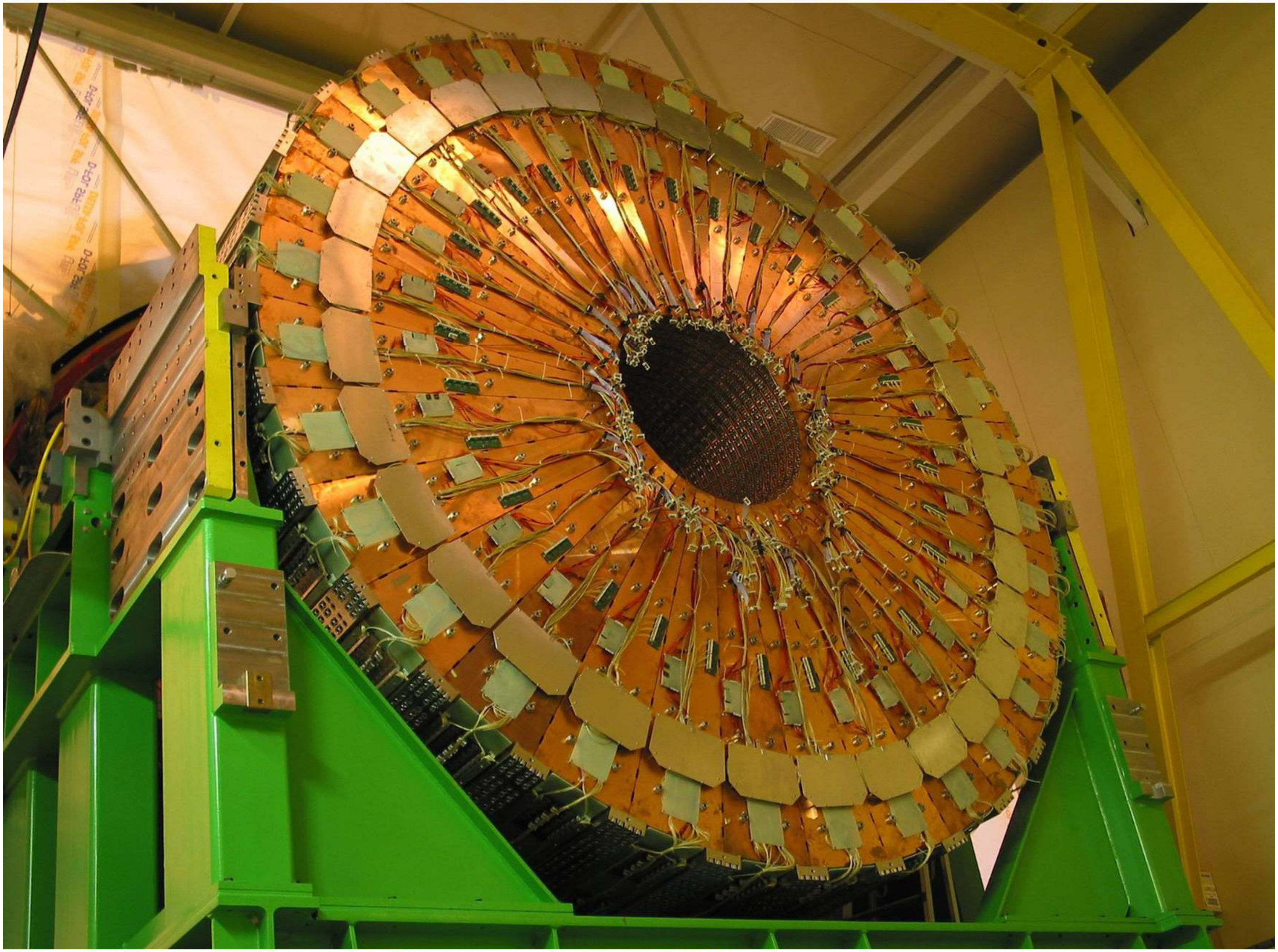

HEC – FCAL Assembly

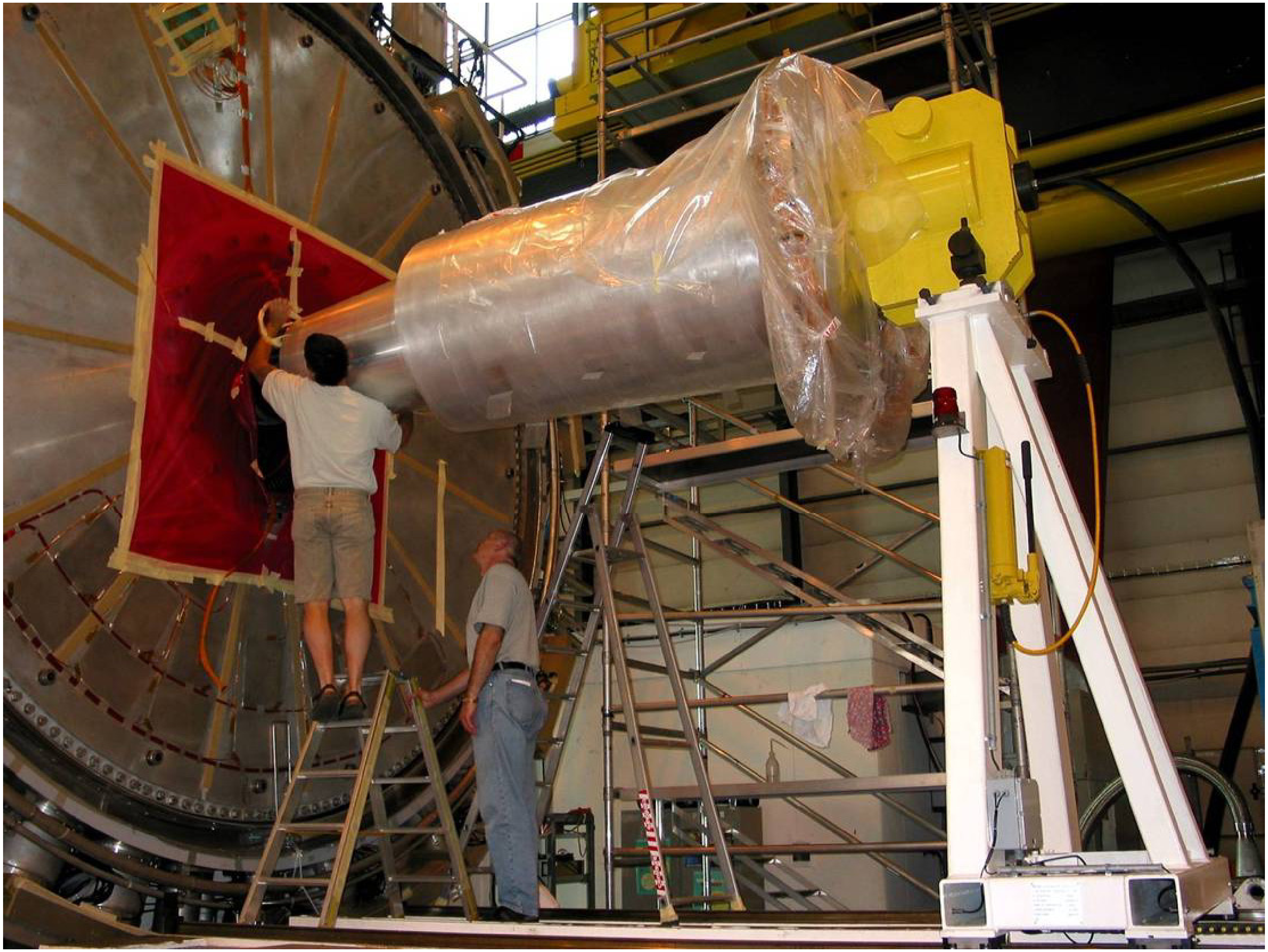

Shaping, Pileup and Electronic Noise

Inelastic pp cross section 70 mb
Average luminosity of 10^{34} $cm^{-2}s^{-1}$
2835 active bunches over 3564 LHC clock cycles

} 23 inelastic events per crossing

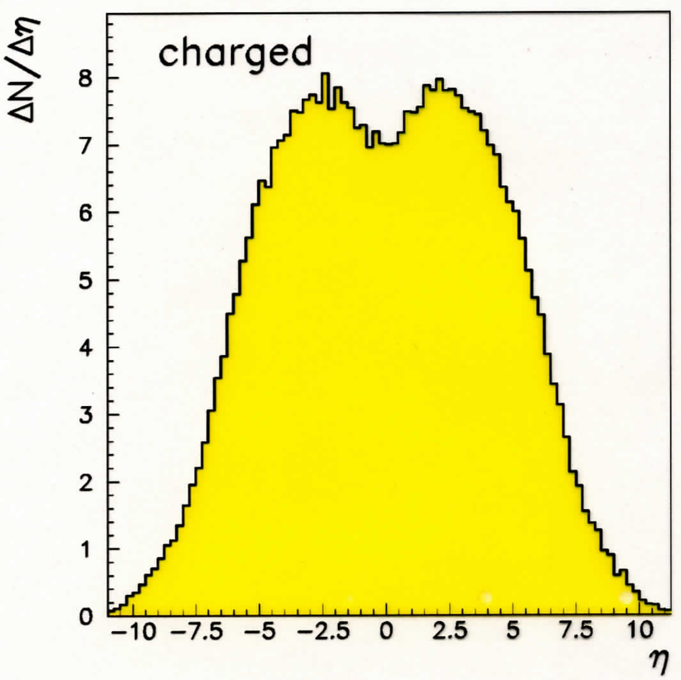

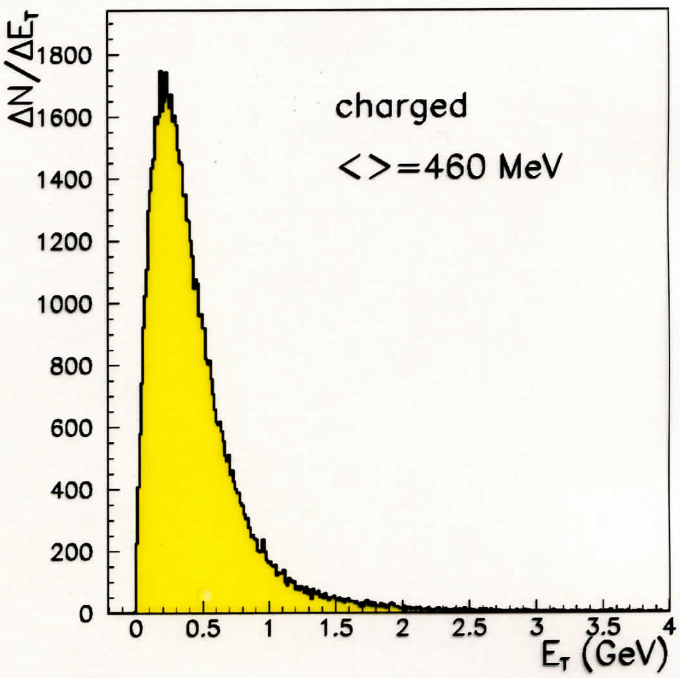

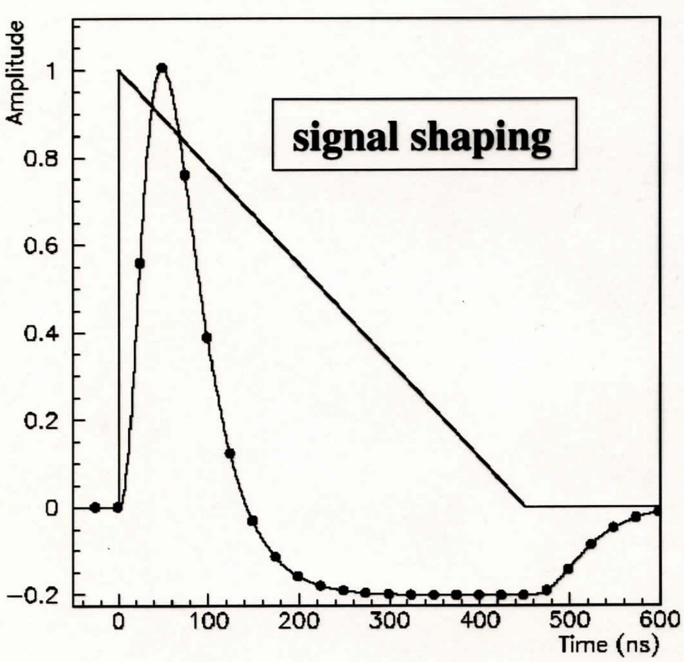

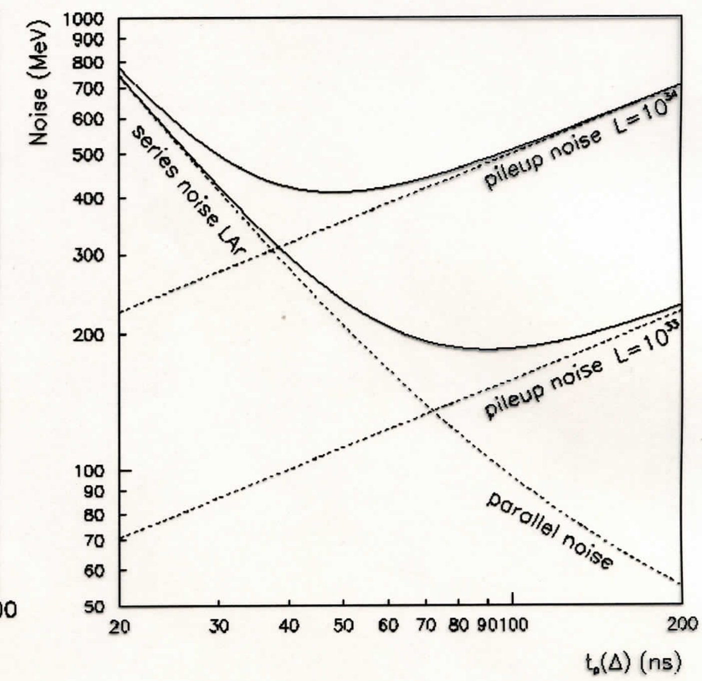

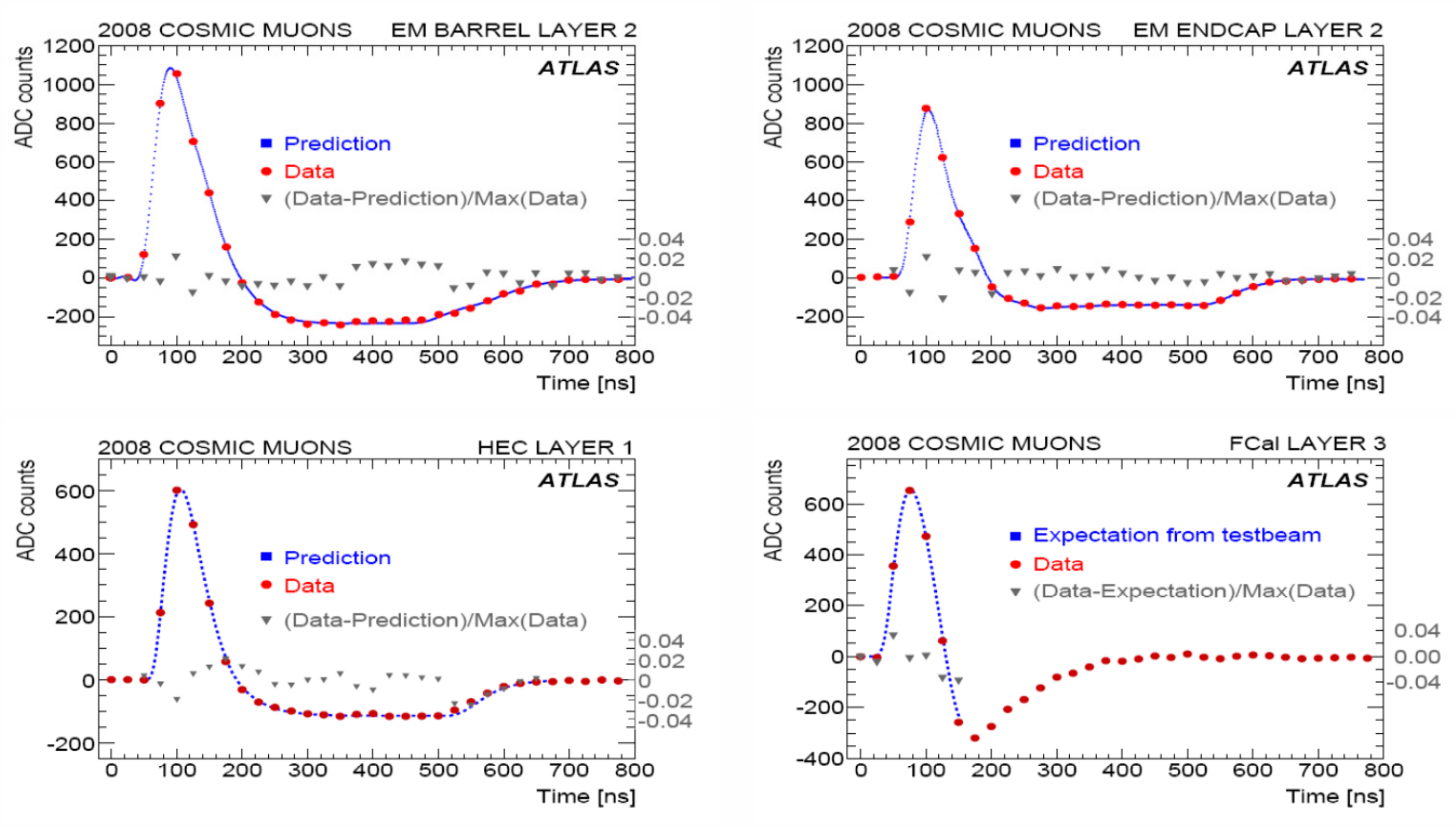

Signal Shape before startup

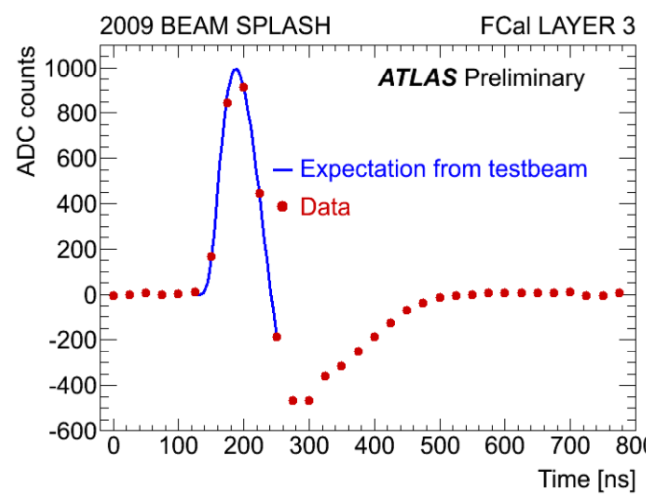

Noise Level in LAr Calorimeters

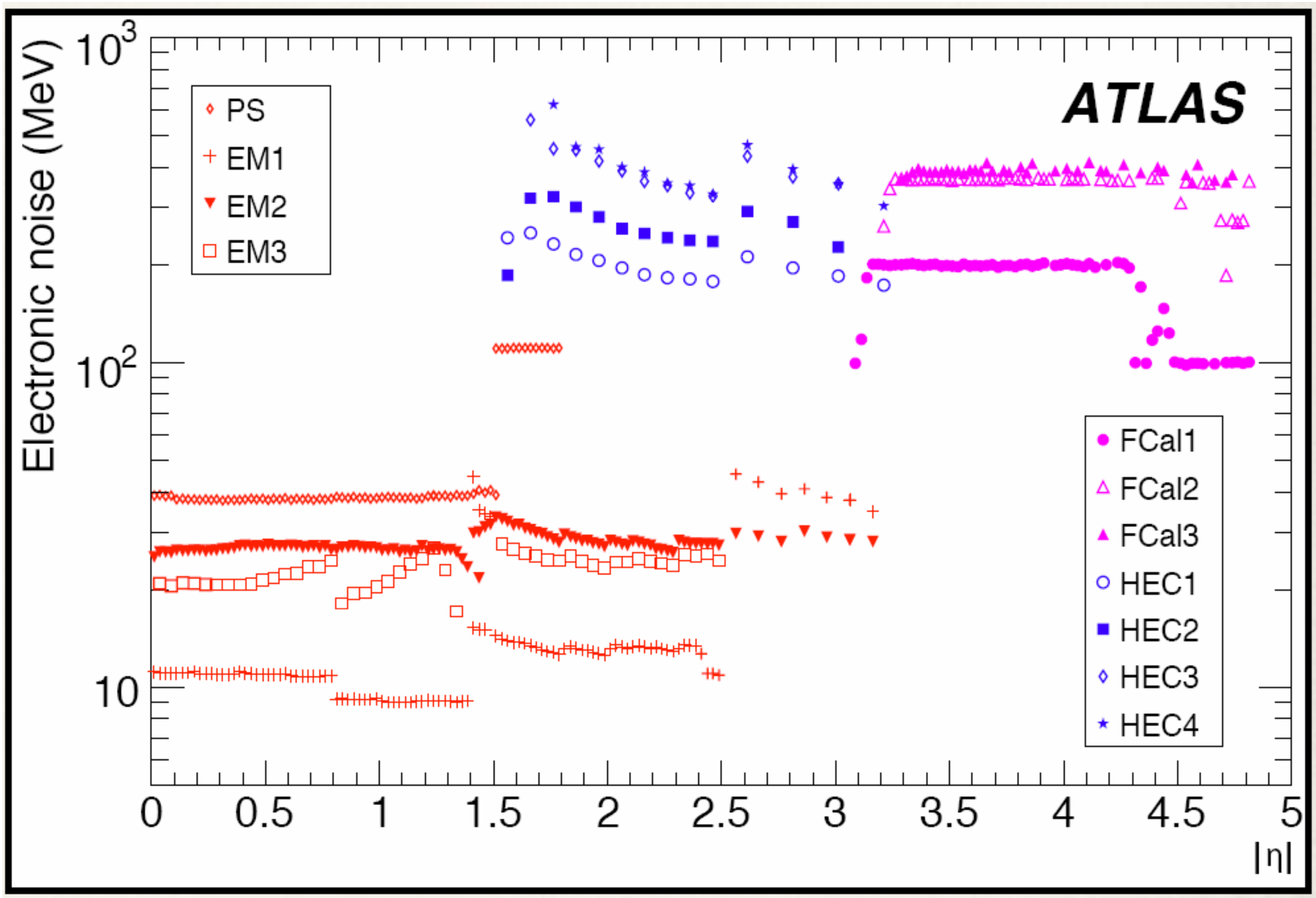

Since the FCal is in the very forward region, these noise levels are OK

Test Beam Energy Resolution

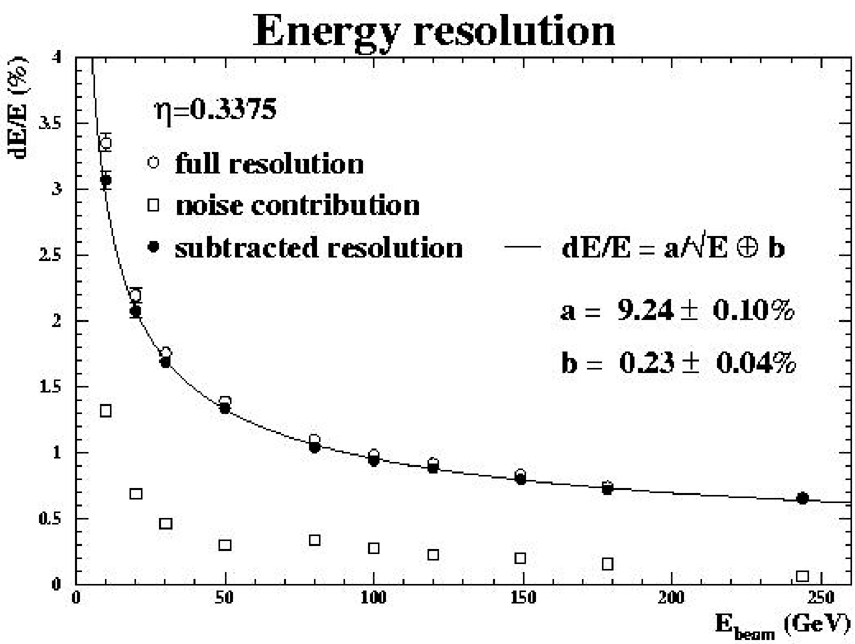

Barrel

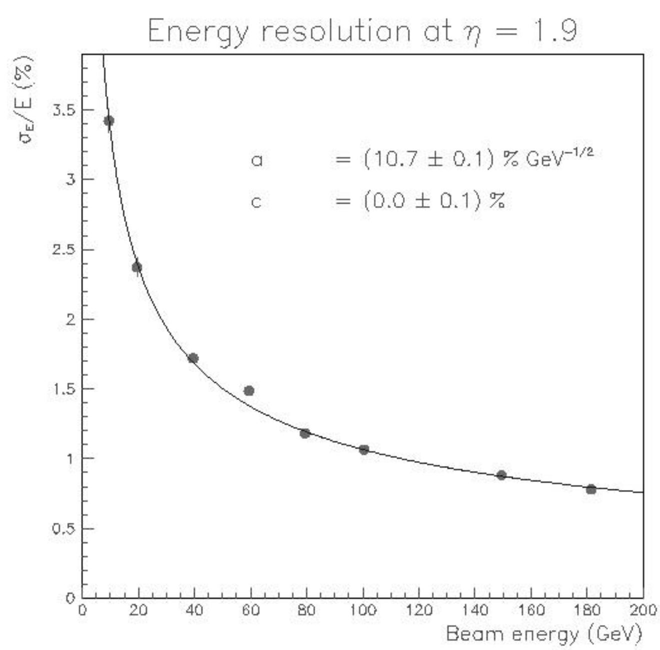

Endcap

Local constant and sampling term in the expected range

Summary of HEC Testbeam Results

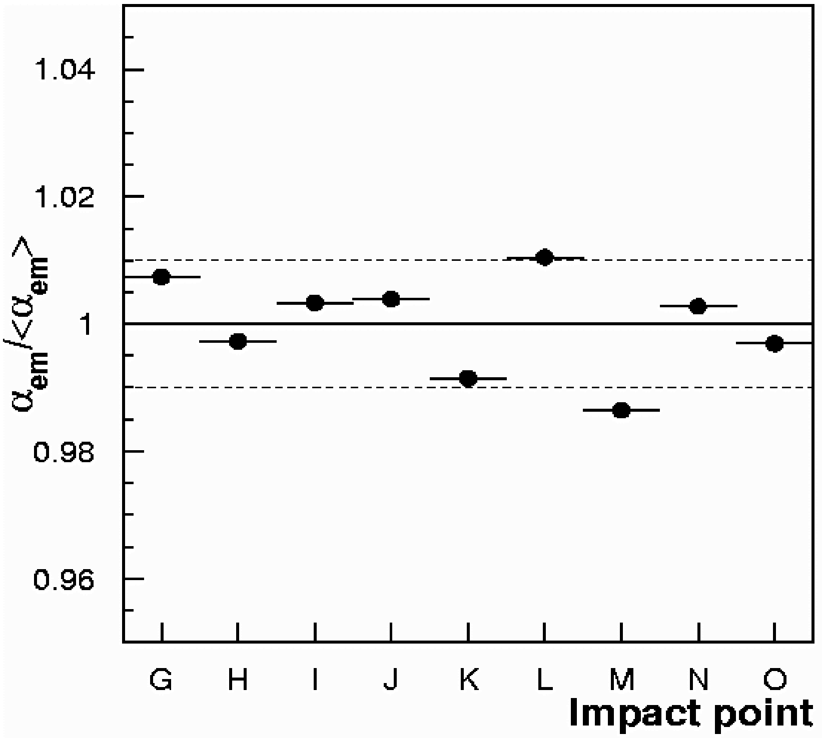

Module Uniform ~ 1%

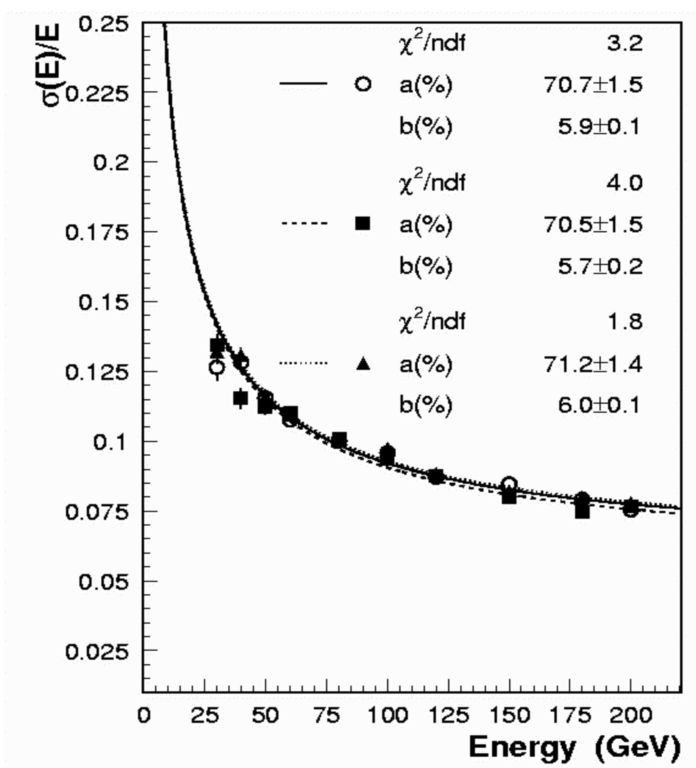

Energy Resolution

Test Beam Single Particle Energy Resolution

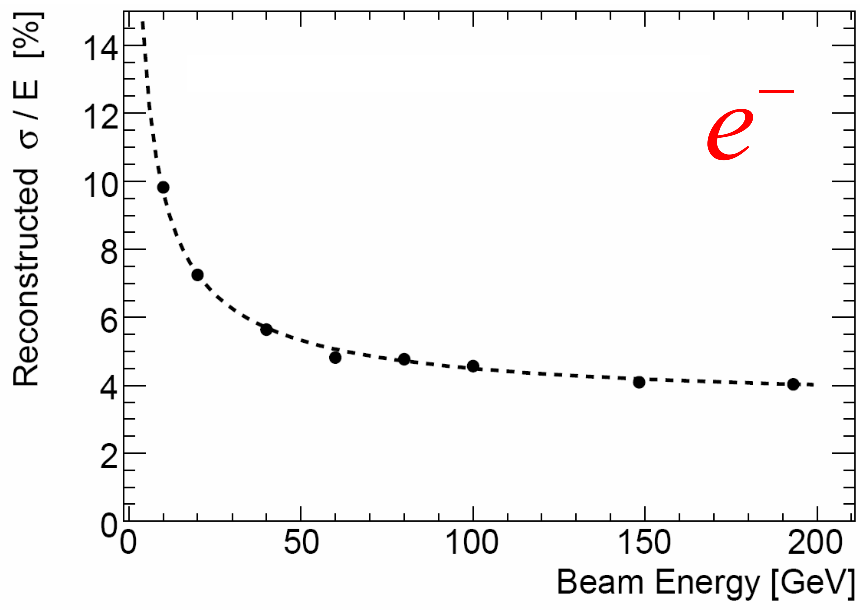

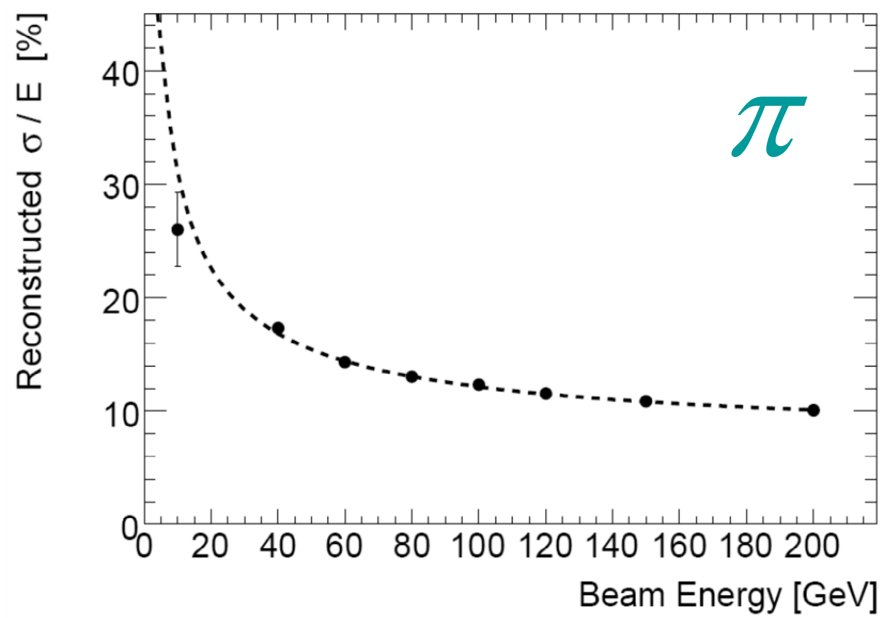

$$\frac{\sigma_E}{E} = \frac{a}{\sqrt{E}} \oplus b$$

Noise subtracted energy resolution

$$a = (28.5 \pm 1.0)\% \cdot \sqrt{GeV}$$

$$b = (3.5 \pm 0.1)\%$$

$$a = (94.2 \pm 1.6)\% \cdot \sqrt{GeV}$$

$$b = (7.5 \pm 0.4)\%$$

Lar Endcap Installed in ATLAS